Mid- to late Holocene seasonal variability in northern Germany and adjacent oceans and its potential impact on human societies

Dissertation in fulfillment of the requirements for the degree “Dr. rer. nat.”

of the faculty of Mathematics and Natural Sciences at Kiel University by

Camille Butruille

Kiel, 2016

First referee: PD Dr. rer. Nat. Mara Weinelt

Second referee: Prof. Dr. Ralph Schneider

Date of the oral examination: 28th of October, 2015

Approved for publication: 31st of May, 2016

Signed: Prof. Dr. Wolfgang J. Duschl

Graduate School « Human Development in Landscapes »

Christian Albrechts University of Kiel

2009-2015

I hereby certify that apart from my supervisor's guidance the content and design of the essay is all my own work; the thesis has not been submitted either partially or wholly as part of a doctoral degree to any other examining body and it has not been published or submitted for publication; in addition, this thesis has been prepared in accordance to the Rules of Good Scientific Practice of the German Research Foundation.

TABLE OF CONTENTS

ABSTRACT

The long term climate evolution in the North Hemisphere during the Holocene is represented by an overall cooling in the high latitudes, punctuated by brief cold episodes every few millennia associated with a slow-down of the Atlantic Meridional Overturning Circulation (AMOC). Some of these cold episodes coincide with important social reorganisations during the Holocene. In northern Germany and southern Scandinavia, the onset of farming occurred around 6000 cal. yrs BP, while agrarian practices were evidenced in surrounding areas for more than a millennium. The sudden transition towards an agrarian system followed by the neolithisation of the region occurs coincidently at the same time as one of the cold events recorded from the North Atlantic, the "5.9 event" that lasted between 6200 and 5800 cal. yrs BP. It is therefore discussed whether the transition towards a Neolithic subsistence in northern Germany and southern Scandinavia could have been shaped by climate change. However, the role of climate is still debated, as high resolution climate reconstructions from the region are lacking or missing the sensitivity to record abrupt climate changes. Interestingly, most of the paleoclimate reconstructions represent the mean annual or the summer climate variability, while some evidence show that winter variability in the North Hemisphere plays an important role during major rapid climate changes of the Holocene.

This dissertation focuses on the reconstruction of mid-to late Holocene winter and warm season thermal conditions based Mg/Ca-paleothermometry and oxygen isotopes on benthic foraminifera from two marine sediment cores. Winter thermal conditions are reconstructed from a core in the deep Skagerrak Basin, while the warm season temperatures are reconstructed from a shallower core in the Skagerrak. Detailed chronologies are established for the marine cores, enabling a correlation to terrestrial records using well known changes in the occurrence of pollen taxa, and thus allowing a direct comparison between climate reconstruction and archaeological records. On the long term, winter temperature reconstructions present a stepwise warming from the mid- to the late Holocene, while the warm season temperatures show an overall cooling. Cold events, roughly corresponding to the Atlantic Bond events, are evidenced during winter in the Skagerrak region over the mid- and late Holocene, and only partially during the warm season. The strongest cooling in

winter is evidenced between 6200 and 5900 cal. yrs BP roughly corresponding to Bond event 4. It is associated with low winter precipitations, and relatively high summer thermal conditions in the region. This abrupt decrease in winter temperatures coincides with the onset of neolithisation in northern Germany and southern Scandinavia. Most likely, it resulted in a shortening of the vegetation growing season, as well as an increased Baltic sea-ice extent that probably affected the marine food resources. This most likely lead the hunter-gatherer-fisher communities to abandon their previous subsistence strategies and adopt an economy based on agriculture. A shift towards more maritime conditions with a decrease in summer temperatures occurred around 5700 cal. yrs BP. This shift coincides with the abandon of naked wheat previously used by the agrarian communities, suggesting that climate conditions were not favorable for the cultivation of this particular cereal type. A rapid and strong cooling occurred again at 4300 cal. yrs BP, this time both evidenced in the winter and summer thermal reconstructions. Coincidently, new archaeological studies in the region report changes in the material culture of the Bronze Age communities happening at 4100 cal. yrs BP, suggesting a climate forcing. Finally, time series analyses conducted on Skagerrak records were used to identify significant periodicities as well as potential recurrent intervals of instability. Multidecadal to centennial scale variability in northern European climate is nowadays mainly associated with fluctuations in the North Atlantic sea surface temperature field and its interaction with the atmospheric system in the northern Hemisphere. Similar cycles are found in the winter and warm season temperature reconstructions, suggesting that variability intrinsic to the ocean-atmosphere system controlled the climate variability over northern Europe during the last 6800 years.

ZUSAMMENFASSUNG

Die langfristige Klimaentwicklung der Nordhemisphäre im Holozän ist in den hohen Breiten durch einen generellen Abkühlungstrend geprägt, ein Trend der in Abständen weniger tausend Jahre mehrfach durch kurzfristige Kaltepisoden unterbrochen wurde. Diese wurden mit Phasen verlangsamter atlantischer meridionaler Zirkulation assoziert. Für einige dieser Phasen wird aufgrund zeitlicher Koinzidenz angenommen, dass sie einen bedeutenden Einfluss auf die Entwicklung menschlicher Gesellschaften hatten. So könnte das späte aber rasche Einsetzen der Landwirtschaft in Norddeutschland und Südskandinavien vor ca. 6000 Jahren im Gegensatz zu angrenzenden Gebieten, wo landwirtschaftliche Praktiken schon über 1000 Jahre früher nachgewiesen wurden, mit veränderlichen Klima- und Umweltbedingungen zusammenhängen. Die Rolle des Klimawandels wird dabei jedoch kontrovers debattiert, nicht zuletzt weil hochauflösende regionale Klimarekonstruktionen noch fehlen bzw. die gewählten Proxies nicht ausreichend sensitiv sind, um abrupten Klimawandel zu erfassen. Das gilt insbesondere für Rekonstruktionen der kalten Jahreszeit, obwohl deren Rolle bzgl. abrupten Klimawandels als besonders relevant gilt.

Die vorliegende Dissertation richtet daher ihren Fokus auf die Rekonstruktion vergangener Winterbedingungen und stützt diese auf Mg/Ca-Paläothermometrie und Sauerstoffisotopensignale benthischer Foraminiferen an einem Sedimentkern aus dem tiefen Skagerrak. Die Temperaturen der warmen Jahreszeit wurden an einer flacheren Station rekonstruiert um die jahreszeitlichen Unterschiede erfassen zu können. Für die marinen Kerne wurden detaillierte Chronologien erstellt, die mit terrestrischen Chronologien korrelierbar sind und so einen direkten Vergleich der Klimaveränderungen mit archäologischen Veränderungen ermöglichen. Die Winterrekonstruktionen zeigen einen langfristigen Trend stufenweiser Erwärmung über das mittlere und späte Holozän, während die Rekonstruktionen der Sommertemperatur eine generelle Abkühlung zeigen. Kalte Ereignisse, die annähernd mit den atlantischen Bondereignissen im Zusammenhang stehen, konnten in der Skagerrak Region in den Winterzeiten im Mittel- und Jungholozän nachgewiesen werden, aber nur zum Teil in den warmen Jahreszeiten. Die stärkste Abkühlung der Wintertemperaturen ist zwischen 6200 und 5900 Jahren vor heute belegt und steht grob im Zusammenhang mit dem Bondereignis 4. Diese Phase ist mit niedrigen

Winterniederschlägen und relativ hohen Sommertemperaturen in der Region gekoppelt. Dieser abrupte Abfall der Wintertemperaturen fällt mit dem Einsetzen der Neolithisierung in Norddeutschland und Südskandinavien zusammen. Es kann angenommen werden, dass dieses Szenario auch zu einer Verkürzung der Vegetationsperiode führte, sowie zu einer Ausdehnung des baltischen Meereises, was widerum auch die marinen Nahrungsgrundlagen beeinträchtigt hätte. Demnach könnten die veränderten Umweltbedingungen die Jäger-Sammler Gemeinschaften veranlasst haben, frühere Subsistenzstrategien aufzugeben und eine landwirtschaftlich geprägte Ökonomie anzunehmen. Eine Verschiebung hin zu maritimen Klima-Bedingungen erfolgte dann vor ca. 5700 Jahren. Diese fällt mit der Aufgabe einer der bis dahin genutzen Hauptgetreidearten (Nacktweizen) zusammen und zeigt möglicherweise, dass die Bedingungen für den Anbau dieses speziellen Typs ungünstig wurden. Schließlich trat eine erneute, abrupte und ausgeprägte Abkühlung vor 4200 Jahren vor heute auf, die diesmal sowohl in den Winter- als auch in den Sommertemperaturen nachgewiesen wurde. Auch hier zeigen neue archäologische Ergebnisse einen parallelen Wandel in der regionalen materiellen Kultur bronzezeitlicher Gemeinschaften, so dass ein Einfluss des Klimawandels in Betracht gezogen werden kann. Zu guter Letzt wurden Zeitreihenanalysen an den Skagerrak Klimakurven durchgeführt, um auffällige Abschnitte sowie sich potenziell wiederholende Intervalle der Instabilität festzustellen.

Klimaschwankungen über Jahrzehnte bis hin zu Jahrhunderten hinweg werden heutzutage hauptsächlich mit den Schwankungen der Oberflächentemperaturen des Nordatlantik und dessen Interaktion mit dem Atmosphärensystem der nördlichen Hemisphäre in Zusammenhang gebracht. Ähnliche Zyklen werden in Rekonstruktionen für kalte und warme Jahreszeiten gefunden, was zu der Annahme führt, dass Veränderungen, die in direkter Verbindung mit dem Ozean-Atmosphärensystem stehen, die klimatischen Veränderungen über Nordeuropa in den letzten 6800 Jahren beinflusst haben.

INTRODUCTION

In northern Germany and southern Scandinavia, the first evidence in the material culture of a "Neolithic package" were found around 6000 cal. yrs BP, witnessing the onset of an agricultural system (Sørensen and Karg, 2014). Agrarian societies were already established for more than a millennium in central Germany (Guilaine, 2000), and communities of hunter-gatherer-fishers of northern Germany and southern Scandinavia had contact with these agrarian societies via trades for instance (Hartz et al., 2007). The sudden transition from Mesolithic hunter-gatherer-fisher communities towards Neolithic societies on a regional scale is suggested to have been influenced by climate change and resulting environmental changes as it occurred almost simulateously with a rapid climate change known from the North Atlantic (Bonsall et al., 2002; Sørensen and Karg, 2014). However, a recent study, comparing the evolution of the population in different regions of northern Europe to climate reconstructions from the northern Hemisphere, shows only low correlation between climate and the transition from the Mesolithic to the Neolithic in the region (Shennan et al, 2013). Yet, the climate records used for their correlation are based on temperature and precipitation reconstructions from archives in Greenland, the North Atlantic, northern Norway and Sweden, and Ireland, and it may be doubted how close they represent the regional climate of the studied societies. Indeed, different climatic developments are apparent on supra-regional scale for instance within northern Europe (Davis et al., 2003). Stacked pollen records from both northwestern and northeastern Europe depict different climate trends (Davis et al., 2003). This highlights a need for high resolution records from archives in the close vicinity of the settlements of past societies from northern Germany and southern Scandinavia that represent regional climate variability in order to identify any potential impact of climate on those societies.

Overall, the Holocene, starting at 11,700 cal. yrs BP (Walker et al., 2009), is regarded as a period of fairly stable climate and environmental conditions compared to the last glacial interval (e.g. Mayewski et al., 2004; Wanner et al., 2008). A general cooling trend documented in most paleoclimate reconstructions describes a cooling in the northern Hemisphere mid- and high latitudes from the early to the late Holocene, driven by the orbital-forced decrease in the summer/mean annual insolation, while a strong seasonality is

expected during the early and mid-Holocene in respect to lower winter insolation, evidenced in pollen-based winter and summer temperature reconstructions (Davis et al., 2003). The early Holocene (11,700 - 8200 cal. yrs BP; Walker et al., 2012) is characterized by remnant ice sheets, a high summer insolation, and ends with the final stages of the deglaciation of the Laurentide and Scandinavian ice sheets. Consequently, the eustatic sea level rose and the retreat of the ice sheet were compensated by the glacial isostatic adjustment of the Scandinavian landmass. At the same time, the Baltic Sea developed from a fresh water lake (Ancylus Lake) to a brackish sea with the opening of the Danish strait (Gyllencreutz et al., 2006). It became connected to the open Atlantic Ocean via the Kategatt and Skagerrak. This is when the modern circulation in the Skagerrak was established, with both the opening of the Danish strait and the English Channel. During the mid-Holocene, climates and environments in northern Europe were generally characterized by high summer and mean annual temperatures, low winter precipitations, and reduced or lacking continental glaciers (Davis et al., 2003; Bjune et al., 2005; Bakke et al., 2008; Seppä et al., 2009). This period is referred as the "Holocene Thermal Optimum" (HTO). It is followed by a transition towards a neoglaciation around 4200 cal. yrs BP that marks the beginning of the late Holocene as recently proposed by Walker et al. (2012). The neoglaciation is associated with a decrease in summer and mean annual temperatures, increased winter precipitations, and re-advancing continental glaciers (Davis et al., 2003; Bjune et al., 2005; Bakke et al., 2008; Seppä et al., 2009).

These general climate trends are punctuated by a series of several abrupt climate changes most notable in the areas surrounding the North Atlantic, the so-called Bond events (Bond et al., 1997; Bond et al., 2001). They were first evidenced in sediments from the Atlantic as repetitive episodes of ice-rafted debris occurring roughly at 1500-years intervals throughout the Holocene and representing large discharge of icebergs into the North Atlantic (Bond et al., 1997). They are supposedly forced by changes in solar intensity and ocean-atmosphere modulation (Bond et al., 1997, 2001; Bianchi and McCave, 1999; Debret et al., 2007; Thornalley et al., 2009), and related to the weakening of the Atlantic Meridional Overturning Circulation (AMOC), which in turn lead to a diminution of the distribution of heat from the tropics towards the poles (Wanner et al., 2008).

Short term variability in modern climate over Northern Europe is mostly associated with the North Atlantic Oscillation or NAO (e.g., Hurrell, 1995; Hurrell et al., 2003). The NAO governs

large-scale atmospheric pressure systems responsible for the redistribution of atmospheric masses between the Arctic and the subtropical Atlantic (Hurrell, 1995; Hurrell et al., 2003). The NAO variability is closely linked to variability in the North Atlantic and in particular changes in the sea surface temperature (SST) fields, also called Atlantic Multidecadal Oscillation (or AMO) (see Sutton and Hodson, 2003). There is also evidence for a non-stationary correlation between AMO and NAO (Walter and Graf, 2002; Wyatt et al., 2012). Besides a variability of one to two years, instrumental records show that the NAO stays predominant in one phase or another on decadal scale (Hurrell, 1995). Since the instrumental records only span about 150 years, it is difficult to discern whether the NAO or the AMO are persistent during the Holocene as periodic drivers in the climate system. However, an increasing number of data-based studies, also supported by simulations, show that multidecadal variability occurred over the Holocene and appears similarly intrinsic to the ocean-atmosphere variability (see Knudsen et al., 2011 and references therein; Wei and Lohmann, 2012). Moreover, climate reconstruction based on tree rings and speleothems for the last 900 years indicate that prolonged phases of the NAO in a dominant state occurred during the Medieval Climate Anomaly (MCA) or the Little Ice Age (LIA) (Trouet et al., 2009, 2012; Moreno et al., 2012; Olsen et al., 2012; Jones et al., 2014 ; Spangehl et al., 2010). Prolonged phases of the NAO in a dominant states seem also to have prevailed during other large-scale changes in the Northern Hemisphere climate for at least the last 5200 years (Olsen et al., 2012).

The abrupt climatic events associated with the Bond events, and the centennial to multidecadal variability such as the NAO are important factors of environmental changes. Indeed, during the Bond events, a general cooling and a shift towards continental-dominated climate conditions are reported in northern Europe (Alley et al., 1997). Bond event 5 (or 8.2 event), occurring around 8200 cal. yrs BP is believed to have induced the expansion of agriculture from the Middle East to Europe (Burroughs, 2005). Other events have also been proven to have had an important impact on the social development during the Holocene, such as the 5.9 event which coincides with the end of the African Humid Period (DeMenocal et al., 2000) and the 4.2 event is known to be related to the collapse and reconstruction of ancient civilization (Gibbons, 1993; Staubwasser et al., 2003; Dixit et al., 2014). Nowadays, the NAO is mostly evidenced during the winter months and changes from one dominant state of the NAO to another are responsible for changes in the seasonal

length, the occurrence of late last-frost, the length of the vegetation growing season (e.g. Gouveia et al., 2008). Additionally, it has an influence on interannual variability of the Baltic Sea seasonal ice cover (Koslowski and Loewe, 1994; Tinz, 1996; Omstedt and Chen, 2001; Jevrejeva et al., 2003).

High-resolution Holocene climate reconstructions from northern Germany and southern Scandinavia present a general cooling trend during the Holocene, yet do not present strong evidence for cold relapses associated with the Bond events (Seppä and Birks, 2001; Seppä et al., 2009; Erbs-Hansen et al., 2011a). Interestingly, those paleoclimate records are generally representing the mean annual or warm season thermal conditions. Yet, major rapid climate changes associated with a shutdown (or decrease in strength) of the AMOC during the last glacial period and the early Holocene, particularly influenced winter variability in the northern Hemisphere high latitudes as a result of high-latitudes remnant ice sheets and low winter insolation (Wanner and Bütikofer, 2008; Wanner et al., 2014, Denton et al., 2005). Indeed, the weakening phases of the AMOC were associated with the extension of Arctic sea ice during winter (Denton et al., 2005; Wanner and Bütikofer, 2008; Wanner et al., 2014), which in turn most likely exacerbated the cooling of high latitudes during winter under decreased winter insolation (Denton et al., 2005; Seppä et al., 2007). The mid-Holocene, however, starts with the melting of the last remnant Laurentide and Scandinavian ice sheets and a change in the insolation regime, and the contribution of winter variability to the annual variability during the mid-Holocene might have change. Nowadays, the short term variability associated with the NAO is also mostly evident during the winter months (Hurrel , 1995). In order to evaluate the potential influence of climate change on past societies in the region, it is therefore necessary to reconstruct regional winter thermal variability during the mid-Holocene.

The Skagerrak is the deepest basin of the North Sea located between Norway and Denmark, and has been considered for the modern time as highly sensitive to the atmospheric climate fluctuations that control the region (Ljøen and Svansson, 1972; Tunberg and Nelson, 1998; Hagberg and Tunberg, 2000; Brückner and Mackensen, 2006). In particular, Skagerrak deep-water renewal monitors nowadays the regional winter thermal variability (Ljøen and Svansson, 1972) and potentially the NAO (Tunberg and Nelson, 1998; Hagberg and Tunberg, 2000; Brückner and Mackensen, 2006). Since most climate or environmental reconstructions in the region represent the mean annual or summer thermal conditions and do not focus in

particular on the mid-Holocene, establishing robust high-resolution reconstructions of winter paleotemperatures for the mid-Holocene, based on archives sensitive to the regional climate variability such as the Skagerrak, is essential in order to understand potential climate and environmental changes that could have affected prehistoric societies from the Mesolithic to the Neolithic in northern Germany and southern Scandinavia. In that perspective, this thesis aims to establish robust chronologies of mid-Holocene winter and the warm season temperatures from the region.

Basically, the main objectives of this study can be outlined as such:

1/ To establish high-resolution reconstructions of past regional climate from Skagerrak marine archives, focusing on winter variability during the mid-Holocene.

2/ To identify the main drivers of past regional climate and in particular, winter variability.

3/ To improve the chronology of mid-Holocene climate reconstructions of the region by establishing robust age models for the marine cores. To do so, we aim to:

a) increase the density of radiocarbon dates over the cores and in particular for the mid-Holocene,

b) use common markers such as tephra layers and pollen assemblages to match the marine climatic records to the terrestrial finely-dated archives of societal and environmental changes relevant to the Neolithic societies in northern Germany and southern Scandinavia.

4/ To identify any potential impact of climate on the environmental and societal evolution from the Neolithic to the Bronze Age in the region.

1.1. STRUCTURE OF THE THESIS

This thesis comprises 8 chapters. **Chapter 1** provides an introduction of the current debates and controversies on the subject of mid-Holocene climate variability, its drivers, and its potential impact on prehistoric societies in the Skagerrak region. **Chapter 2** outlines the main area of interest of the thesis: Skagerrak modern hydrograhy; the modern regional climate; and the evolution of Mesolithic to Bronze Age societies in northern Germany and southern Scandinavia. The material and methods used in this thesis are described in **chapter 3**. Chapter 4 to 7 present the results and discussions of the thesis divided in different manuscripts, as follow:

Chapter 4 focuses on the establishment of robust age models for marine cores IOW225514 and IOW225517 from the Skagerrak. Complementary radiocarbon dates were added to the already existing age models. The age models were additionally tested by comparing the XRF records of both cores. The correlation gives a satisfactory result of 0.83. In a second step, the correlation between the marine chronostratigraphies and on-land stratigraphies of archaeological and environmental reconstructions is explored. Tephra layers were sought in the marine cores, in order to identify specific eruptions that occurred during the Holocene. However, tephra particles appeared to be reworked over time and we could only identify one eruption. A pollen diagram for core IOW225517 was also established in order to identify remarkable events in environmental changes on-land. Remarkable changes in on-land vegetation were identify in the marine cores. According to our results, a radiocarbon reservoir age of 400 years can be accounted for the Skagerrak during the mid-Holocene.

Chapter 5, published as a manuscript to the journal The Holocene in April 2015, focuses on mid- to late Holocene climate reconstructions from the Skagerrak. Benthic foraminifera Mg/Ca paleothermometry and isotope reconstructions of $\delta^{18}O_{sea\text{-}water}$ are performed on core IOW225514 in the deepest part of the Skagerrak basin, allowing us to reconstruct winter thermal variability since the mid-Holocene, in comparison to wam season temperature reconstructions based on benthic foraminifera Mg/Ca paleothermometry from the shallower core IOW225517. Our results show that the mid-Holocene was characterized by generally cold winter conditions and relatively warm summers, followed by a shift towards milder winter conditions and colder summers over the North Sea around 3500 cal. yrs BP. The late Holocene shift was most likely related to the onset of a regime of intensified winter westerly

winds (Westerlies) directed towards northern Europe and an increased inflow of North Atlantic water into the Skagerrak/North Sea reflecting more maritime climate conditions. These periods were punctuated by cold phases mainly distinct in the winter thermal reconstruction, matching with low winter precipitation phases in western Norway. The cold phases seem to correlate with distinct increases in ice rafted debris (IRD) in North Atlantic sediments, suggesting that phases of iceberg discharge in the Atlantic were associated with cold and dry winter conditions over northern Europe.

Chapter 6 present the spectral analyses of the time series reconstructed in chapter 5 from cores IOW225514 and IOW225517 in order to identify possible drivers of past regional climate. Potential cycles and non-stationary behaviour are sought: ≈1000-1200 years periods are found and most likely reflect the influence of the Bond events on the regional climate. Additionally, multidecadal variability of 50 to 110 years is found in Skagerrak records. This periodicity most likely indicates an influence of short term variability similar to the Atlantic Multidecadal Oscillation (AMO) and possibly the North Atlantic Oscillation (NAO) on the regional thermal conditions since the mid-Holocene.

Chapter 7 discusses the potential impact of climate on the prehistoric societies in northern Germany and southern Scandinavia, based on the climate reconstructions from chapter 5. The focus is made on three particular changes in the economy of past societies in the region that occurred from the Mesolithic to the Bronze Age. 1/ The transition from hunter-gatherer-fisher communities towards an agricultural system: the onset of agriculture in the region occurred directly after Bond event 4, which is evidenced in our records as an abrupt period of particularly severe winters. Most likely, those resulted in late onset of spring and late last-frosts, both responsible for a shortening of the vegetation growing season, as well as an increased Baltic sea-ice extent. In turn, prolonged ice sea cover might have lead to hypoxia in the Baltic Sea that largely affected the marine food resources. Hunter-gatherer-fishers, well adapted to their environments were probably vulnerable to such environmental changes which resulted in the adoption of an agrarian subsistence. 2/ A change in the main cultivars used at 5700 cal. yrs BP, at the establishment of a fully developed agrarian system, coincides with a decrease in summer temperatures, and relatively mild winter conditions. Since some of the crops used need relatively warm summers, a decrease in summer temperatures might have influence the change in crop cultivation around 5700 cal. yrs BP. 3/ A transition from a period of boom in the economy of Bronze Age societies towards a period

of crisis is evidenced at 4100 cal. yrs BP, coinciding with a strong winter cooling at 4200 cal. yrs BP that could have led to worse conditions for agriculture, as the growing season for vegetation must have shortened. At 3700 cal. yrs BP, a new period of economic boom is evidenced in the material culture, that more or less coincides with an abrupt increase in winter temperature and the onset of a period of milder winters, probably more favorable to agriculture. Each subchapters of the discussion are planned to be submitted as independent manuscripts.

The main conclusions of the thesis are synthesized in **chapter 8**, together with future outlooks.

2. WORKING AREA

2.1. THE SKAGERRAK

The Skagerrak is a marine basin in the north-eastern part of the North Sea (Figure 2.1). The modern circulation inside the Skagerrak is anti-clockwise. It consists of North Atlantic waters entering the Skagerrak along the southern slope of the Norwegian trench and that join the Jutland Current and Central North Sea water along the coast of Denmark. The resulting water mass flows along the Swedish coast and exits the Skagerrak along the northern slope of the Norwegian trench. The Jutland current, along the west coast of Denmark, is the most erosive current entering the Skagerrak. It has the highest concentration of suspended sediment, collecting waters from the shallow south and central North Sea served by numerous rivers such as the Elbe, the Rhine, and the Thames. Being the deepest basin of the North Sea, the Skagerrak constitutes a trap for the suspended sediments and therefore provides high-resolution paleoclimatic and hydrographical records for the Holocene.

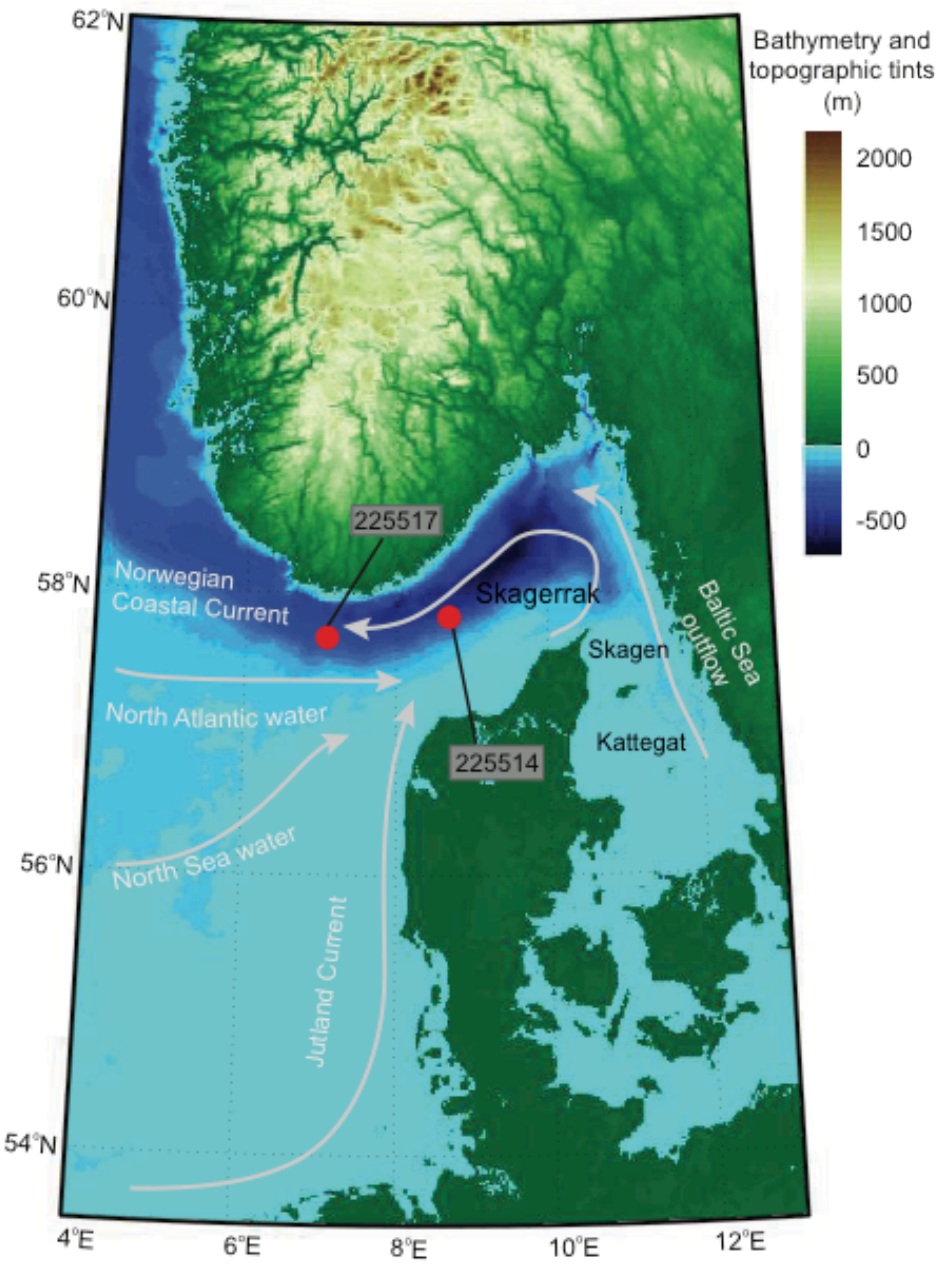

Figure 2.1: General circulation and bathymetry in the eastern North Sea and Skagerrak-Kattegat (Map modified from Gyllencreutz, 2005). The cores used in this study are marked with red dots.

Basically, the modern circulation of the Skagerrak was established about 8500 years ago, as a result of four important changes (eg Gyllencreutz et al., 2006): i) a strengthening of the Atlantic inflow about 9000 years ago, ii) the progressive widening of the Danish Strait between about 10 000 to 8000 years ago, allowing the exchange of water masses with the brackish Baltic Sea, iii) the opening of the English Channel between 9000 and 7700 years ago, and iv) the isolation of the Dogger Bank about 9000 years ago, allowing the penetration of saline Atlantic water from the SW North Sea towards the west coast of Denmark, a pathway

blocked throughout the last glacial period. The last two events enabled the formation of the Jutland Current (see Figure 2.1). The strengthening of the Atlantic inflow and the opening of the Danish Strait are responsible for the establishment of the anti-cyclonic circulation and an increased transport of suspended sediments. About 8000 years ago, the coastlines of the eastern North Sea had mostly reached their current shape and all major elements of the modern circulation were established. Afterwards, the Jutland Current underwent a phase of intensification between 6300 to 3800 years BP, gradually developing towards the present system (i.g. Gyllencreutz et al., 2006).

According to Ljøen and Svansson (1972), there is a significant contrast in the long-term variations of temperatures between waters above and below the sill depth (about 300m). Above 300m, the main processes of exchanging water masses are advective, reflecting the character of water flowing into Skagerrak from the surrounding seas with their interannual temperature variability (from 0 to 15°C or more). This is where the main transport occurs (around 200 to 300m water-depth). Below the sill level, the variation in temperatures (between ca. 4-8°C for the modern time) reflects the renewal of the deep waters by denser waters every few years, with a rapid cooling phase and a longer period of warming, especially pronounced below 400m (Ljøen and Svansson, 1972). Instrumental measurements of temperature, salinity and derived density show that the deep waters are renewed by waters from the central North Sea during cold winters: since the central North Sea is shallow and characterized by slow movements and strong mixing, dense waters are formed during a cold period. They later flow down the southern slope of the Skagerrak, injecting cold, well-oxygenated waters into the deep basin. A single renewal cycle is completed over a period of four to five months. In years of mild winters, the waters from the North Sea do not reach the density for vertical overturning of the deep waters. The latter therefore mix with the upper waters, gradually warming up, until a new renewal is triggered by the next cooling. This warming phase of the deep waters can take up to two and a half years depending on the degree of the precedent cooling and the timing of the next one. This rhythm of the deep-water renewal has been shown to be positively correlated to the phases of the NAO for the last decades (Tunberg and Nelson, 1998; Hagberg and Tunberg, 2000; Brückner and Mackensen, 2006).

2.2. Modern regional climate variability

Today, one of the most prominent climatic phenomenons affecting Europe is represented by large-scale atmospheric pressure systems that drive the redistribution of atmospheric masses between the Arctic and the subtropical Atlantic. This phenomenon of atmospheric circulation is also referred to as the North Atlantic Oscillation (NAO), mostly evidenced during the winter months (Hurrell, 1995; Hurrell et al., 2003). It governs the wind tracks over the North Atlantic (Westerlies) that transport heat and moisture towards Europe, and the intensity and number of storms. Intensified pressure gradients between the Icelandic Low and the Azores High (positive state of the NAO) lead to periods of maritime-dominated climate, characterized by strong Westerlies bringing mild and moist air masses over Northern Europe. In contrast, low pressure gradients between the Icelandic Low and the Azores High (negative NAO) lead to a shift of the Westerlies towards southern Europe, and a shift of the continental anticyclone from Russia towards northwestern Europe. Summers are thus warm and dry, while winters are cold and dry (see Hurrell, 1995; Hurrell et al., 2003). The fluctuations between the different modes of the NAO are responsible for interannual variations in the seasonal length and the occurrence of late last-frost (e.g. Gouveia et al., 2008), as well as interannual variability of the Baltic Sea seasonal ice cover (Koslowski and Loewe, 1994; Tinz, 1996; Omstedt and Chen, 2001; Jevrejeva et al., 2003). Therefore, the NAO has a strong influence on interannual environmental variability in Europe.

Moreover, besides the short-term variability of one to two years, the NAO is known to stay predominant in one phase or another on decadal scale (Hurrell, 1995). The NAO was also probably locked in one phase during prolonged periods such as the Medieval Warm Period (MWP) or the Little Ice Age (LIA) (Trouet et al., 2009, 2012; Moreno et al., 2012; Olsen et al., 2012; Jones et al., 2014 ; Spangehl et al., 2010).

2.3. Prehistoric societies in northern Germany and southern Scandinavia

The late Mesolithic in southern Scandinavia and northern Germany is represented by the Ertebølle culture that was present in the region between 7400 and 6100 cal. yrs BP, consisting of communities of hunter-gatherer-fishers (Hartz et al. 2007 and references therein). Agrarian communities were already established in central Germany, and evidence

of trades with the Ertebølle culture is documented (Hartz et al., 2007). Then, a period of radical changes in the economy of the Mesolithic communities occurred at 6100 cal. yrs BP, with the introduction of domesticated animals and to less extend the use of cereals, as the first evidence of a « Neolithic package ». It was however at first still associated with a hunter-gatherer-fisher subsistence until around 5700-5500 cal. yrs BP, when farming strategies were fully adopted and a new social organization was established represented by the Funnel Beaker culture (or Trichterrandbecherkultur, TRB) (Müller, 2011; Dörfler et al., 2012; Feeser et al., 2012; Kirleis et al., 2012; Sørensen and Karg, 2014). Traces of the TRB groups are found in a large part of northern Europe, from the Netherlands in the West to Poland in the East, and from northern Germany to southern Sweden. The new agricultural economy probably improved their living conditions, since a boom in the regional population density is evidenced (Hinz et al., 2012). It also most likely enabled extra investments into infrastructure, as manifested in the edification of at least 30,000 megalith graves in a really short period of 300 to 400 years (Hinz et al., 2012). However, around 5100 cal. yrs BP, the population collapsed and forests recovered, until the late Neolithic around 4900 cal. yrs BP and the development of the Single Grave Culture (Hinz et al., 2012; Müller, 2011; Feeser et al., 2012). The Single Grave Culture represents the late Neolithic and the early Bronze Age in the region.

3. MATERIAL AND METHODS

3.1. SEDIMENT CORES

The main focus of the present project is climate variability inferred from the Skagerrak based on foraminifera analyses. Planktonic foraminifera are scarce in the Skagerrak because the surface water is influenced by the outflow of brackish water from the Baltic Sea. We therefore focused on benthic foraminifera paleothermometry to reconstruct past climate variability.

Interestingly, Skagerrak deep-water temperatures have the particularity to keep a regional winter signal over the year (Ljøen and Svansson, 1972), and knowledge about past winter climate conditions are rare due to the biological origin of most proxies. Therefore, a gravity core from the deep basin of the Skagerrak, core IOW225514 (57°50.279' N, 8°42.226' E, 420m water depth, 405cm long) was chosen in order to reconstruct past winter variability in the Skagerrak region. Additionally, a shallower gravity core was chosen, core IOW225517 (57°40.002' N, 7°05.465' E, 293 m water depth, 455cm long). Both cores were retrieved during Alkor cruise 159 in 2000. The water masses at that depth are expected to have faced a seasonal variability (Ljøen and Svansson, 1972). Paleothermometry based on benthic foraminifera at that depth are therefore expected to represent the signal of the season in which the foraminifera grow. Planktonic blooms in the North Sea region mainly occur during spring to autumn (Joint and Pomroy, 1993; Blanz et al, 2005 and references therein), resulting in organic flux to the sea floor with a strong seasonality influence on the growth of benthic foraminifera (Gooday, 2003). Therefore, it is more likely to assume that benthic foraminifera growth in the Skagerrak occurs during spring to autumn, and thus, paleothermometry based on benthic foraminifera from core IOW225517 is likely to reflect a warm season signal.

Both stations dispose of an array of available paleoceanographic data from previous studies (Hass, 1996; Emeis et al., 2003; Brückner and Mackensen, 2006, 2008; Brückner, 2008). The uppermost part of core IOW225517 was lost during its recovery and a correlation with a multicore from the same station was performed by comparison of sediment facies, physical

properties and organic carbon concentrations. 41.5 cm were reported to be missing. To simplify the reading, we will use uncorrected depth in this thesis, unless mentionned otherwise. Earlier age models for both cores, based on six and seven ^{14}C dates respectively, were published by Emeis et al. (2003). They also provided first high-resolution sea surface temperature (SST) records using the alkenones un-saturation ratio $U^{K'}_{37}$ on lipid extracts produced by phytoplankton (Emeis et al., 2003). Krossa et al. (2015) used a revised method (Leduc et al., 2010) to improve the analytical sensitivity for alkenone sea surface temperatures (SST) reconstructions, and applied this method on cores from an east-west transect in the Skagerrak, including cores IOW225514 and IOW225517. Stable isotope records as well as abundance data of benthic foraminiferal species from core IOW225514 were published by Brückner and Mackensen (2006) and Brückner and Mackensen (2008). Granulometry and stable oxygen isotopes records were built from a core from the same station as core IOW225514 (Hass, 1996) and were used to reconstruct climatic variability during the late Holocene.

3.2. SAMPLING MATERIAL

For our study, core IOW225514 was sampled every centimeter between 227 and 405 cm, and at 2 to 5 cm intervals for the remainder of the core. Slices of 1cm thickness were wet sieved to collect the sediment fraction between 125 µm and 2 mm. Benthic foraminifera were hand-picked from the >150 µm coarse fraction and mono-specific samples were prepared for stable isotopes ($\delta^{18}O$, $\delta^{13}C$) and Mg/Ca analyses on calcareous tests. Core IOW225517 was sampled every 1 to 2 cm between 159 and 307 cm and every 10 or more cm for the remainder of the core. *Melonis barleeanus, Uvigerina mediterranea* and *Bulimina marginata* are the three most abundant benthic foraminifera species in the Skagerrak during the Holocene (Brückner, 2008). The author also reported that individuals of these species seemed to be the least affected by carbonate dissolution and re-precipitation (after preparation for stable isotope measurements), as inferred from microscopic and SEM investigations. We therefore focused on those species for radiocarbon dating, and in particular on *Melonis barleeanus* for Mg/Ca and stable isotopes analyses.

3.3. AGE MODEL

Refined and robust age models are of high importance in this project, in order to compare terrestrial and marine archives. Previous reconstructions by Hass (1996) and by Brückner and Mackensen (2006) and Brückner and Mackensen (2008) are based on a different dating method than the usual radiocarbon age model, using the «excess» ^{210}Pb method and the «supported» ^{210}Pb method (Erlenkeuser and Pederstad, 1984; Erlenkeuser, 1985). The «supported» ^{210}Pb method has not been developed further or used in recent paleoclimatological and paleoceanological studies. It gives large discrepancies when compared to radiocarbon dating, the further back in time we go: around 310 cm depth in core IOW225514, the «supported» ^{210}Pb method gives an estimated age of about 3450±375 yrs BP (Brückner and Mackensen, 2006), which differs from the radiocarbon method by about 2000 years (Emeis et al., 2003). The radiocarbon dating method, on the other hand, is widely accepted as a reliable dating method for the Holocene and is used to date the marine and terrestrial archives of interest for this study. Radiocarbon dating is therefore the method of dating used in this study. Yet, there are potential biases associated with this method that need to be considered, such as possible preferential re-sedimentation/reworking of individual foraminifera species and reservoir ages for marine archives or hard water effects for fresh-water archives. The potential biases that could affect radiocarbon dating in our case will be discussed.

3.3.1. Radiocarbon dating

The age models of core IOW225514 and IOW225517 are based on radiocarbon dates of benthic foraminifera, previously published by Emeis et al. (2003) and expanded with two and five new radiocarbon dates, respectively (see chapter 4). In order to minimize problems of possible preferential re-sedimentation/reworking of individual foraminifera species, which may bias dating, samples of selected species were used in this study for radiocarbon dating. All ^{14}C data were recalibrated using the online software CALIB (Calib7.0, © 1986-2014: M. Stuiver and P. Reimer) and the Marine13 curve (Reimer et al., 2013), with a standard reservoir age of 400 years as generally used in the Skagerrak (e.g. Erbs-Hansen et al., 2011a, 2011b; Krossa et al., 2015). Potential reservoir ages will be discussed in chapter 4. We also

sought for tephra layers along the cores and built a pollen stratigraphy on core IOW225517, aiming at an independent age control to link the marine records to the terrestrial records. XRF ratios are used to improve the correlation between both marine cores.

3.3.2. Tephra layers

During the Holocene, a number of major eruptions occurred in Iceland, and in particular from the Hekla volcano, ashes from which were found in many sediment archives over Northern Europe (Dugmore et al., 1995; Pilcher and Hall, 1996; van den Bogaard et al., 2002; Zillén et al., 2002; Wastegård, 2005; Vorren et al., 2007; Dörfler et al., 2012). Since an eruption occurs on a really short time (days to weeks), tephra should represent isochronous surfaces independent of the environment and distance from their source. Regional tephra occurrences mostly represent the airborne ashes of distant volcanoes, and thus provide a unique chance to directly link chronologies of different archives, be it marine or terrestrial. Skagerrak lies for instance under the influence of ash plumes from the Hekla eruptions 3 and 4, occurring respectively around 3120-3068 cal. yrs BP and 4417-4266 cal. yrs BP, and found in lakes from Northern Germany (Dörfler et al., 2012), close to the archaeological study area of this project. Those particular eruptions were therefore sought in the marine core IOW225514 and IOW225517 used in this study.

In order to find defined layers of tephra, sections of the cores were first sampled according to the presumed position of known tephra layers following the ^{14}C chronology. Sample groups of 3 to 5cm intervals were first analyzed to detect the presence of volcanic ash. In case of presence, sub-samples of 1cm were then taken and analyzed to identify peak occurrences. The samples were prepared using HCl (10%) to dissolve carbonates, NaOH (10%) to eliminate diatom silicates, and concentrated H2SO4 and HNO3 to get rid of organic material. Samples were then sieved to isolate the 6 to 100 µm fraction (range for main tephra particles). In order to separate tephra shards from heavier particles, a separation using heavy liquid with a density of 2.5 was practiced on this fraction. The lighter particles (including tephra) were then precipitated on micro slides, and tephra particles were counted under an optical microscope. Samples of 1cm, with significant number of tephra particles

were redissolved to be deposited on a special relief-free diamond-polished slide. A carbon coating was applied (using a high-vacuum carbon evaporator) to make the sample electrically conductive. Those slides were then brought for geochemical analyses to the GEOMAR-Helmholtz-Zentrum für Ozeanforschung, in Kiel. Major elements (oxides) were measured using an Electron Microprobe JEOL JXA 8200 (X-ray). In order to identify the potential volcanic eruptions that lead to the deposition of the tephra layers found in our cores, we then compare the geochemical signals to those from tephra layers identified in the region.

3.3.3. Pollen analyses

General patterns of vegetation changes on a regional scale are reflected in pollen diagrams. Synchronous (or quasi-synchronous) changes in vegetation are used to link chronologies of the different archives. Therefore, we performed pollen analyses on core IOW225517 in order to identify remarkable changes in the pollen of singular plants and directly link terrestrial and marine chronologies.

Twelve samples of about 1,5 cm^3 from 1cm-thick slices were taken for pollen analyses in core IOW225517 between 213 and 300cm. To facilitate calculation of pollen concentration, *Lycopodium* tablets were added at known concentration (Stockmarr, 1971). Samples were treated with KOH, HCL, HF and acetolysed following the standard pollen procedures (Moore et al., 1991). The coarse fraction was removed by initial sieving (120µm mesh size). Also particles under 6µm were removed by ultrasonic sieving. The residue was mounted in Glycerol and pollen grains were counted at x400 magnification. Phase contrast and x1000 magnification were used in case of critical grains. A pollen sum of about 180 grains per samples was generally achieved.

3.3.4. X-Ray Fluorescence (XRF) scans

X-Ray Fluorescence is a non-destructive method for elemental and chemical analyses. The method consists of bombarding a material with high-energy X-rays and measuring the resulting emission of fluorescent X-rays (secondary X-rays). The secondary X-ray being

characteristic of an element, the elemental composition of the material can be deduced. XRF measurements were carried out using the XRF Avaatech core scanner from Kiel University, with the following settings: 15 seconds measurement time in a 1.2x1 cm rectangle, operated at 10kV and 30kV.

XRF scanning with the XRF Avaatech core scanner need to be performed on a continuous and even surface. Core IOW225514 was heavily sampled prior to 158 cm during previous studies (Brückner, 2008) which prevented the possibility of XRF analyses on this section. Other shorter sections were not analysed for similar reasons on both core IOW225514 and IOW225517. Apart from these short sections, measurements were performed every centimeter, and yield relatively continuous, high resolution records of elemental composition.

3.4. BENTHIC FORAMINIFERA ANALYSES

3.4.1. Mg/Ca analyses and derived temperatures estimates

Paleotemperatures from the Skagerrak were reconstructed using Mg/Ca-thermometry. The incorporation of Mg into the foraminifera shell is expected to reflect the temperature of the ambient water (Nürnberg et al., 1996; Lea et al., 1999). Mg/Ca ratios in the carbonate tests of foraminifera vary exponentially with the temperature at which the test was formed but are species-dependent. Therefore species-dependent calibrations are used to deduce the water temperature from the composition of Mg of benthic and planktonic foraminifera shells. Nonetheless, carbon ion concentration at lower temperatures (<3-4ºC) and salinity might affect Mg incorporation in the foraminifera shells (e.g. Elderfield et al., 2006; Raitzsch et al., 2008), and need to be considered when using benthic foraminifera Mg/Ca as a paleothermometer.

Bulimina marginata, Melonis barleeanum and *Uvigerina mediterranea* are benthic foraminifera species that were abundant in the Skagerrak over the Holocene and seemed to be the least affected by carbonate dissolution and re-precipitation as inferred from microscopic and SEM investigations (Brückner and Mackensen, 2006). They were therefore species of preference for the reconstruction of paleotemperatures. However, upon initiation

of this study, the only robust calibration existing for Mg/Ca-derived temperatures for those species was for *Melonis barleeanus* (e.g. Kristjánsdóttir et al., 2007). Mono-specific samples of *M. barleeanus* (15-30 individuals) were therefore prepared for Mg/Ca analyses: they were weighed using an ultra-precision scale (Sartorius ME5 OCE) and gently crushed to reveal the inner chamber walls. Following the protocol originally developed by Martin and Lea (2002) and later adapted in the Kiel laboratory for Mg/Ca analyses, samples were successively cleaned with methanol to remove clays, with hydrazine, ammonium hydroxide and ammonium citrate to remove metal oxides (reduction step), and with sodium hydroxide to remove organic matter (oxidation step). Finally, dissolution and dilution were applied so that the final solution contains about 50 (25–75) $mg.L^{-1}$ of Ca. The samples were then analyzed on a radial viewing simultaneous ICP-AES (SPECTRO *Ciros*^{CCD} *SOP*) at the Institute for Geosciences, Kiel. Standards for foraminifera were used to calibrate the results afterwards, following de Villiers et al. (2002). Carbonate reference materials (ECRM 752–1, BAM RS3) were analyzed for monitoring analytical accuracy (Greaves et al., 2008). Replicate samples from anterior analyses were run; the typical external error is 0.1% rel. (1sigma) for Mg/Ca. Matrix effects caused by the easily ionized element Ca were investigated and found to be negligible. Samples with a recovery in Ca concentration of less than 20% were rejected. To prevent the use of samples potentially contaminated with metal oxides or ashes for example, Fe/Ca, Al/Ca and Mn/Ca ratios were additionally monitored, and samples showing a significant correlation between Fe/Ca, Al/Ca, Mn/Ca and Mg/Ca values were excluded (Schmidt et al., 2004).

From the available temperature calibrations for *M. barleeanus* Mg/Ca, the calibration developed by Kristjándóttir et al. (equation (1), Kristjánsdóttir et al., 2007) was selected because the derived temperature estimates with this equation best fit the instrumental temperatures of the deep Skagerrak (close to 6-7°C). The Mg/Ca ratios were converted into temperature using the following equation:

$$Mg/Ca = 0.658 \pm 0.07 * \exp(0.137 \pm 0.020 * T) \quad (1)$$

3.4.2. Stable isotope analyses and derived δw estimates

Benthic foraminifera $\delta^{18}O$ ratios are used in this study to trace variation in the water salinity. The incorporation of oxygen isotopes into foraminifera shells is dependent of both

temperature and salinity of the ambient water, and is specie-dependent. The relationship between $\delta^{18}O$ ratios of foraminifera shells and temperature and salinity of the ambient water is reflected in Shackelton's equation (Shackleton, 1974):

$$T(°C) = 16.9 – 4 * (\delta^{18}Oc – \delta w) \quad (2)$$

in which $\delta^{18}Oc$ is the isotope composition of calcite (measured), and δw the $\delta^{18}O$ ratio of marine waters. Therefore, using Mg/Ca-based temperatures and $\delta^{18}Oc$ after correction for vital effects, it is possible to reconstruct δw directly linked to salinity.

Mono-specific samples of benthic foraminifera (*M. barleeanus*, 7-15 individuals) were crushed into large fragments, stirred in ethanol in an ultrasonic bath for about 20 seconds, and then dried at 40 °C in a stove. Stable carbon and oxygen isotopes were measured with a Finnigan MAT 251 mass spectrometer at the Leibniz Laboratory, Kiel. The system is coupled online to the Carbo-Kiel Device (Type I) for automated CO_2 preparation from carbonate samples (for stable isotopic analyses). Samples were reacted by individual acid addition (99 % H3PO4 at 73 °C). Standard external error is better than ±0.07 ‰ for $\delta^{18}O$ and ±0.04 ‰ for $\delta^{13}C$ as documented by the performance of international and laboratory-internal carbonate standard materials.

Melonis barleeanus $\delta^{18}O$ was corrected for vital effect and a systematic deviation from equilibrium, following Kristjánsdóttir (2005) and Kristjánsdóttir et al. (2007):

$$\delta^{18}O \text{ (corrected)} = \delta^{18}O \text{ (calcite VPDB)} + 0.276 \quad (3)$$

In order to reconstruct salinity based on δw, different issues have to be taken into account. The $\delta^{18}O$ of the ocean varies depending of the amount of water stored in global ice caps. Therefore, an ice volume correction was applied, based on the calibration curve from Fairbanks (Fairbanks, 1989) for the period prior to 6000 years. Since the general isotopic composition of the world ocean has not changed significantly afterwards (about 0.05‰ according to Fairbanks,1989) no correction was done for this interval. Moreover, the slope of the relationship between the salt contained in the water and the δw differs on regional scales and $\delta^{18}O$-salinity mixing lines must be constructed regionally from modern values. Numerous $\delta^{18}O$-salinity mixing lines have been reconstructed for Skagerrak and surrounding areas and some could apply for Skagerrak deep waters (Mikalsen and Sejrup, 2000; Austin et

al., 2006; Harwood et al., 2008). After testing the different mixing lines (not presented here), we decided to directly reconstruct past δw of the deep Skagerrak waters to represent a qualitative salinity. To do so we used $\delta^{18}O_c$ (after correction for vital effects) and Mg/Ca-derived temperatures within Shackelton's equation (2). A quantitative reconstruction of salinity is not proposed here as the different mixing-lines give a wide range of results for the deep-water salinity. However, a qualitative reconstruction of salinity was sufficient for the purpose of this study.

3.5. TIME SERIES ANALYSES

3.5.1. Spectral analyses

Time series analyses were used in this study to identify low and high frequencies in the regional climate reconstructions. Spectral analyses were used to assess the power (proportional to amplitude squared) of periodic components at all possible frequencies. These periodic components are generally assumed to be sinusoidal, each with a certain amplitude and phase. The method applied in this study is described by Schulz and Mudelsee (2002), using the REDFIT software. Spectra of paleoclimatic time series frequently show a continuous decrease of spectral amplitude with increasing frequency (red-noise). Compared to the conventional spectral analysis, REDFIT removes the bias of the Fourier transform for unevenly spaced data (most paleoclimate time series) by correcting for the effect of correlation between Lomb– Scargle Fourier components. A critical false-alarm level of (1-1/n)*100% was calculated, following Thomson (1990).

3.5.2. Wavelet analyses

In addition, wavelet analysis were used to study time series at multiple scales simultaneously (i.e. at low and high frequencies), thus allowing us to detect potential non-stationary periodicities. With wavelet analyses, the size of the window of study is adjusted to fit the frequency analyzed, with wide windows at low frequencies and narrow windows at high frequencies. The number of oscillations in the window remains constant, while the so-called

mother wavelet is stretched or compressed to fit the window observed. Here we used the software PAST (Hammer et al., 2001) to perform a Morlet transform on our data sets which consists of a plane wave modulated by a Gaussian function, capturing oscillatory behavior as it will return information about both amplitude and phase. A significance level of p=0.005 was chosen.

MANUSCRIPTS

4. LINKING MARINE ARCHIVES FROM THE SKAGERRAK AND TERRESTRIAL ARCHIVES FROM CENTRAL NORTHERN EUROPE

This chapter corresponds to the following manuscript to be submitted: C. Butruille; W. Dörfler; C. van den Bogaard: Linking marine archives from the Skagerrak and terrestrial archives from central northern Europe.

The first author established the age model based on radiocarbon dating, tephra analyses and pollen analyses. Radiocarbon dates were measured at the Leibniz Institute (Kiel); pollen analyses were performed at the pollen laboratory in the Ur und Frühgeschichte Institut (UFG, Kiel). The first author counted the tephra particles and prepared the material to be analyzed at GEOMAR (Kiel). The analyses were performed by the first author with the help of C. van den Bogaard. Post-processing analyses for the tephra were done by C. van den Bogaard. Walter Dörfler and Christel van den Bogaard contributed to the discussion of this chapter.

4.1. ABSTRACT

In order to directly link marine climate records from the Skagerrak and terrestrial archaeological records from northern Germany and southern Scandinavia, we attempted to identify tephra layers from two marine cores from central Skagerrak (cores IOW225514 and IOW225517). Radiocarbon chronologies from both cores were completed with additionnal ^{14}C dates and XRF measurements performed on the cores allow us to perfectly match the chronology of both marine cores. The seek for tephra layers was unfruitful as the light ash particles did not settle in the Skagerrak into definite layers. However, remarkable events in pollen analyses carried out on core IOW225517 enable the direct comparison between terrestrial and marine archives and suggest that a reservoir age of 400 years for the Skagerrak during the mid- and late Holocene is a reasonable estimation.

4.2. INTRODUCTION

Regional climate reconstructions are important for archaeological studies in order to understand the potential response of human societies to climate change. Terrestrial reconstructions of climate change (based on pollen analyses for example), are often used in this context as they can be conducted on site or from local peats or lakes. They are however patchy, likely as a result of an overprint by human activity (e.g. pollen diagram recording deforestation) which differs on a local scale. Choosing marine archives to reconstruct climate variability can therefore be a better option at a time when human impact on the environment started to be noticeable. However, in order to test the robustness of marine chronologies depicting climate variables and to compare marine-based climate variability with archaeological and environmental reconstructions, refined age models of the marine cores are required.

In the frame of the Priority Program "*Early Monumentality and Social Differentiation, on the origin and development of Neolithic large-scale buildings and the emergence of early complex societies in Northern Central Europe*", we aim to assess the role of climate variability and its potential impact on Neolithic societies in Northern Central Europe. Terrestrial reconstructions of climate change exist for the Holocene in Northern Europe, such as reconstructions based on pollen records, but they are either potentially biased by human activities (Seppä and Birks, 2001), or are missing the short term variability needed to compare with archaeological studies. High resolution climate reconstructions from Skagerrak marine sediment cores, spanning the mid-and late Holocene, show short term variability of winter conditions over the North Sea and adjacent lands, associated with an atmospheric reorganization (Butruille et al., in press; Krossa et al., 2015). However, in order to improve the correlation with terrestrial archives, this also implies to better identify radiocarbon reservoir ages, since the magnitude in reservoir ages can change over time. For instance, the reservoir age of the Norwegian Sea varies between 400 to 1300 ^{14}C year during the last deglaciation while for the North Atlantic the calculated magnitude of reservoir ages varies between +1300 ^{14}C year and -1100 ^{14}C year (Björck et al., 2003).

In an attempt to improve the knowledge of Skagerrak reservoir age, estimated at 400 years for the recent time (Heier-Nielsen et al., 1995), we pursued to identify tephra layers in the marine cores, and potential remarkable predominant environmental changes using pollen analyses. We based our search for tephra layers in the marine cores on series of well-known tephra layers of Icelandic volcano eruptions, precisely dated in peat bogs (e.g. van den Bogaard and Schmincke, 2002; van den Bogaard et al., 2002; Hall and Pilcher, 2002; Wastegård, 2005) as well as in lacustrine series (e.g. Dörfler et al., 2012; Wastegård, 2005; Zillén et al., 2002) from Northern Europe. Remarkable environmental changes were sought in the pollen record, such as the increasing impact of human activity on its environment at the onset of agriculture in southern Scandinavia.

4.3. MATERIAL AND METHODS

Two marine sediment cores from different stations and water depth from the Skagerrak (core IOW225514,57°50.279' N, 8°42.226' E, 420m water depth, 405cm long and core IOW225517, 57°40.002' N, 7°05.465' E, 293 m water depth, 455cm long) were used in this study.

To improve the radiocarbon age models, and to test the legitimacy of the ^{14}C age model, questioned by Brückner and Mackensen in 2006, we added radiocarbon dates to the existing age models (Emeis et al., 2003) and performed XRF analyses to compare both marine cores. We made an attempt to identify tephra layers from Icelandic eruptions in the marine records, in particular Hekla 3 and 4 whose plumes are expected to extend over the Skagerrak region around 3000 and 4200 years BP respectively (e.g. overview of the tephra layers identified in Scandinavia by Wastegård, 2005; Dörfler et al., 2012) and were likely to be deposited in these marine deposits. Where concentration peaks of tephra particles were found in the cores, glass shards were concentrated and geochemical analyses were carried out on single shards, to enable a correlation to their possible source volcano. This ^{14}C independent chronostratigraphy would enable us to infer the variable reservoir age of the Skagerrak waters over time. We additionally used pollen analyses to detect potential remarkable environmental changes.

4.3.1. Radiocarbon dating

The age models from core IOW225514 and IOW225517 are based on radiocarbon dates of benthic foraminifera, previously published by Emeis et al. (2003) and expanded with two and five new radiocarbon dates, respectively.

In order to avoid problems of possible preferential re-sedimentation/reworking of individual foraminifera species, as known to be often the case in near-shore sediments to bias dating, samples of three species were used in this study for radiocarbon dating: *Hyalinea balthica, Bulimina marginata* and *Uvigerina mediterranea*. Two of the species are reported by Heier-Nielsen et al. (1995) to give reliable radiocarbon ages (*Uvigerina mediterranea* and *Bulimina marginata*). Core IOW225517 was adjusted in depth for sediment loss at the core top of the gravity core by comparison with multicore already by Emeis et al., (2003). Since the depth correction does not present a particular issue, and for clarity, we will use uncorrected depth in this thesis, unless mentionned otherwise. Dates were calibrated using the online software CALIB (Calib7.0,1986-2014: M. Stuiver and P. Reimer; http://calib.qub.ac.uk/calib/calib.html) and the Marine13 curve (Reimer et al., 2013). A standard reservoir age of 400 years is used, generally supported for the recent time in the marine area around the Danish coast (Heier-Nielsen et al., 1995) and generally used in the Skagerrak (e.g. Erbs-Hansen et al., 2011a; Erbs-Hansen et al., 2011b; Krossa et al., 2015). The radiocarbon reservoir age will be discuss later in this chapter.

4.3.2. XRF measurements

To further improve the age model and to accordingly choose outliers for the radiocarbon dates, we conducted XRF measurements on core IOW225514 and compared the results to the well-dated XRF records of core IOW225517. XRF measurements were carried out for both cores using the XRF Avaatech core scanner from Kiel University, with the following settings: 15 seconds measurement time in a 1.2x1 cm rectangle, operated at 10kV and 30kV. High-resolution geochemical records were produced and analyses of the results were performed following the recommendation from Weltje and Tjallingii (Weltje and Tjallingii, 2008).

XRF analyses have to be performed on a continuous and even surface to avoid artefacts during the measurements. Previous sampling on part of cores IOW225514 and IOW225517 prevented the possibility of XRF analyses on short sections, and on the uppermost part of core IOW225514 prior to 158 cm. Apart from these sections, measurements were performed every centimeter, and yield relatively continuous, high resolution records of elemental composition.

4.3.3. Tephra particles

Sections of the cores were first sampled according to the presumed position of known tephra layers following the ^{14}C chronology in order to test the latter. Sample groups of 3 to 5cm intervals were first analyzed to detect the presence of tephra particles (Figure 4.1). Where particles were found, sub-samples of 1cm were then taken and analyzed.

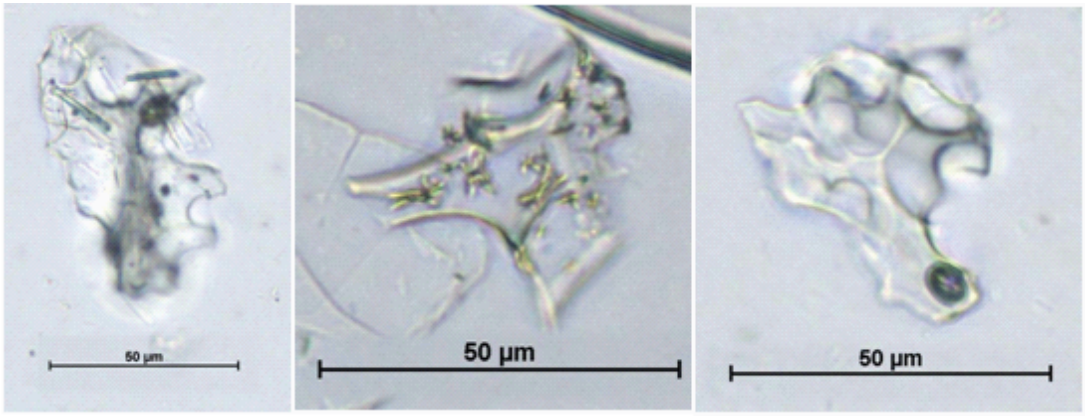

Figure 4.1: Tephra particles from core IOW225514. Particles in picture 1 and 2 contain microlites.

The samples were prepared using HCl (10%) to dissolve carbonates, NaOH (10%) to eliminate diatom silicates, and concentrated H_2SO_4 and HNO_3 to remove organic material. Samples were then sieved to isolate the 6 to 100 µm fraction, which we considered the range for main tephra particles. In order to separate tephra shards from heavier particles, a separation using heavy liquid with a density of 2,5 was practiced on this fraction. The lighter particles (including tephra) were then embedded in glycerin on micro slides, and tephra particles were counted under an optical microscope. Samples of 1cm, with significant numbers of

tephra particles were re-dissolved to be deposited on a special relief-free diamond-polished slide. A carbon coating was applied (using a high-vacuum carbon evaporator) to make the sample electrically conductive. The glass shards were then analyzed be electron microprobe at to the GEOMAR-Helmholtz-Zentrum für Ozeanforschung, in Kiel. Major elements, S, Cl and F, were analyzed with a JEOL JXA 8200 (X-ray) electron microprobe. Analytical conditions were those described in detail in Bogaard et al. 2014. This lab participated in the inter-comparison of tephrochronology laboratories confirming the high quality of the microprobe results (Kuehn et al., 2011). Near source material from the assumed source volcanoes was analyzed at the same time.

4.3.4. Pollen analyses

Pollen analyses were also performed to improve the age models. Twelve samples of about 1,5cm^3 from 1cm-thick slices were taken for pollen analyses in core IOW225517between 213 and 300cm. To facilitate calculation of pollen concentration, *Lycopodium* tablets were added at known concentration (Stockmarr, 1971). Samples were treated with KOH, HCL, HF and acetolysed following the standard pollen procedures (Moore et al., 1991). The coarse fraction was removed by initial sieving (120µm mesh size). Also particles under 6µm were removed by ultrasonic sieving. The residue was mounted in Glycerol and pollen grains were counted at x400 magnification. Phase contrast and x1000 magnification were used in case of critical grains. A pollen sum of about 180 grains per samples was generally achieved. Though too low for assessing environmental changes precisely, these samples are still sufficient enough to confidentially identify major features such as the start of cereal cultivation in north-western Europe.

4.4. RESULTS

4.4.1. Radiocarbon age models

Radiocarbon dates are listed in Table 4.1, with both the dates measured by Emeis et al. (2003) and new ones produced during this study. Core IOW225514 shows some apparent

age reversals, while the age-depth control of core IOW225517 appears more robust with steadily increasing ^{14}C ages (Table 4.1). Our choice for the outliers and reservoir age will be discussed. After removing the outliers, age-depth models were established using linear interpolation between each calibrated radiocarbon date.

Table 4.1: Radiocarbon dates of core IOW225514 and IOW225517. Calendars years are recalculated for all data using Calib7.0, with ΔR=0. The discarded dates are in grey.

Sample	Depth (cm)	^{14}C (yrs BP)	Median Cal. Age (yrs BP)	1σ range (yrs BP)	From	Fraction dated
Core IOW225514 (57T50.279N, 842.226'E), 420 m water depth						
KIA14028	10,5	810 $^{+}/_{-}$ 30	454	429-483	Emeis et al.	Mixed benthic foraminifera
KIA14029	105,5	1780 $^{+}/_{-}$ 35	1323	1284-1352	Emeis et al.	Mixed benthic foraminifera
KIA14030	105,5	1165 $^{+}/_{-}$ 30	707	670-731	Emeis et al.	Bivalve
KIA14031	135,5	2710 $^{+}/_{-}$ 35	2407	2342-2451	Emeis et al.	Mixed benthic foraminifera
KIA14032	135,5	1980 $^{+}/_{-}$ 30	1540	1502-1587	Emeis et al.	Bivalve
KIA14033	155,5	2755 $^{+}/_{-}$ 45	2481	2368-2545	Emeis et al.	Mixed benthic foraminifera
KIA43703	218,5	3545 $^{+}/_{-}$ 35	3431	3377-3472	This study	Mixed benthic foraminifera
KIA14034	250,5	4280 $^{+}/_{-}$ 45	4397	4337-4480	Emeis et al.	Mixed benthic foraminifera
KIA43704	300,5	4250 $^{+}/_{-}$ 60	4353	4257-4430	This study	Mixed benthic foraminifera
KIA14035	310,5	6400 $^{+}/_{-}$ 45	6876	6810-6939	Emeis et al.	Mixed benthic foraminifera
KIA14036	375,5	5680 $^{+}/_{-}$ 45	6086	6022-6160	Emeis et al.	Mixed benthic foraminifera
Core IOW225517 (57"40.002'N, 7'05.465'E), 293 m water depth						
KIA15116	40,5	2185 $^{+}/_{-}$ 30	1781	1728-1823	Emeis et al.	Mixed benthic foraminifera
KIA15117	80,5	3065 $^{+}/_{-}$ 35	2828	2772-2868	Emeis et al.	Mixed benthic foraminifera
KIA47690	95,5	3250 $^{+}/_{-}$ 60	3070	2980-3157	This study	Mixed benthic foraminifera
KIA47691	154,5	4150 $^{+}/_{-}$ 60	4222	4133-4322	This study	Mixed benthic foraminifera
KIA15118	160,5	4305 $^{+}/_{-}$ 30	4434	4396-4487	Emeis et al.	Mixed benthic foraminifera
KIA15119	190,5	4610 $^{+}/_{-}$ 30	4830	4800-4854	Emeis et al.	Mixed benthic foraminifera
KIA43705	211,5	5015 $^{+}/_{-}$ 30	5369	5314-5409	This study	Mixed benthic foraminifera
KIA15120	230,5	5165 $^{+}/_{-}$ 35	5528	5505-5571	Emeis et al.	Mixed benthic foraminifera
KIA47693	250,5	5295 $^{+}/_{-}$ 30	5647	5601-5681	This study	Mixed benthic foraminifera
KIA15121	310,5	6485 $^{+}/_{-}$ 40	6988	6919-7053	Emeis et al.	Mixed benthic foraminifera
KIA43706	362,5	7850 $^{+}/_{-}$ 40	8320	8282-8369	This study	Mixed benthic foraminifera
KIA15122	410,5	9825 $^{+}/_{-}$ 50	10751	10656-10831	Emeis et al.	Mixed benthic foraminifera

4.4.2. Identifying tephra layers

A wide array of identified eruption deposits mainly of Icelandic origin have been described in bogs and lakes sequences from all over Northern Europe (i.g. Dugmore et al., 1995; Pilcher and Hall, 1996; Hall and Pilcher, 2002; van den Bogaard and Schmincke, 2002; van den Bogaard et al., 2002; Zillén et al., 2002; Wastegård, 2005; Vorren et al., 2007; Dörfler et al., 2012). Hekla 3 (H3) and Hekla 4 (H4) are remarkable eruptions from Iceland that occurred during the mid-Holocene and tephra layers from these eruptions are widely found in Northern Europe. In the view of their geographical distribution, they are expected to be found in the Skagerrak.

Dörfler et al. (2012) give a time window between 3068-3120 cal. years BP (2σ) for H3 deposition and between 4266-4417 cal. years BP (2σ) for H4 deposition, using an age model based on radiocarbon dates improved by varve counting. We therefore based our search for H3 and H4 on those results. We used the radiocarbon age model of core IOW225514 and core IOW225517 to narrow down sections of the cores where deposition of tephra particles from Hekla 3 and 4 can be expected. With this, we expected to find H3 around 190 - 200 cm in core IOW225514 and 90 - 100 cm in core IOW225517 and H4 around 290 - 300 cm in core IOW225514 and 150 – 160 cm in core IOW225517.

We choose broader sections to sample and look for peaks of tephra particles. One concentration peak of tephra particles was found between 177 and 183 cm depth in core IOW225514 (Figure 4.2), reaching its maximum at 180 cm. We could not investigate lower down in the core IOW225514 for lack of material. In total, 18 geochemical measurements were made on 13 particles from the concentration peak at 180cm (hereafter called IOW14-180). Two maxima of tephra shards were found in core IOW225517 between 91 and 99, and 147 and 160 cm depth respectively (Figure 4.2). Eleven samples were analyzed for their geochemical composition (sample depths: 94, 95, 97, 98 cm and 150, 151, 152, 155, 156, 158 and 159 cm). Some of the samples contained particles of critical measurement size, which had to be discarded. We did not take into account measurements with a sum of total oxides below 90%. Samples IOW17-95 and IOW17-151 for example, yielded no satisfying results.

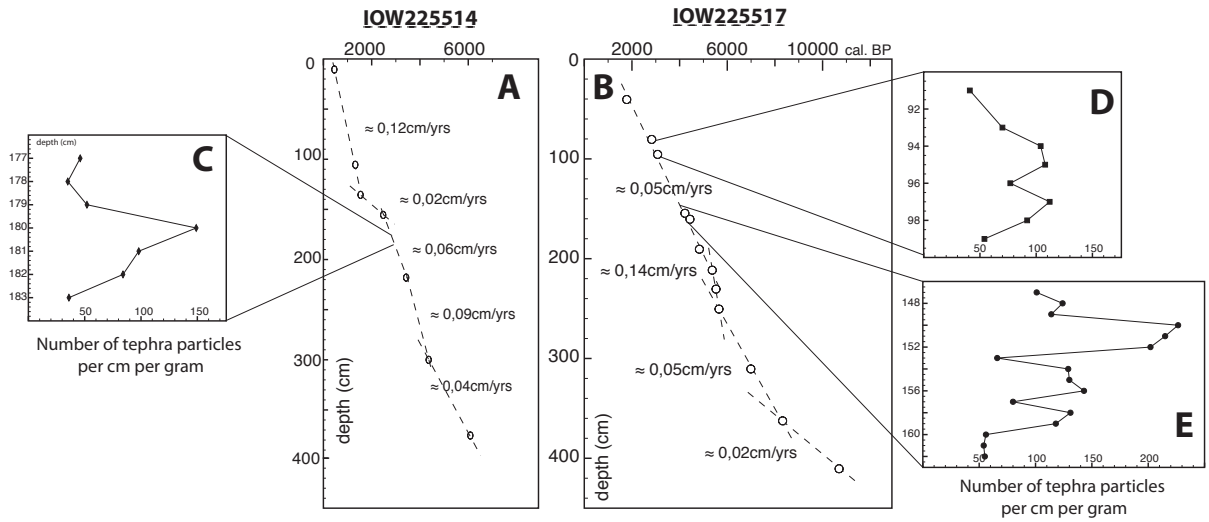

Figure 4.2: A-B: Age-depth relation of radiocarbon calibrated age model for core IOW225514 (A) and IOW225517 (B), and resulting sedimentation rates; C-D-E: Amount of particles in core IOW225514 between 177 and 183 cm (C) and in core IOW225517 between 91 and 99 cm (D) and between 148 and 162 cm (E).

4.4.3. Pollen analyses

Pollen analyses were performed in core IOW225517, between 213 and 300cm, which correspond to the period between 5380 and 6750 cal. years BP according to the ^{14}C-based age model of the marine core, with a standard reservoir age of 400 years (Figure 4.3). Various types of pollen were detected in the marine core, from arboreal to grasses and herbs types. As expected, a large number of *Pinus* pollen grains were detected in the marine core since they are airborne types and are known to be transported by the wind over large distance. They can therefore be directly transported on-site as well as by the water masses flowing in the Skagerrak.

Although not very remarkable, there is a constant decrease in arboreal pollen from the beginning of the sequence (95% at 6750 years BP) until the end (85% at 5380 years BP). The concentration of *Ulmus* pollen grains is increasing and decreasing between 6750 and 6600 years BP, with the highest values in the early part of the sequence. Between 5600 and 5500 years BP, *Ulmus* pollen grains appear to be lacking and then the concentration is steadily increasing again thereafter, until the end of the sequence (5380 years BP). A discrete appearance of both *Poaceae* and *Artemisia* pollen grains is visible at 6440 years BP, but a remarkable increase and thereafter constant content is visible at ca. 6100 and 5775 years BP

respectively. Cereal-type pollen appears also around 6200 years BP and *Plantago lanceolata* around 5900 years BP.

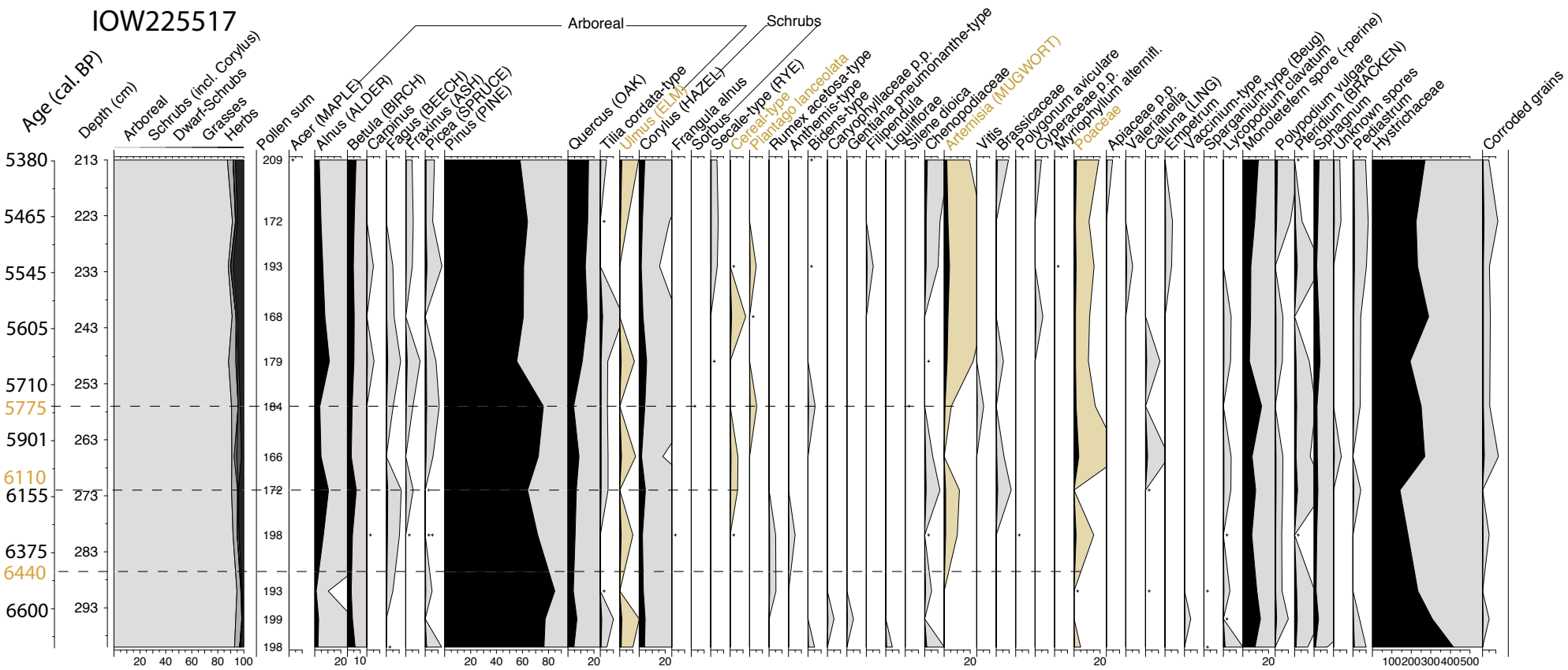

Figure 4.3: Pollen diagram from core IOW225517. The interesting taxa for the discussions are highlighted in light brown. Stippled-lines indicate the timing of major changes occuring in the pollen assemblage from core IOW225517 (see discussion in the text).

4.5. DISCUSSION

4.5.1. Outliers in the radiocarbon chronology

As shown in table 4.1, core IOW225514 possesses some age reversals, while the age-depth control of core IOW225517 appears more robust with steadily increasing ^{14}C ages. Some dates in the radiocarbon age model of core IOW225514 therefore need to be discarded as outliers, and the resulting age model needs to be tested. This can be done using XRF measurements conducted on cores IOW225514 and IOW225517. The XRF analyses do not cover prior to 158cm in core IOW225514 due to lack of material. Therefore, testing the radiocarbon age models using grahical comparison of the XRF records is only possible for the deeper/older part of the cores, namely for the dates prior to 158 cm – around 2500 cal. years BP. The general aim of this study is to establish high-resolution records of climate variability with robust chronologies during the end of the mid-Holocene and the beginning of the late Holocene, mostly between around 7000 and 3000 cal. years BP. The uncertainty of the radiocarbon age models prior to 3000 cal. years BP is therefore of minor importance for this study. For the youngest dates, prior to 158cm, we trusted in the age model established by Emeis and co-authors (2003).

For the deeper part of the core, where XRF analyses are available, we first decided to discard the eldest date when two dates were contradicting. The robustness of the resulting age model was then confirmed by curves of selected element ratios (here Ca/K) and graphically compare them (Figure 4.4).

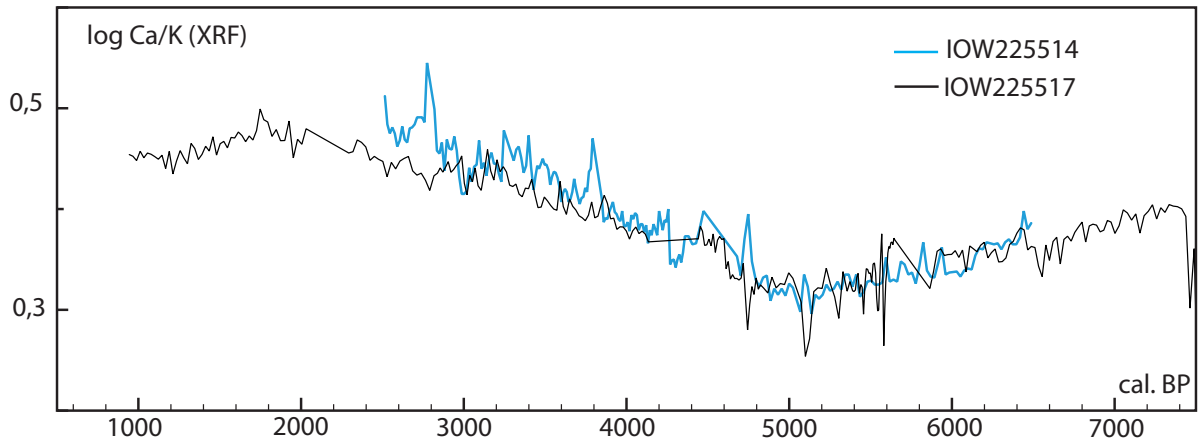

Figure 4.4: Ca/K ratio from XRF measurements on core IOW22514 (blue) and IOW225517. XRF measurements were performed on XRF Avaatech core scanner from Kiel University, with the following settings: 15 seconds measurement time in a 1.2x1 cm rectangle, operated at 10kV and 30kV. The comparison was used to confirm the choice of outliers in core IOW225514, without re-adjustment of the age models. The missing section prior to ≈2500 cal. years BP in core IOW225514 is due to lack of material for the measurement (see method section 4.3.2).

No adjustment of the age models was done based on the XRF records. The XRF curves were only used to determine how well both cores were correlated after the removing of the outliers. Using the age models presented in table 4.1 and figure 4.2, the match between the Ca/K ratio of both core is of R^2=0.83 (Figure 4.4). This excellent match supports the age models chosen. Other choice of outliers yields less significant matches between the Ca/K curves.

The presence of outlier might raise the question of the fiability of other records based on core IOW225514. However the good matching and the resemblance of Ca/K records from both cores, retrieved at different sites in the Skagerrak, therefore not subject to the same local disturbances, suggests that the outlier data are only due to punctual reworking, and not a continuous disturbance at the site of core IOW225514.

The good agreement of the radiocarbon age models of two Skagerrak cores and the well matched Ca/K XRF ratios, suggests a robust correlation between both marine cores, under similar oceanographic and climatic forcing prior to 2500 cal. years BP.

4.5.2. Radiocarbon reservoir ages

Although the good correlation between cores IOW225514 and IOW225517 suggests a robust choice of radiocarbon dates, issues concerning potential changes in the radiocarbon reservoir age during the mid- and late Holocene need to be addressed if we want to improve the linkage between ocean and terrestrial archives. For this purpose, we sought to identify tephra layers and remarkable features from pollen assemblages in the marine cores. The analyses were mainly performed on core IOW225517, which seems less affected by punctual reworking. We sought the remarkable events using the previously calculated age model with a radiocarbon reservoir age of 400 years, and the reservoir age is then tested.

Identifying tephra layers

There are three remarkable tephra layers identified in both cores: two in core IOW225517 peaking around 95 and 150 cm (corected depth) respectively, and one in core IOW225514 around 180 cm. In core IOW225517, the tephra layer found between 92 and 98 cm yields radiocarbon dates of 3020 and 3127 (±60) cal. years BP, according to the radiocarbon age model. The one between 150 and 160 cm in core IOW225517 yields radiocarbon dates of 4134 (±60) and 4434 (±30) cal. years BP. In core IOW225514, the tephra layer found between 179 and 182 cm yields radiocarbon dates of 2835 and 2881 (±45) cal. years BP.

Table 4.2 show the timing of the three different layers found in the Skagerrak cores and the coinciding well known eruptions found over Northern Europe.

Table 4.2: Tephra layers found in this study with their radiocarbon dates using a reservoir age of 400 years, and the potential corresponding erruptions identidied in archives over Northern Europe with their respective ages. Calibrated dates were calculated in this study using Calib6.0 with Intercal09, when un-calibrated dates were given in the articles.

Tephra layers from this study		**Identified erruptions in the litterature**			
Location	**Age cal. BP**	**Name of tephra**	**Found in**	**Age Cal. BP**	**References**
IOW17 92-98 cm	3020 – 3127 (±60)	Hekla 3	Lake Belau (N-Germany)	3068 - 3120 (2σ)	(Dörfler et al., 2012)
IOW17 155-160 cm	4134 (±60) – 4434 (±30)	Hekla 4	Lake Belau (N-Germany)	4266 - 4417 (2σ)	(Dörfler et al., 2012)
IOW14 179-182 cm	2835 – 2881 (±45)	”Microlite tephra” Barnsmore tephra	Bogs (Germany)	2614 - 2680	(van den Bogaard and Schmincke, 2002; van den Bogaard et al., 2002)
			Bogs (Ireland)	ca. 2650	(Hall and Pilcher, 2002)
		Gullbergby tephra	Gullbergbymo -ssen bog (Sweden)	ca. 2700	(Wastegård, 2005)

As seen in table 4.2, the tephra layer found between 92 and 98 cm in core IOW225517 could correspond to Hekla 3 (H3). Indeed, in lake Belau, the deposition of H3 dates between 3068 and 3120 cal. years BP (2σ) (Dörfler et al., 2012), while the layer in core IOW225517 dates between 3020 and 3127 (±60 years) which falls withing the error margins. Similarly, the tephra layer found between 150 and 160 cm in core IOW225517 could correspond to Hekla 4 (H4). In lake Belau, the deposition of H4 dates between 4266 and 4417 cal. years BP (2σ) (Dörfler et al., 2012), while the layer in core IOW225517 dates between 4134 (±60 years) and 4434 (±30 years) cal. years BP, which onset also falls withing the error margins. If geochemical analyses of the tephra particles found in the layers at 92-98 cm and 150-160 cm yield results corresponding to H3 and H4 respectively, this would suggest that a radiocarbon reservoir age of 400 years is reasonable for the Skagerrak at least around 4500 and 3100 cal. years BP.

In core IOW225514, the layer found does not coincide with the deposition of H3, but is closer in timing to the Gullbergby or the Barnsmore tephra (see table 4.2), however, with about 200 years difference.

However, all particles analysed from the different layers in the Skagerrak cores actually present traits of an evolved magma, ranging from rhyolite to andesite, and chemically close to Hekla 4 (Figure 4.5). This would be expected for the layer deposited between 150 and 160 cm in core IOW225517 but not for the others.

We therefore have to conclude that the different layers probably represent a repeated re-deposition of Hekla shards subsequent to the initial eruption and depostion. It is possible that the layer deposited between 150 and 160 cm in core IOW225517 around 4134 (±60 years) and 4434 (±30 years) cal. years BP correspond to the initial deposition, after the eruption Hekla 4. However, since we did not seek tephra layers deeper than 160 cm, it can only be assumed.

The iterated presence of shards with an Hekla 4 signature over the cores could be explained by the repeated suspension and deposition of the small tephra particles over time, and does not mean that the entire cores are completely reworked. Indeed, tephra particles are extremely light and trap air bubbles in their matrix, making them prone to long residence time in the water column prior to deposition, as well as to easy re-suspension once deposited. Similar re-deposition patterns have already been evidenced in other Atlantic cores (K.L. Knudsen, personal communication). Moreover, there could have been secondary influx of Hekla 4 particles into the Skagerrak from on-land. In lacustrine environments, bogs or different marine basins, the deposition of tephra particles in delimited layers is rendered possible by small catching basins or relatively stratified conditions preventing the re-suspension of deposited particles. However, the Skagerrak has a wide catching basin and is subject to an internal circulation that could explain the re-suspension of extremely light material, such as tephra particles, without necessarily reworking other coarser material.

In conclusion, it is not really possible to use tephrochronology in the Skagerrak, except by seeking the earliest deposition of a particular eruption. The tephra layer deposited around 150 and 160 cm in core IOW225517, could correspond to the original deposition of Hekla 4 particles after the eruption. This would mean that a radiocarbon reservoir age of 400 years is correct for the Skagerrak at least around 4500 cal. years BP. Further investigations are however needed.

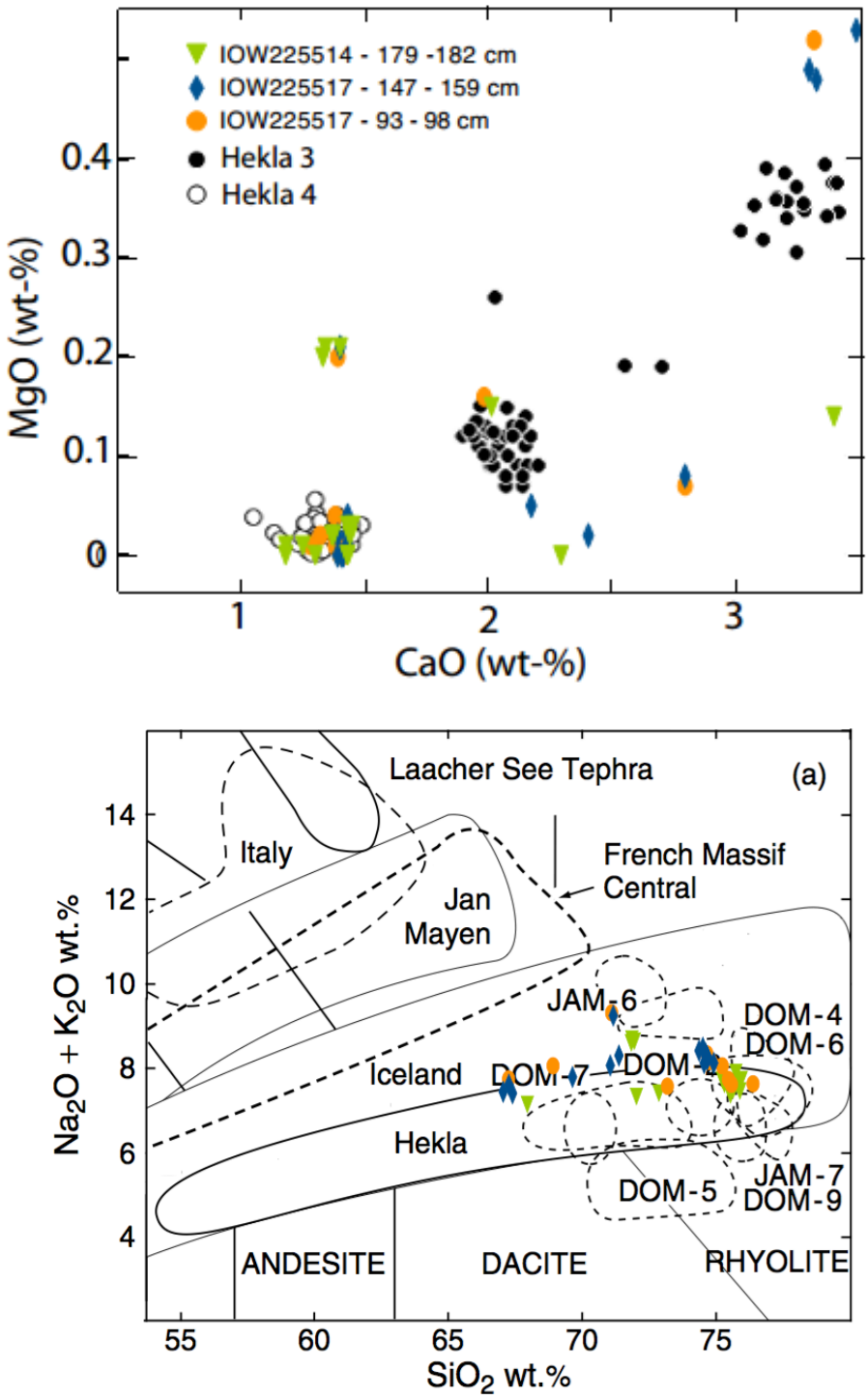

Figure 4.5: Geochemistry of the layers found in core IOW225517 and IOW225514 as compared to the composition of different eruptions.

Pollen assemblages

Another possibility we had to ascertain the radiocarbon reservoir age in Skagerrak, after the tephrochronology was not as successful as initially expected, was to seek remarkable events in pollen assemblages described from terrestrial archives, such as the “Elm decline” or the onset of agriculture in northern Europe. The "Elm decline" is a feature found in most of the pollen diagrams from northern Europe, reflecting the decline of the elm population probably due to the combined effect of the outbreak of a disease and the intensification of deforestation by human populations (e.g. Parker et al., 2002). This decline in the Elm population started between 6343 and 6307 cal. years BP and ended between 5420 and 5290 cal. years BP (Parker et al., 2002). Another remarkable event is the beginning of cereal cultivation in northern Europe, around 6250 to 5950 cal. years BP (e.g. Cappers and Raemaekers, 2008; Kirleis et al., 2011).

The Skagerrak is a depocenter basin surrounded by the Great Britain islands, Northern Germany, the Netherlands, Denmark, Norway and Sweden. It gathers waters from the different coastal regions, therefore variations in pollen assemblages recorded in the Skagerrak are expected to yield a supra-regional signal. Pollen grains can be directly brought by the wind (e.g. *Pinus*), but most of them are more likely transported via the different rivers into the sea or directly coming from coastal environments, and subsequently transpoted within the water masses that form the circulation in the North Sea and the Skagerrak. Since the core is located on the southern slope of the Skagerrak, it is doubtfull that pollen from southern Norway and Sweden can be transported by the water masses to the site, but we expect to find pollen from the southern coastal regions of the Skagerrak (Northern Germany, the Netherlands, Denmark) and from the Great Britain islands.

Although the “Elm decline” depicts only weakly in the diagram, a distinct increase in pollen grains from plants indicative of Neolithic human-activities (*Artemisia, Poaceae* and cereal-types) is evident starting at 6100 cal. BP in core IOW225517. *Poacea* and *Artemisia* are naturally found in various environments and as for example in coastal regions. However they are also used as an indicator of human activities such as the opening of the landscape. The significant increase pollen grains from those particular plants between 6100 and 5700 years BP in the Skagerrak is matching the increase in predominant human impact during the Neolithic in the region. Increased Poacea values are found for example in Northern Germany around 5600 cal. BP (Dörfler et al. 2012). Another specificity of the beginning of the Neolithic

in Northern Europe is the start of cereal cultivation. The presence of cereal-type pollen in Skagerrak core starting around 6100 years BP might appear early, since the adoption of intensive agricultural production in Northern Central Europe and Southern Scandinavia really started around 5750 cal. BP. However, cereal cultivation on a smaller scale in the region is assumed to have started around 6250 cal. BP (e.g. Cappers and Raemaekers, 2008; Müller, 2011; Kirleis et al. 2014). Cereal-type pollen grains could have reached the Skagerrak from the Netherland coastal region for instance, where early small-scale cereal cultivation is known (Cappers and Raemaekers, 2008).

There are in the end many uncertainties that prevent the narrowing down of the reservoir age using Skagerrak pollen assemblages. For instance, the broad origin of the pollen grains; the amount or the surface of cereal cultivated that would be sufficient enough to have cereal pollen grains transported into the Skagerrak; the time needed for the transport of those pollen grains from their origin to the marine basin; or the precise dating of the first cultivation of cereal in northern Europe. Remarkable events in pollen assemblages reconstructed from the Skagerrak can therefore not give a precise determination of Skagerrak radiocarbon reservoir age but suggest that a radiocarbon reservoir age of 400 (±150) years is conceivable around 6000 cal. years BP.

4.6. CONCLUSION

Here, we extended the existing radiocarbon age models for cores IOW225514 and IOW225517 with two and five additional dates respectively. The excellent match (R^2=0.83) after 2500 cal. years BP between the Ca/K XRF ratios from both cores suggest a robust choice for the radiocarbon outliers in core IOW225514 for that period.

The attempt to refine the reservoir age for the Skagerrak using tephra layers or pollen assemblages was not completely successful. The tephra layer deposited around 150 and 160 cm in core IOW225517 could correspond to the original deposition of Hekla 4, allowing for a radiocarbon reservoir age of 400 years for the Skagerrak around 4500 cal. years BP. However, we concluded that teprhochornology in the Skagerrak can only be pursued by seeking the original deposition of particular eruptions. The timing of remarkable events in pollen assemblages reconstructed from the Skagerrak does not contradict a reservoir age of

400 years for the period around 6000 cal. years BP, but cannot give a precision better than ±150 years.

In the end, the attempt to assess potential biases in radiocarbon dating of Skagerrak archives, although not completely successful, helped building age models as robust as possible for core IOW225514 and IOW225517. Using these age models, seasonal climate variability based on foraminifera stable isotopes and Mg/Ca records from the Skagerrak cores is reconstructed from the Mid- to the Late Holocene (Butruille et al., in press; chapter 5).

Acknowledgements: We thank Walter Dörfler and Christel van den Bogaard for their help with tephra and pollen analyses, and for the many discussions on the subject. Many thanks also to the persons who did the analyses of the pollen at the laboratory of the UFG and of the radiocarbon date at the Leibniz Institute for their help, and the Hiwis that helped me with the many cleaning procedures. The work has been founded by the DFG SPP 1400 project "Early Monumentality and Social Differentiation".

5. RECONSTRUCTION OF MID- TO LATE HOLOCENE WINTER TEMPERATURES IN THE SKAGERRAK REGION USING BENTHIC FORAMINIFERA MG/CA AND $\delta^{18}O$

This chapter corresponds to the following manuscript, in press in the Holocene:

C. Butruille; V.R. Krossa; C. Schwab; M. Weinelt; 2016. Reconstruction of mid- to late Holocene winter temperatures in the Skagerrak region using benthic foraminifera Mg/Ca and $\delta^{18}O$. The Holocene. DOI: 10.1177/0959683616652701

All material was prepared by the first author. The Mg/Ca analyses were performed at the Institut für Geowissenschaften (IFG, Kiel), stables isotope analyses at the Leibniz Institute (Kiel). The interpretation of the results and the discussion were done by the first author, with the contribution of all co-author.

5.1. ABSTRACT

Reconstruction of Skagerrak deep-water renewal is used to assess regional changes in winter thermal conditions over the past 6800 cal years BP. Changes in winter climate conditions from the Skagerrak region are in turn linked to shifts in Holocene large-scale atmospheric circulation patterns prevailing over northern Europe. We use *Melonis barleeanus* Mg/Ca and δ18O from a sediment core in the deep central Skagerrak to reconstruct temperature and salinity of Skagerrak deep-water, monitoring Skagerrak deep-water renewal. *Melonis barleeanus* Mg/Ca from a sediment core at shallower depth is used to reconstruct Skagerrak intermediate-water temperatures. Waters at intermediate depth consist of the Atlantic Inflow and possess an inter-annual thermal variability. Our results show that the Skagerrak deep-water experienced phases of particularly enhanced renewal during the mid-Holocene reflecting severe winter conditions, followed by a general shift to reduced renewal as a consequence of milder winter conditions over the North Sea around 3500 cal years BP. The late Holocene shift was most likely related to the onset of a regime with intensified winter westerly winds (Westerlies) directed towards northern Europe and an increased inflow of North Atlantic water into the Skagerrak/North Sea reflecting more maritime climate conditions. On millennial scale, cold phases in our deep-water records match with low winter precipitation phases in western Norway. They are associated with distinct increases in ice rafted debris (IRD) in North Atlantic sediments, suggesting that phases of iceberg discharge in the Atlantic were associated with cold and dry winter conditions over northern Europe. Interestingly, the cold event centered around 5900 cal years BP appears to be only associated with winter variability, while the following one at 4200 cal years BP is documented in our winter record, as well as in records related to warmer seasons.

5.2. INTRODUCTION

In northwestern Europe, climate conditions during the mid-Holocene period were characterized by generally high summer and mean annual temperatures, lower winter precipitation rates, and reduced or lacking continental glaciers (Bakke et al., 2008; Bjune et al., 2005; Davis et al., 2003; Seppä et al., 2009). The end of the mid-Holocene «climate optimum » occurred in Northwestern Europe around ~4200 cal years BP (Davis et al., 2003), followed by a transition towards the late Holocene that was associated by a decrease in summer and mean annual temperatures, increased winter precipitation, and re-advancing continental glaciers (Davis et al., 2003; Bjune et al., 2005; Bakke et al., 2008; Seppä et al., 2009).

Until now, most paleo-temperature reconstructions from northwestern Europe are based on biological proxies that are biased towards the warm season as productivity mainly occur during spring to autumn in the North Sea region and biological production during winter is normally low (Joint and Pomroy, 1993; Andersen et al., 2004; Moros et al., 2004; Blanz et al., 2005; Leduc et al., 2010; Liu et al., 2014). However, many pieces of evidence point to the stronger importance of winter variability compare to summer variability in Europe over the Holocene (O'Brien et al., 1995; Oppo et al., 2003; Mangini et al., 2005, 2007; Xoplaki et al., 2005). On the short-term, modern climate in Europe are governed by large-scale atmospheric pressure cells responsible for changes in strength and direction of North Atlantic wind fields (Hurrel et al., 2003). Because the vigor of the flow is related to meridional pressure gradient, the westerly winds (or Westerlies) carrying warmth and moisture across the North Atlantic are strongest during winter months. But, it is still under debate whether or not this phenomenon, also known as the North Atlantic Oscillation (NAO) has prevailed during the Holocene (Trouet et al., 2009, 2012; Spangehl et al., 2010; Moreno et al., 2012; Olsen et al., 2012; Jones et al., 2014). On millennial-scale, cold events during the early Holocene are expected to have mainly influenced winter variability as a result of high-latitudes remnant ice sheets and low winter insolation (Wanner and Bütikofer, 2008; Wanner et al., 2014, Denton et al., 2005). The mid-Holocene, however, starts with the melting of the last remnant Laurentide and Scandinavian ice sheets and a change in the insolation regime, and the contribution of winter variability to the annual variability during

the mid-Holocene might have change. Most reconstructions of northwestern European temperatures spanning the mid- to late Holocene are however biased towards the warm season, and therefore underestimate the potential temperature variability occurring during winter months.

The Skagerrak, deepest basin of the North Sea, is known to be sensitive to regional atmospheric circulation. In particular, Skagerrak deep-water renewal is influenced by changes in winter conditions over the North Sea for the last 1200 years at least (Ljøen and Svansson, 1972; Brückner and Mackensen, 2006). Here, we will argue that the renewal of the deep water has been occurring at least since the onset of the modern circulation about 8500 cal yrs BP, and has been reflecting winter atmospheric temperatures over the region. Subsequently, Skagerrak deep archives can be use to trace past winter variability since the onset of the modern circulation. Using *Melonis barleeanus* Mg/Ca and δ18O from a core in the deep basin (IOW225514), we have reconstructed deep-water temperature (DWT) and, therefore, traced winter atmospheric temperatures for the last 6800 cal. yr BP. We will also argue that intermediate-water temperature (IWT) reconstructions based on benthic foraminifera Mg/Ca from a core at intermediate depth (IOW225517) are biased toward the warm season.

To complete our understanding of past climate variability in the Skagerrak region, we compare our records with alkenonebased sea surface temperature (SST; Krossa, personal communication, 2015) from core IOW225514, interpreted as a proxy for regional mean annual temperatures. Changes in seasonal thermal gradient are discussed in terms of regional atmospheric circulation, as well as the seasonal imprint of mid- and late Holocene Bond events on northwestern Europe climate.

5.3. Regional setting

The Skagerrak is a marginal basin in the northern part of the North Sea and forms a connection between the North Atlantic and the Baltic Sea (Figure 5.1). It has a fjord-like shape with maximum depths of around 700 m at its north-eastern rim (Rodhe, 1987). A sill separates the Skagerrak from the rest of the North Sea at a water depth of ~270 m, and creates a boundary between upper and lower water masses (Ljøen and Svansson, 1972; Figure 5.1).

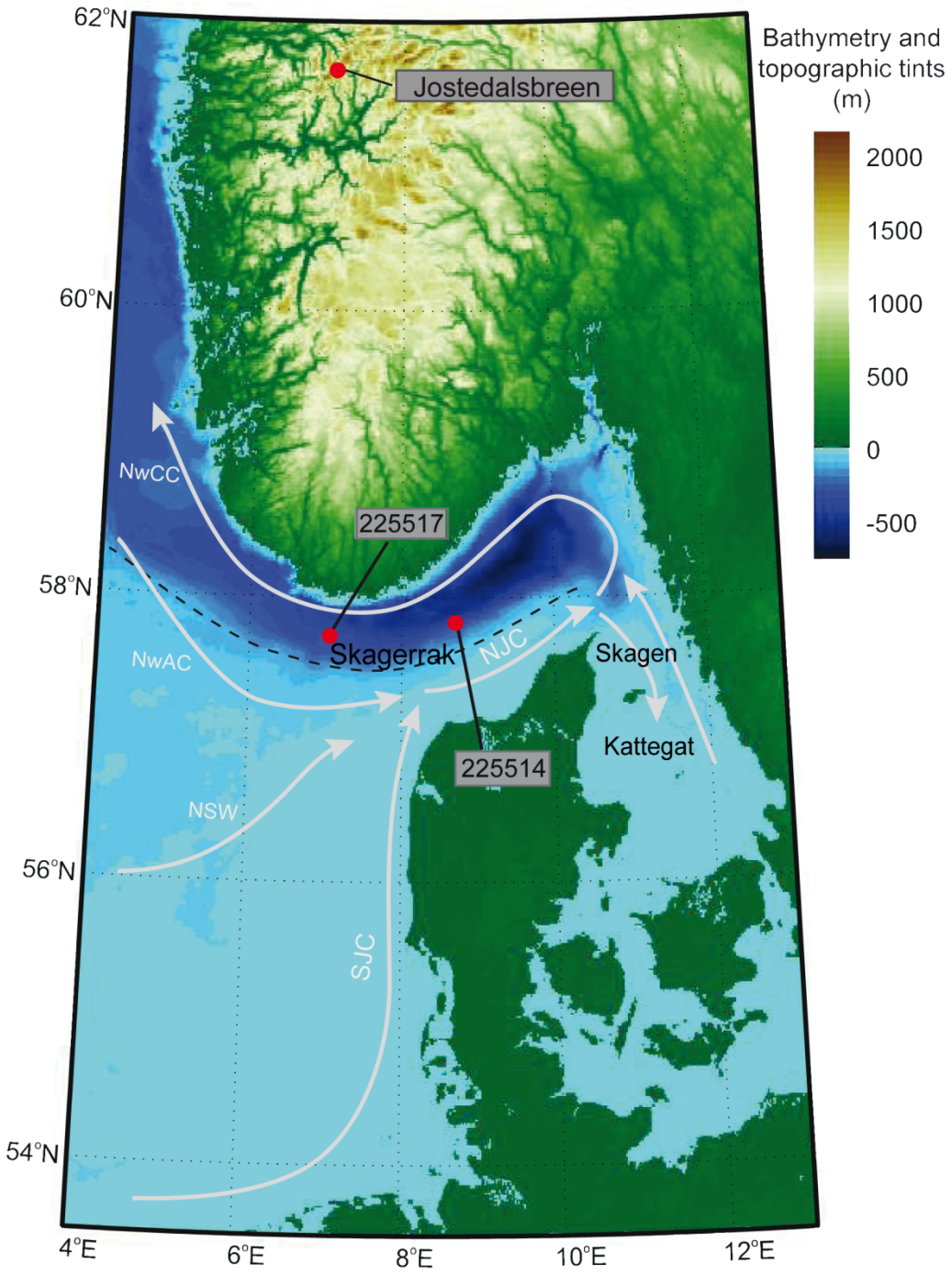

Figure 5.1: General circulation and bathymetry in the eastern North Sea and Skagerrak-Kattegat. The cores used in this study are marked with dots. The main transport is located around 200 to 300m water-depth (Svansson, 1975; Rodhe, 1987).

The modern circulation pattern has been established around 8500 cal years BP as a consequence of the opening of the English Channel and the Danish Strait (Gyllencreutz et al., 2005). It is governed by the inflow of North Atlantic water and the outflow of Baltic Sea water (Svansson, 1975; Rodhe, 1987; Otto et al., 1990). North Atlantic water enters the

Skagerrak from the North-West, forming the Norwegian Atlantic Current and the central North Sea water, and from the South-West through the English Channel, forming the South Jutland Current (Figure 5.1). Those currents subsequently mix to form the North Jutland Current. As this water mass passes Skagen thereby entering the Skagerrak/Kattegat border, it mixes with fresher and colder Baltic Sea water. It subsequently slows down, allowing fine-grained sediments to accumulate at high rates in the central and northeastern parts of the Skagerrak (Rodhe and Holt, 1996). The resulting water mass exits the Skagerrak flowing along the Norwegian coast as the Norwegian Coastal Current, forming an anti-clockwise circulation pattern (Figure 5.1).

The surface layer is permanently stratified mainly due to the outflow of fresher Baltic Sea water, in addition to a thermal stratification component during summer (Otto et al., 1990). Throughout the complete annual cycle, the temperatures in the surface waters range from 4 to 15ºC (Locarnini et al., 2010). The intermediate water in the western Skagerrak is strongly influenced by the inflow of a branch of North Atlantic water. The temperature ranges between 4-8ºC, showing intra-annual variations in temperature (Ljøen and Svansson, 1972; Figure 5.2). Finally, the deep waters are dissociated to the main circulation process. They stay stagnant for a few years until they are replaced by cold and dense water coming from the central North Sea. This process is known as Skagerrak deep-water renewal and is strongly driven by temperature and to a lesser extent by salinity of the central North Sea surface water mass (Ljøen and Svansson, 1972). The deep-water temperatures do not possess a intra-annual variability but present a multi-annual variability with temperatures ranging between 4 and 8ºC (Ljøen and Svansson, 1972; Figure 5.2).

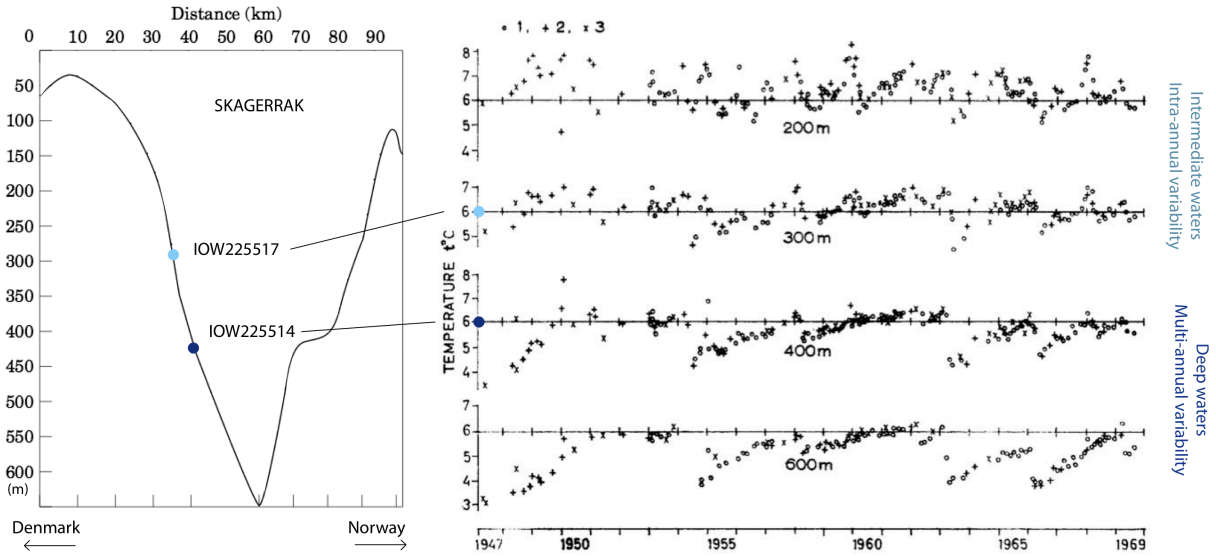

Figure 5.2: Evolution of instrumental temperatures at different depths in the Skagerrak basin, depicting the difference between the intermediate and the deep-waters annual variability between 1947 and 1969 CE (from Ljøen and Svansson, 1972). The cores used in this study are represented at their respective depth on a profile of the Skagerrak basin.

5.3.1. Deep-water renewal and regional climate

During severe winters, slow currents and strong vertical mixing of the water mass of the central North Sea enable cooling of the whole water body in this part of the North Sea. The resulting cold and therefore dense water mass subsequently cascades down into the Skagerrak basin and replaces less dense waters prevailing in the deep basin. Trapped in the deeper basins for several years, the deep-water mass preserves the winter temperature signal (Ljøen and Svansson, 1972). The present-day process of deep-water renewal is characterized by a cooling phase of a few months in the deep-water, followed by a period of a slight temperature increase that might last a few years. Temperature variability of the deep waters has been positively correlated to winter atmospheric temperatures over the region. It has been documented for the period between 1947 and 1969 (Ljøen and Svansson, 1972), extended here until 2010 (Figure 5.3), and for the last 1200 years (Brückner and Mackensen, 2006). Finally, the frequency of the deep-water renewal has been positively correlated to the phases of the North Atlantic Oscillation (NAO) for the last decades (Brückner and Mackensen, 2006; Hagberg and Tunberg, 2000; Tunberg and Nelson, 1998).

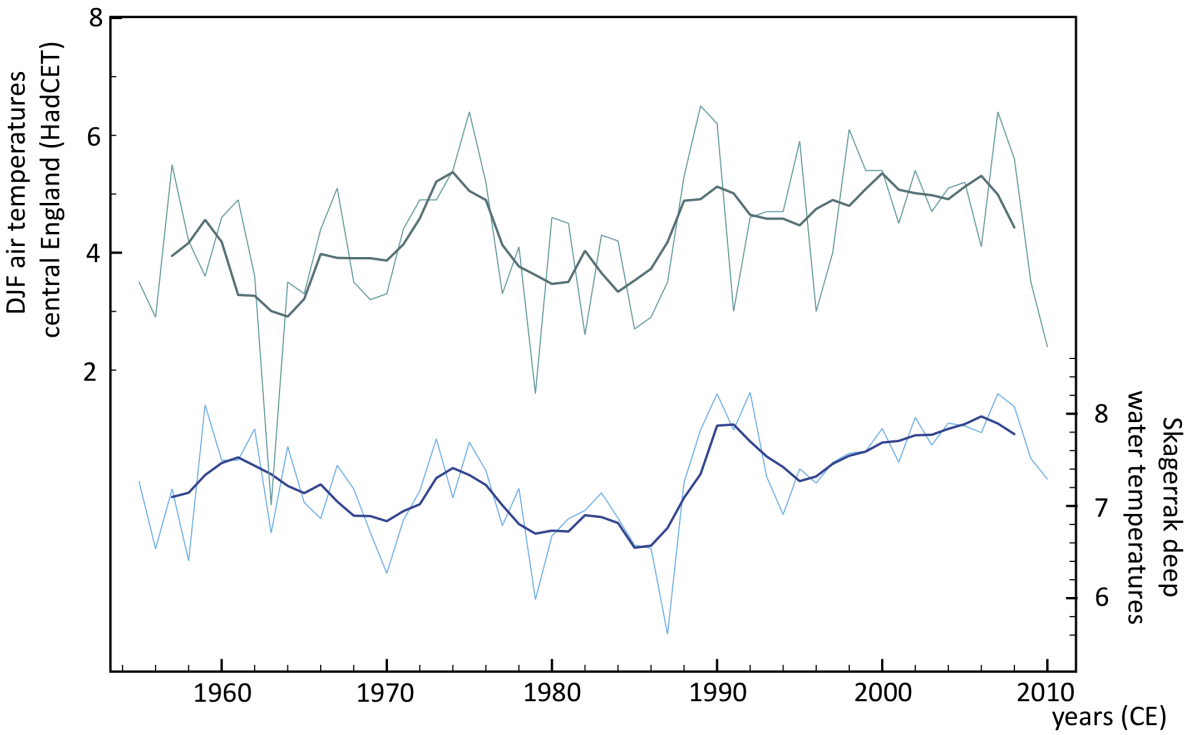

Figure 5.3: Winter air temperatures from central England (mean of December, January and February, from the HadCET dataset) and Skagerrak deep-water temperatures (bottle data from the Ocean Data View, measurements below 400m) between 1950 and 1960 CE. The thicker lines represent a five years average.

Today, winter climate conditions affecting the North Sea are largely governed by large-scaled atmospheric pressure systems that drive variations in strength and direction of wind fields. This phenomenon of atmospheric circulation is also referred to as the NAO (Hurrell, 1995; Hurrell et al., 2003). The corresponding index, which describes the winter NAO pattern, is defined by differences in atmospheric pressure cells over Iceland and the Azores (NAO index) (Hurrell, 1995). During periods of a positive NAO index, the difference between the pressure cells is high, leading to westerly winds (Westerlies) shifted towards Northern Europe. The Westerlies bring mild and moist air masses from the North Atlantic over Norther Europe (Hurrell, 1995; Hurrell et al., 2003). During periods of a negative winter NAO index, the difference is low and consequently, Westerlies are weaker, preventing mild and moist air masses to influence the climate in northwestern Europe. A positive NAO is associated with moist and mild winters over Northern Europe, while, a negative NAO is associated with severe and dry winters. The winter NAO index varies from year to year. However, it also exhibits the tendency to remain on one phase for several years (Hurrell, 1995).

5.4. MATERIALS AND METHODS

5.4.1. Sample material

We used two gravity-cores from the central Skagerrak (Figure 1, Table 1) to reconstruct Skagerrak DWT and IWT. Gravity-core IOW225514 is located at 420 m water depth, thus in the range of the deep-waters. IOW225517 was cored around sill depth, at 293 m water depth, consequently in the range of the intermediate waters. Both gravity-cores consist of homogeneous olive-green silty clay, and an array of pale-oceanographic data is available for both stations on these specific cores (Brückner and Mackensen, 2006, 2008; Emeis et al., 2003; Hass, 1996; Krossa et al., 2015). We sampled material of 1 cm slices and wet sieved the sediment fractions between 125 µm and 2 mm. Benthic foraminifera were obtained from the >150 µm coarse fraction, and mono-specific samples (*Melonis barleeanus*) were prepared for δ18O and Mg/Ca analyses (see below). We chose *M. barleeanus* to reconstruct past changes in Skagerrak deep-water conditions, as it is abundant continuously during the Holocene in the Skagerrak and is one of the species reported to be only slightly affected by carbonate dissolution and re-precipitation (Brückner, 2008)..

5.4.2. Mg/Ca analyses and temperature reconstructions

Ten to twenty-five specimens of *Melonis barleeanus* were weighed using an ultra-precision scale (Sartorius ME5 OCE) and gently crushed to reveal the inner chamber walls. Subsequently, they were prepared for Mg/Ca analyses following the protocol originally developed by Martin and Lea (2002). The samples were successively cleaned with methanol to remove clays and with hydrazine, ammonium hydroxide, and ammonium citrate to remove metal oxides (reduction step), and with sodium hydroxide to remove organic matter (oxidation step). Finally, the samples were dissolved and diluted in order to achieve a final solution containing about 50 (25–75) mg.L−1 of Ca.

The samples were analysed on a radial viewing simultaneous ICP-AES (SPECTRO CirosCCD SOP) at the Institute for Geosciences, Kiel. Standards for foraminifera were used to calibrate the results, following de Villiers et al. (2002). Carbonate reference materials (ECRM 752–1, BAM RS3) were analysed for monitoring analytical accuracy (Greaves et al., 2008). The

typical external error is 0.1% rel. (1sigma) for Mg/Ca. According to replicate samples, the standard deviation is about 0.1 mmol.mol−1 Mg/Ca for *M. barleeanus*. Samples with a recovery in Ca concentration of less than 20% were rejected. To check for potential contamination from metal oxides or ashes, trace elements were additionally monitored, and samples showing a significant correlation between Fe/Ca, Al/Ca, Mn/Ca and Mg/Ca values were excluded (Schmidt et al., 2004).

Temperatures were derived from Mg/Ca ratios using the following calibration for *M. barleeanus* (Kristjánsdóttir et al., 2007):

$Mg/Ca = (0.658 \pm 0.07) * \exp((0.137 \pm 0.020) *T)$

5.4.3. Mg/Ca as a deep-water temperature proxy in the Skagerrak

Foraminifera Mg/Ca is largely used in paleoceanography as a proxy for reconstructing past temperatures. However, studies argue that carbon ion concentration at lower temperatures (<3-4ºC) and also salinity might affect Mg incorporation in the foraminifera shells (Elderfield et al., 2006; Raitzsch et al., 2008), consequently influencing the temperature reconstructions. Both modern observations (Ljøen and Svansson, 1972) and temperature reconstructions over the past 1200 cal years BP (Brückner and Mackensen, 2006) show that Skagerrak deep-water temperatures are generally higher than 3-4ºC. Additionally, as deep-water masses in the Skagerrak originate from North Atlantic waters and are not affected by fresher Baltic Sea water (Ljøen and Svansson, 1972), the deep-water salinity does not vary enough to influence the Mg incorporation. Therefore, we do not expect the carbonate ion or salinity to bias the Mg incorporation and subsequently our Mg/Ca-derived temperature record. Supportingly, benthic foraminifera Mg/Ca has also been successfully applied to reconstruct past deep-water temperatures in the northeastern Skagerrak (D. R. Erbs-Hansen et al., 2011).

5.4.4. $\delta^{18}O$ analyses

Four to fifteen individuals of *M. barleeanus* were crushed into large fragments, stirred in ethanol in an ultrasonic bath for about 20s, and then dried at 40°C in a stove. We measured

stable carbon and oxygen isotopes using a Finnigan MAT 251 mass spectrometer at the Leibniz Laboratory at the University of Kiel. The system is coupled online to the Carbo-Kiel Device (Type I) for automated CO2 preparation from carbonate samples (for stable isotopic analyses). Samples were reacted by individual acid addition (99% H3PO4 at 73°C). Standard external error is lower than ±0.07‰, as documented by the performance of international and laboratory-internal carbonate standard materials.

Values were corrected for vital effect of 0.276 on *M. barleeanus* δ18O values (Kristjánsdóttir et al., 2007). After correction of the vital effect, δ18O of calcite in the shells of benthic foraminifera can be used to reconstruct past changes in temperature when knowing the isotopic composition of water (δw) (Shackleton, 1974):

T (°C) = 16.9 – 4 (δ 18Oc – δ w)

Consequently, as we know the temperature reconstructed using Mg/Ca (see above), we can infer past changes in δw, which is dependent on the salinity of the water mass and also ice volume. Prior to 6000 cal years BP, $\delta^{18}O$ values were corrected for an ice volume effect of 0.11‰ per 10 m sea-level change (Fairbanks, 1989). After 6000 cal years BP, the general isotopic composition of the world ocean did not changed significantly (Fairbanks, 1989), and therefore no correction was applied. Therefore, after correction for ice volume effect, past changes in salinity in the Skagerrak can be estimated.

In the Skagerrak, Brückner and Mackensen (2006) reconstructed past deep-water temperatures using a mixing-line from Sognefjorden in western Norway (Mikalsen and Sejrup, 2000). They found no significant changes in salinity and consequently δw over the past 1200 cal years BP. However, when applying Mikalsen and Sejrup (2000) mixing-line or the more recently proposed Skagerrak mixing-lines (Austin et al., 2006; Harwood et al., 2008), we document a relationship of salinity and δw, which results in a much larger influence of salinity on the δ18Oc signal. Additionally, as the Skagerrak mixing-lines were proposed for a present-day situation of deep-water renewal, it is possible that under different deep-water renewal conditions -for instance no renewal at all for a period longer than recorded nowadays- the relationship between the salinity and the δw was different in the past ~6800 cal years BP. To avoid complications regarding mixing-lines, we used paired Mg/Ca and δ18O from benthic foraminifera to reconstruct δw, thereby using δw only to infer

qualitative changes in past salinity. Plus, δ18O and δw will only be used in this study in parallel to deep-water temperatures, to test the robustness of the latter.

5.4.5. Age model

The gravity-cores were dated using the AMS14C method on specific foraminifera species (Table I). The 14C data, including those previously published by Emeis et al. (2003) were calibrated using the online software CALIB (Calib7.0, Ó1986-2014: M. Stuiver and P. Reimer; http://calib.qub.ac.uk/calib/calib.html) and the Marine13 curve (Reimer et al., 2013), with a standard reservoir age of 400 years as generally used in the Skagerrak (e.g. Erbs-Hansen et al., 2011; Erbs-Hansen et al., 2011; Krossa et al., 2015). Our results are presented on a calibrated age scale before Present (cal years BP, AD 1950). Age-depth models were established using linear interpolation between each calibrated radiocarbon date.

No inverted ages occur for gravity-core IOW225517, while four inverted dates are found for core IOW225514 (Figure 4), which can either be explained by bioturbation, re-deposition, or changes in habitat depth of benthic foraminifera.

High resolution geochemical records were produced using XRF, and analysed of the results were performed following the recommendation from Weltje and Tjallingii (Weltje and Tjallingii, 2008). Using XRF Ca/Al records of both gravity-cores, we were able to find a good correlation (0.8) between both records. This was done by considering the 14C too old as outlier when an inversion was occurring (Figure 4), which suggests that outlier dates in core IOW225514 are due to punctual reworking such as bioturbation or re-deposition. For the youngest dates, not covered by the XRF records, we used the date chosen by Emeis and co-authors (2003). After removing the outliers in core IOW225514, the good agreement between both XRF curves from both cores (0.8) suggest that the age models are robust. Additional comparisons with regional terrestrial records were done using for instance pollen data (not presented here), and showed that the chronostratigraphy of both cores IOW225514 and IOW225517 were robust (Butruille, in preparation).

Table 5.1: Radiocarbon dates of core IOW225514 and IOW225517. The material dated is mixed benthic foraminifera except for samples KIA14030 and KIA14032 where it is bivalves. Calendars years are recalculated for all data using Calib7.0, with Marine13. The discarded dates are in grey.

Core IOW225514 (57"50.279'N, 842.226'E), 420 m water depth					
Sample	**Depth (cm)**	**^{14}C (years BP)**	**Median Cal. Age (cal. years BP)**	**1σ range (cal. years BP)**	**From**
KIA14028	10,5	810±30	454	429-483	Emeis et al.
KIA14029	105,5	1780±35	1323	1284-1352	Emeis et al.
KIA14030	105,5	1165±30	707	670-731	Emeis et al.
KIA14031	135,5	2710±35	2407	2342-2451	Emeis et al.
KIA14032	135,5	1980±30	1540	1502-1587	Emeis et al.
KIA14033	155,5	2755±45	2481	2368-2545	Emeis et al.
KIA43703	218,5	3545±35	3431	3377-3472	This study
KIA14034	250,5	4280±45	4397	4337-4480	Emeis et al.
KIA43704	300,5	4250±60	4353	4257-4430	This study
KIA14035	310,5	6400±45	6876	6810-6939	Emeis et al.
KIA14036	375,5	5680±45	6086	6022-6160	Emeis et al.

Core IOW225517 (57"40.002'N, 7'05.465'E), 293 m water depth					
Sample	**Depth (cm)**	**^{14}C (years BP)**	**Median Cal. Age (cal. years BP)**	**1σ range (cal. years BP)**	**From**
KIA15116	40,5	2185±30	1781	1728-1823	Emeis et al.
KIA15117	80,5	3065±35	2828	2772-2868	Emeis et al.
KIA47690	95,5	3250±60	3070	2980-3157	This study
KIA47691	154,5	4150±60	4222	4133-4322	This study
KIA15118	160,5	4305±30	4434	4396-4487	Emeis et al.
KIA15119	190,5	4610±30	4830	4800-4854	Emeis et al.
KIA43705	211,5	5015±30	5369	5314-5409	This study
KIA15120	230,5	5165±35	5528	5505-5571	Emeis et al.
KIA47693	250,5	5295±30	5647	5601-5681	This study
KIA15121	310,5	6485±40	6988	6919-7053	Emeis et al.
KIA43706	362,5	7850±40	8320	8282-8369	This study
KIA15122	410,5	9825±50	10751	10656-10831	Emeis et al.

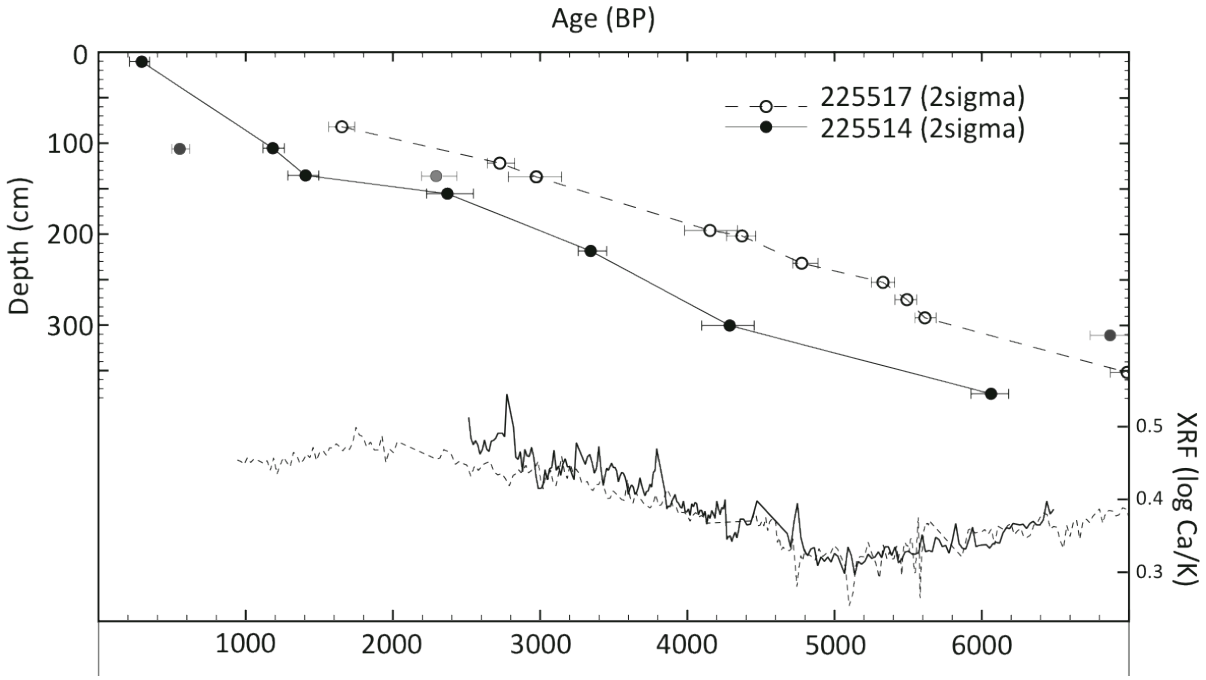

Figure 5.4: Top: Age-depth relation of radiocarbon calibrated age model for core IOW225514 and IOW225517. Bottom: Ca/K ratio from XRF measurements for core IOW225514 and IOW225517. XRF measurements were performed on XRF Avaatech core scanner from Kiel University, with the following settings: 15 seconds measurement time in a 1.2x1 cm rectangle, operated at 10kV and 30kV.

5.5. RESULTS

Mg/Ca-based temperatures, and δ18O from core IOW225514 (420 m water depth) are used in this study to reconstruct Skagerrak deep-water temperatures (DWT) and deep-water δw, respectively. Mg/Ca-based temperatures from core IOW225517 (290 m water depth) is used in to reconstruct intermediate-water temperatures (IWT). The records cover the period between 6800 and 700 cal years BP.

Over this period, the general trends in DWT and δw show an increase (+1°C and + 0.3o/oo respectively). In contrast, IWT seem to have had higher values in the early part of the record compared to the latest part, although the resolution is too low after 4200 cal years BP to confidently document a trend.

Several distinct shifts superimposed on the general trend are observed in the DWT and δw records (Figure 5). The interval between 6800 and 3500 cal years BP is characterized by strong variability in the DWT with high frequency and amplitude (+/- 4.7°C). The two coldest episods of deep waters are found during that interval, between 6300 and 5700 cal years BP

(minimum of 2.8°C), and 4300 and 3500 cal years BP (minimum of 4°C). Episods of low δw occur at the same time.

A strong increase in DWT (+~1.5ºC) and δw (+ 1.3o/oo) occurs at 3500 cal years BP, followed by a period of prevailing high DWT and δw and lower amplitude in DWT variability (+/- 2.9°C) until the end of the record at 700 cal years BP. During the late Holocene, we observe periods of decreased deep-water temperatures and in particular δw, centered around 2800 and 1400 cal years BP respectively, but of less amplitude than prior events.

Bewteen 6400 and 4300-4200 cal years BP, the IWT varied around 6.8°C in average, with high frequency and amplitude variability where values range between 4.6 and 10.2°C. Between 4300-4200 and 3500 cal years BP the IWT decreased to reach around 5.5°C. The IWT has low resolution afterwards.

Towards the end of the deep-water records, at 1500 cal years BP, a rapid increase in temperatures of ~2°C within a few centuries is documented, that culminated around 1200 cal years BP, followed by a rapid decrease of about the same amplitude over a few centuries.

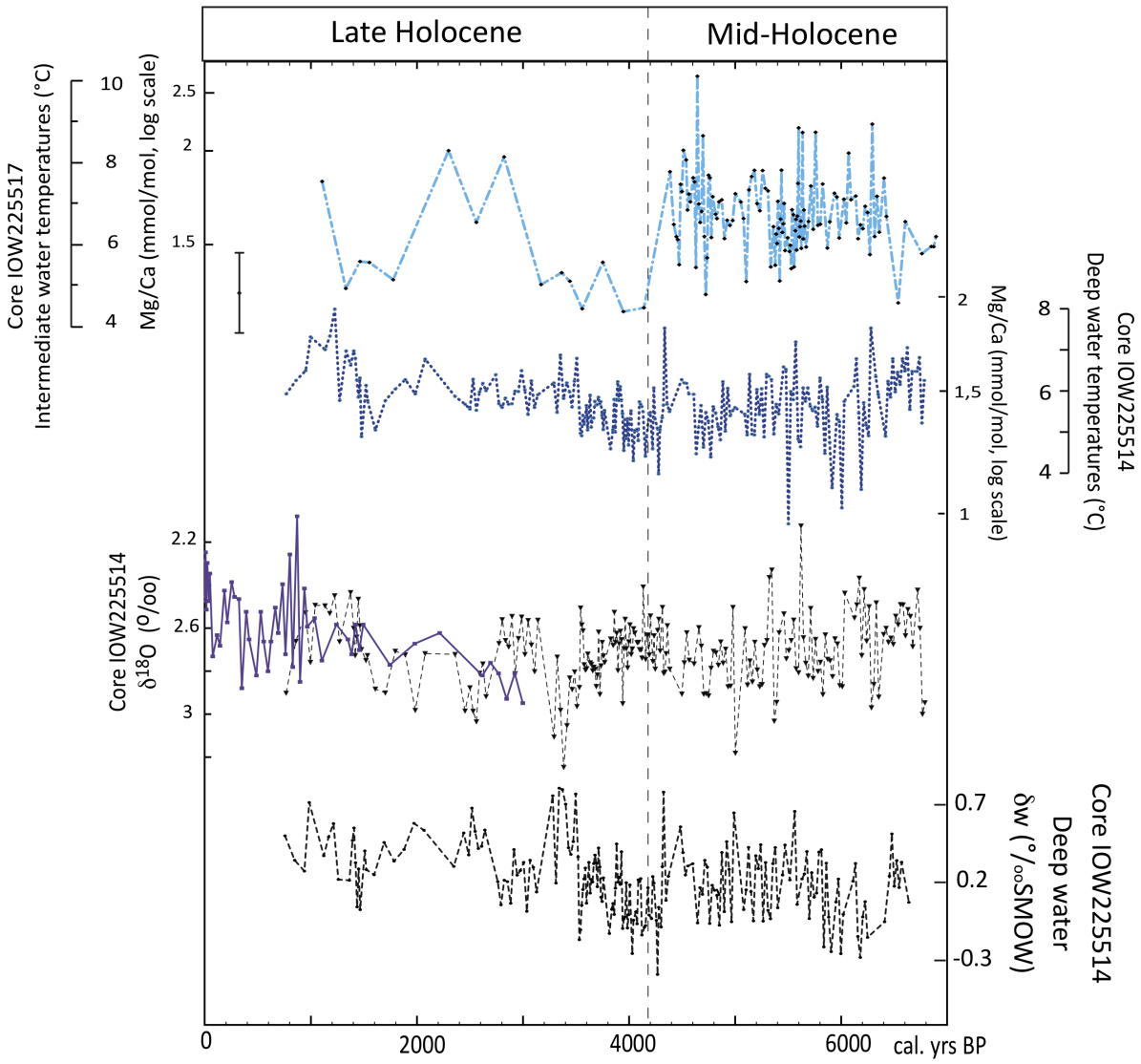

Figure 5.5: *M. barleeanus* Mg/Ca on intermediate (IOW225517) and deep (IOW225514) cores and *M. barleeanus* $\delta^{18}O$ of the deep core, and derived temperature reconstructions. The error bar indicates analytical error for Mg/Ca reconstructions. The stable isotope record is corrected for vital effect and ice volume (see references in the methods).

5.6. Discussion

5.6.1. Approach to assess deep- and intermediate-water temperature signals in the Skagerrak

In the North Sea region, the main planktonic blooms occurs during spring to autumn (Blanz et al., 2005; Joint and Pomroy, 1993), resulting in organic flux to the sea floor with a strong seasonality influence on the growth of benthic foraminifera (Gooday, 2003).

Temperature measurements from the surface and intermediate water (up to 350m) in the Skagerrak reflect seasonal-like atmospheric temperature variability (Ljøen and Svansson, 1972). Benthic foraminifera dwelling at intermediate depths will integrate into their shell the thermal conditions during their growing season which is mainly between spring to autumn as discussed previously. As a consequence, we expect low (high) Mg/Ca-based temperatures from benthic foraminifera of core IOW22517 (292 m water depth) to reflect warm (mild) conditions during the warm season (spring to autumn).

However, DWT measurements and reconstructions over the past 1200 cal years BP reflect the thermal conditions of the winter months (Brückner and Mackensen, 2006; Ljøen and Svansson, 1972). This is the result of the renewal of Skagerrak deep-waters, occurring after particularly severe winters (Ljøen and Svansson, 1972). During severe winters, slow currents and strong vertical mixing of the water mass enable the cooling, and therefore increase in density, of the whole water body of the central North Sea. This dense water mass subsequently flows downward into the central Skagerrak basin where it is trapped for several years until a new episode of deep-water renewal occurs, thus preserving the winter temperature signal (Ljøen and Svansson, 1972). Benthic foraminifera in the deep Skagerrak basin, although precipitating their shells during spring to autumn, will therefore record temperatures reflecting winter conditions.

The deep-water renewal is a particular process controlled by the topography and circulation in the North Sea. The shallowness of the central North Sea enables the formation of a cold dense water mass during severe winters on the whole water column, and the circulation brings this water mass into the Skagerrak where it cascades down into the deep basin and is trapped until a new renewal (Ljøen and Svansson, 1972). Since the topography has not considerably changed since the onset of the modern circulation at 8500 cal years BP (Gyllencreutz, 2005), it is reasonable to expect that the conditions that allows the process of Skagerrak deep-water renewal were established at least since the establishment of the modern circulation at 8500 cal years BP. The frequency of the renewal will itself depends on winter thermal conditions. As a consequence, low (high) Mg/Ca-based temperatures from benthic foraminifera of the deep core IOW22514 should reflect strong (weak) renewal of the deep-water following a period of severe (mild) winters, at least for the last 8500 years.

In summary, using Mg/Ca-based temperatures from benthic foraminifera at both deep and intermediate depth give an insight on past atmospheric temperature variability during both

warmer season and winter, here, for the last 6800 cal years BP which is the time covered by the cores. In addition, we compare our results to alkenone-derived sea surface temperature records from the same cores, representing mean annual temperatures (Krossa, personal communication, 2015).

5.6.2. Long term temperature trends in the Skagerrak region

The records in Figure 5.6 show that the long-term trends in the surface and intermediate-water temperatures (SST and IWT, respectively) are inversed compared to the long term trend of the deep-water temperatures (DWT; Figure 5.6). Indeed, SST and IWT, representing the mean annual and warm season atmospheric temperatures, respectively, are decreasing over the course of the record, while DWT, representing winter temperatures, are increasing. This is consistent with a decrease in mean-annual/summer insolation and increase in winter insolation at northern high latitudes (Laskar et al., 2004).

We observe a strong contrast in Skagerrak water temperatures at different depths prior to 4400-4200 cal years BP, with high SST and IWT, and low DWT. The contrast suggests a strong seasonal gradient, with warm summers and severe winters, indicating prevalent continental conditions prior to 4300-4200 cal years BP. Most likely, the Westerlies that transport warm and moist air from the Atlantic towards NW Europe were weakened between 6800 and ~4400-4200 cal years BP. Consequently, cold and dry continental air masses from the north or the east influenced the climate conditions in northern Europe, probably resembling the spatial atmospheric configuration of a negative phase of the North Atlantic Oscillation (NAO) (Hurrell, 1995). In contrast, we document lower differences in temperatures between the SST/IWT and the DWT after 4400-4200 cal years BP. We note a decrease in all records, but of stronger importance in the SST and IWT records at ~4400-4200 cal years BP, followed by an abrupy increase in DWT at 3500 cal years BP. This suggests a transition towards a lower seasonal gradient, probably related to a stronger dominance of maritime conditions reflective of a strengthening in the Westerlies that in turn bring warm and moist air over northern Europe, resembling the spatial configuration of a positive phase of the NAO at present (Hurrell, 1995). The transition from a period of strong seasonal gradient to a period

of low seasonal gradient at 4200 cal years BP is associated with a period of instability in the temperature records of the different seasons between ~4400-4200 and 3500 cal years BP.

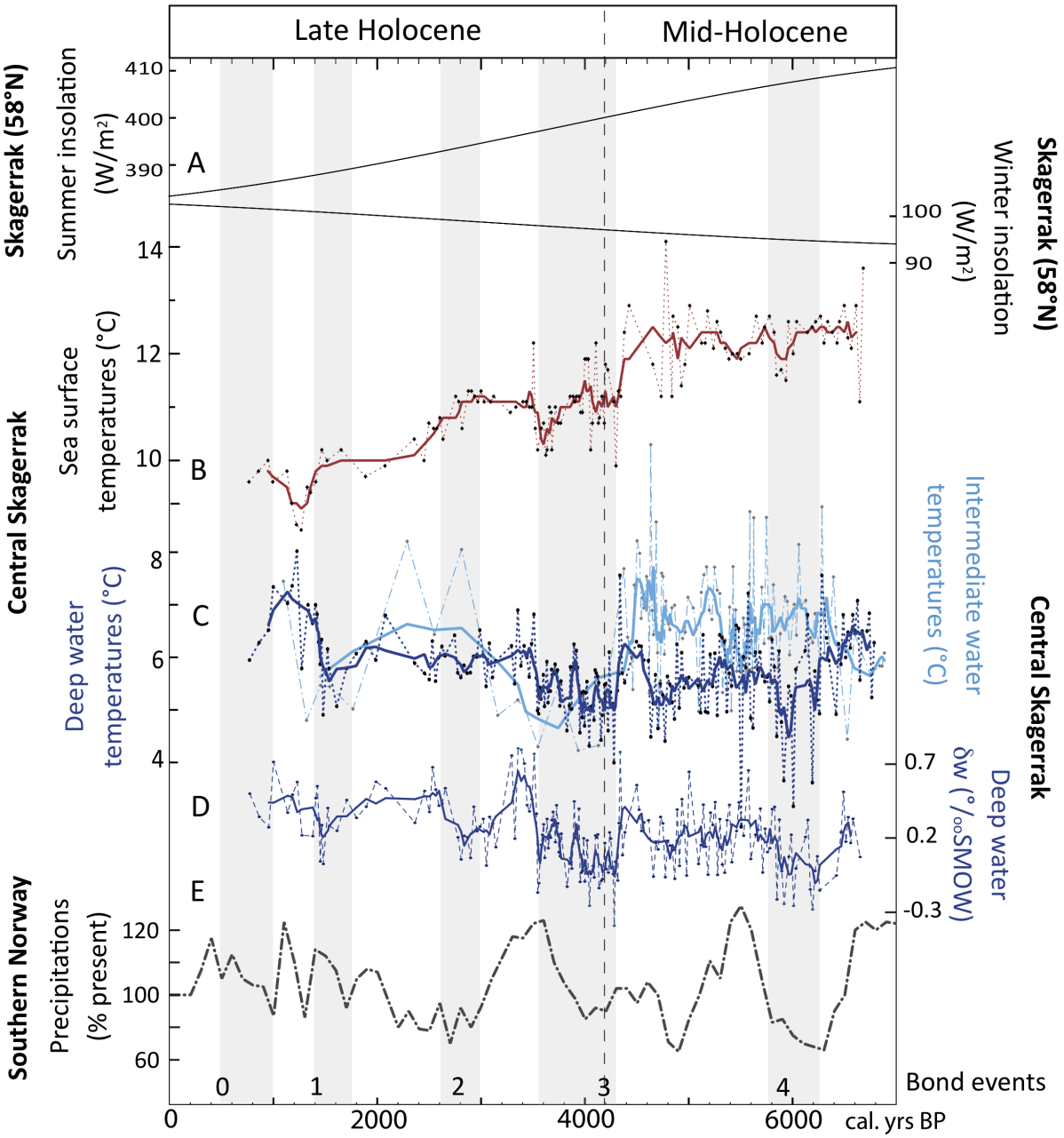

Figure 5.6: A) Winter and summer insolations at 58°N (Laskar et al., 2004), B) Skagerrak sea surface temperatures, core IOW225514 (Krossa, personal communication, 2015), C) intermediate and deep-water temperatures, D) deep-water salinity (represented by δw), E) winter precipitations documented from Norway (Nesje et al., 2001). Note that the solid lines in B, C, and D represent a 5 points running mean. Periods of relatively cold and less saline deep waters are highlighted by grey areas.

This is consistent previous climate reconstructions from the region and the North Atlantic (Bakke et al., 2008; Bjune et al., 2005; D. R. Erbs-Hansen et al., 2011; Krossa et al., 2015;

Moros et al., 2004; Nesje et al., 2001; Risebrobakken et al., 2003; Snowball et al., 1999), where a change from a period of strong seasonal gradient to a period of low seasonal gradient has been documented between ~4000 and 3500 cal years BP. However the timing of the transition is not clearly established in regional records. In western Norway, retreating or even lacking glaciers related to reduced winter precipitation rates and warm summers are documented prior to ~4000 cal years BP, followed by a period of re-advancing glaciers (Bakke et al., 2008; Bjune et al., 2005; Nesje et al., 2001). Paleoclimate records from the open North Atlantic that are expected to reflect a winter signal, suggest a colder mid-Holocene and a warmer late Holocene with a transition at around 3700 cal years BP (Moros et al., 2004). In the Skagerrak, an increased influence of Atlantic in the eastern basin, probably associated with an increased strength of the Westerlies, is documented starting around 4350 (D. R. Erbs-Hansen et al., 2011), while an increase in Baltic outflow is documented starting at ~3500 cal years BP most likely associated with an increase in winter precipitation over the catchment area under maritime conditions (Krossa et al., 2015). The period of instability between 4400-4200 and 3500 cal years BP evidenced from our Skagerrak records could explain the different timing for the transition from dominant continental to dominant marine climate conditions, documented in the regional records.

According to those results, the transition from mid- to late Holocene in the region is placed in this study at ~4200 years BP, at a time when changes occurred in regional temperature records of both the cold and the warm seasons. The choice of this date has been proposed by Walker and co-authors in a recent attempt to formally fix the appellations “early”, “mid-” and “late” Holocene (Walker et al., 2012).

5.6.3. Abrupt temperature variations in the Skagerrak

The long trends describe above are punctuated in our records by multi-centennial fluctuations, particularly distinct during the mid-Holocene in the evolution of the deep-water renewal. These fluctuations are evidenced in both the Mg/Ca-based temperature records and in the $\delta 18O$ record from the deep core, suggesting a robust signal. We observe periods of relatively low DWT between ~6300 and 5800 , 4800 and 4600, 4300 and 3600 cal years BP, and two last centered around 2800 and 1400 cal years BP, concomitant with periods of

relatively warm deep-water. These periods of decreased DWT suggest strong deep-water renewal reflecting particularly cold winter conditions.

Moreover, the different cold and warm winter phases recorded in the DWT match with winter precipitation reconstruction from Norway (Nesje et al., 2001; Figure 5.6). Low (high) DWT suggesting cold (mild) winter conditions are associated with dry (wet) winters in Norway. The cold and dry winter conditions are most probably reflecting a decreased strength of the Westerlies, while mild and wet winter conditions are most probably reflecting a strengthening of the Westerlies.

Interestingly, the coupled cold and dry winter conditions documented from our records and precipitation reconstructions from Norway (Nesje et al., 2001) also match with the Bond Events represented by increases in ice rafted debris (IRD) in northern North Atlantic sediments (Bond et al., 2001; Figure 6). The IRD occurred in the North Atlantic roughly at 1500-years intervals and supposedly are forced by changes in solar intensity and ocean-atmosphere modulation (Bianchi and McCave, 1999; Bond et al., 1997, 2001; Debret et al., 2007; Thornalley et al., 2009). During these events a general cooling and a shift towards continental-dominated climate conditions are reported in northern Europe (Alley et al., 1997).

Bond event 4, centered around 5900 cal years BP is particularly marked in our DWT record, as well as in the winter precipitation records from Norway (Nesje et al., 2001). However, Bond event 4 is seldom found in the Skagerrak climate records (Emeis et al., 2003; D. R. Erbs-Hansen et al., 2011; Krossa et al., 2015). Moreover, it is not marked in either the IWT or the SST records (this study; Krossa, personal communication). This suggests that Bond event 4 mainly affected winter climate conditions in Northern Europe. Accordingly, stacked atmospheric temperature records based on pollen from southern Sweden coherently document a cooling event in the annual temperature reconstruction between ~6300 and 5500 years BP, which is only slightly visible in the summer temperature reconstructions (Seppä et al., 2009). The cooling during winter can be linked to a reduction of AMOC associated with the Bond event (Wanner and Bütikofer, 2008), most likely resulting in the extension of Artic ice cover during winters and a continental climate over the mid- and high latitudes, as documented for previous Bond events (Denton et al., 2005).

However, Bond Event 3 (~4200 cal years BP, coinciding with the 4.2 event) is associated in our records with both a period of intense renewal of the deep-water (low DWT) and a strong

cooling in IWT and SST between about 4200 and 3500 years BP. This suggests that the cooling event at that time did not only prevailed during winter time in the Skagerrak region, but also clearly affected the whole year. The difference with the previous period is maybe related to the lower summer/annual insolation at that time, possibly delaying the melting of the extended ice cover.

The following Bond events (2 and 1), centered around 2800 and 1400 cal years BP respectively, are also evidenced in our deep-water records by a decrease in temperature and in particular in salinity, but with less significance than prior cold events. Our intermediate-water record does not have the resolution to comment on such short-term events, but the SST record does not show any particular cooling (Figure 6). This suggests that those events did not have a strong impact on the climate of the Skagerrak region.

In summary, our records suggest that the 5.9 event was associated with particularly cold and dry winter conditions in the Skagerrak region, and relatively warm summers, implying continental conditions. In contrast, Bond event 3 appear to have affected the climate in the Skagerrak region not only during winter but also during warmer seasons as documented in the intermediate and sea surface temperature records. Afterwards, during the late Holocene, cold events appear moderate in all seasons, except maybe for the Little Ice Age (LIA) which is not entirely covered in our records. The reason for the different seasonal sensitivity of the region to the Bond events may be explained by different insolation at the time of those cold events.

5.6.4. The "Medieval Warm Period"

Over the past two millennia, the "Medieval Warm Period" (MWP) and the LIA are the most prominent features in Skagerrak climate records (Hebbeln et al., 2006). The MWP is evidenced in the region between ~1300 to 900 cal years BP, as reported by Hebbeln et al. (2006), and is covered in our deep-water record. During the MWP, we observe the most pronounced deep-water warming within the complete record, indicating an interval of weakest deep-water renewal and also increased salinity. In 2006, Hebbeln et al. suggested that an increased advection of warm and saline North Atlantic water reaching the deeper basins in the Skagerrak occurred during the MWP. Our data support that hypothesis and may also suggest that the North Atlantic saline inflow did not only reached deeper levels, but

probably filled the whole deep basin of the Skagerrak during a period of particularly weak deep-water renewal.

There is an on-going debate about whether the climate conditions during the MWP were driven by a persistent positive mode of the NAO (Jones et al., 2014; Moreno et al., 2012; Olsen et al., 2012; Trouet et al., 2009, 2012). Such predominance in one phase of the NAO is attributed to an oceanic modulation by the Atlantic Meridional Overturning Circulation (AMOC) that is enhanced/weakened after a positive/negative phase of the NAO (Delworth and Greatbatch, 2000; Robson et al., 2012), which in turn results in a prolonged phase of a locked ocean-atmosphere system (Trouet et al., 2009, 2012). Previous observational and paleoclimate studies have indicated that deep-water renewal in the Skagerrak correlates highly to the NAO (Brückner and Mackensen, 2006; Hagberg and Tunberg, 2000; Tunberg and Nelson, 1998). The exceptional conditions in the Skagerrak during the MWP, with potentially no renewal of the deep-water as suggested by our data set, would support such prevailing positive-like NAO conditions during the MWP (Moreno et al., 2012; Trouet et al., 2009, 2012).

5.7. Conclusion

We used benthic Mg/Ca and stable isotopes from a gravity-core located at ~420 m water depth in the Skagerrak to reconstruct changes in past deep-water temperatures over the last 6800 years that are linked to deep-water renewal during cold winter conditions. We also used benthic Mg/Ca from a gravity-core at intermediate water depth (~270 m) to infer past changes in warm season temperatures in order to comment on seasonal variability in temperature. Overall, the mid-Holocene period was characterized by cold and low-saline deep-water and generally warm intermediate waters, suggesting a continental-dominated atmospheric circulation pattern marked by cold and dry winters and also a strong seasonal contrast in temperature. At ~3500 years BP, warmer deep-water temperatures and increased salinity occurred associated with a cooling in the SST, indicating a shift towards a more maritime-dominated atmospheric circulation pattern over the late Holocene period. Superimposed on the general temperature trends, the deep-water records documented periods of relatively frequent/intense deep-water renewal concomitant with dry conditions in Norway and increases in IRD in North Atlantic sediments. The 5.9 event seem to be only

associated with winter variability, while younger events appear to be associated with variability during winter and warmer months. During the MWP there were apparently no renewal of the deep-waters which could indicate a period of long-lasting positive-like NAO conditions supporting observations from previous studies. A higher resolution record of the deep-water renewal during the late Holocene would add to the discussion about winter thermal conditions and seasonality over North-Western Europe for that period.

Acknowledgements: We thank all co-authors for their contribution to the discussion. We would also like to thank Dieter Garbe-Schönberg and Marcus Regenberg for their support with the Mg/Ca analyses, Nils Andersen for his help on the stable isotopes analyses. We would also like to express our thanks towards Alte Nesje who provided us with the winter precipitation data. We thank Thomas Blanz and Sylvia Koch for their work on the alkenone analyses on core IOW225514, following the method described in Leduc et al., 2010. The work has been founded by the DFG SPP 1400 project "Early Monumentality and Social Differentiation".

6. MULTIDECADAL TO MILLENNIAL SCALE CLIMATE VARIABILITY IN THE SKAGERRAK REGION OVER THE LAST 6800 YEARS

Carsten Lemmen initiated Camille Butruille to time series analyses. Camille Butruille performed and interpreted all the time series analyses in this chapter. Carsten Lemmen and Mara Weinelt contributed to the discussion.

6.1. ABSTRACT

Time series analyses are performed on Skagerrak deep and intermediate-water temperature and salinity reconstructions for the Holocene. Our aim is to identify potential cyclicity and non-stationary behaviour possibly linked to the open North Atlantic system or to external forcing. Millennial variability is found in the deep-water temperature and $\delta^{18}O$ records, both representing winter thermal conditions (Butruille et al., in press). Additionally, multidecadal variability of 60 to 110 years is found in both records, and cycles of 50 years are found in the intermediate record. Both the millennial and the multidecadal variability can be attributed to the North Atlantic system. Millennial variability is associated with the Bond events and cold relapse in Northern Europe, especially during winter. The 50-110 years periodicity is related to the Atlantic Multidecadal Oscillation (AMO), the Atlantic Meridional Overturning Circulation (AMOC), and possibly the North Atlantic Oscillation (NAO). Interestingly, multidecadal instability in the winter conditions seems particularly strong during or just after Bond events.

6.2. INTRODUCTION

Millennial-scale climate variability during the Holocene is generally associated with the so-called Bond events (Bond et al., 1997; Bond et al., 2001), corresponding to large discharge of icebergs from the boreal high-latitudes towards the South, that affected the climate and environments on a global scale (see review in Wanner et al., 2011). These events have a near 1500-year periodicity (Bond et al., 1997; Bond et al., 2001) although a clear cyclicity has not been found (Wanner et al., 2011). They are expected to be mainly driven by a weakening of the Atlantic Meridional Overturning Circulation (AMOC) and by sun activity which have an internal variability around 1500-2000 and 1000 years, respectively (Bond et al., 1997, 2001; Bianchi and McCave, 1999; Debret et al., 2007; Thornalley et al., 2009). These rapid climate changes had a strong influence on winter variability in the northern Hemisphere high latitudes during the early Holocene (Denton et al., 2005). The associated shutdown (or decrease in strength) of the North Atlantic meridional overturning circulation (AMOC) caused the extension of Arctic sea ice during winter (Denton et al., 2005; Wanner and Bütikofer, 2008; Wanner et al., 2014, and references therein) which most likely exacerbated the cooling of high latitudes during winter (Denton et al., 2005; Seppä et al., 2007). The following cold relapses, during the mid- and late Holocene, occurred under different orbital and predominant ice covers conditions, but are also associated with a reduced AMOC and extended Arctic sea ice (Wanner et al., 2014), and a new study shows that abrupt cooling particularly prominent during winter in Northern Europe roughly coincide with the Bond events (Butruille et al., in press).

Short term variability in the modern climate in northern Europe is strongly governed by large-scale atmospheric pressure systems, in a sea-saw atmospheric phenomenon also known as the North Atlantic Oscillation (NAO) (e.g., Hurrell, 1995; Hurrell et al., 2003). The NAO controls changes in the mean wind speed and direction over the Atlantic (Westerlies), the heat and moisture transport between the Atlantic and the continent, and the intensity and number of storms, and is mostly evidenced during the winter months. Its variability is closely linked to climate variability in the North Atlantic and in particular to changes in the sea surface temperature (SST) fields, also called Atlantic Multidecadal Oscillation (or AMO) (Sutton and Hodson, 2003), with evidence for a non-stationary correlation between AMO

and NAO (Walter and Graf, 2002; Wyatt et al., 2012). Nowadays, the NAO is responsible for the short term variability in northern European climate (Hurrel, 1995) and environment, (Koslowski and Loewe, 1994; Tinz, 1996; Omstedt and Chen, 2001; Jevrejeva et al., 2003; Gouveia et al., 2008). Besides a variability of one to two years, instrumental records show that the NAO stay predominant in one phase or another on decadal scale (Hurrell, 1995). However, since instrumental records only span about 150 years, it is difficult to discern whether the NAO or the AMO are persistent during the Holocene as periodic drivers in the climate system. Yet, climate reconstructions based on tree rings and speleothems for the last 900 years indicate that prolonged phases of the NAO in a dominant state occurred during the Medieval Climate Anomaly (MCA) or the Little Ice Age (LIA) (Trouet et al., 2009, 2012; Moreno et al., 2012; Olsen et al., 2012; Jones et al., 2014 ; Spangehl et al., 2010). Moreover, an increasing number of data-based studies, supported by simulations, show that multidecadal variability during the Holocene is similarly intrinsic to the ocean-atmosphere variability (see Knudsen et al., 2011 and references therein; Wei and Lohmann, 2012). Moreover, prolonged phases of the NAO in a dominant states also seem to have prevailed during other large-scale changes in the Northern Hemisphere climate for at least the last 5200 years (Olsen et al., 2012). Additional investigations are however needed to document if multidecadal variability intrinsic to the ocean-atmosphere variability (AMO, NAO) existed further back during mid-Holocene, for instance during the emergence of agrarian cultures in northern Europe, potentially influenced by climate change.

The Skagerrak, located between Norway and Denmark, is the deepest basin of the North Sea and has been considered for the modern time as highly sensitive to the atmospheric climate fluctuations that control the region, and in particular to the NAO (Ljøen and Svansson, 1972; Tunberg and Nelson, 1998; Hagberg and Tunberg, 2000; Brückner and Mackensen, 2006). Additionally, high-resolution records of mid- to late Holocene summer and winter temperatures have been recently reconstructed from the Skagerrak (Butruille et al., in press; chapter 5). Here, we aim to improve the knowledge on multidecadal to millennial scale variability, by performing time series analyses on those summer and winter temperature reconstructions from the Skagerrak. Skagerrak records allow us to identify millennial to multidecadal periodicity from the winter temperature records and thus to explore potential links to the North Atlantic variability, Bond cycles, the AMO and possibly the NAO.

6.3. WORKING AREA – THE SKAGERRAK

The main circulation in the Skagerrak occurs at intermediate depth and seasonal variability is reflected in the temperature field of the intermediate-depth water (Ljøen and Svansson, 1972). The upper water layers in the Skagerrak are mostly stratified with respect to salinity over the year, due to the meeting of the saline Atlantic Inflow and the brackish Baltic Outflow. During summer, the waters will in addition have a thermal stratification, restricting convective exchanges between deep and surface waters. Skagerrak deep-water renewal is therefore mostly due to advective processes. The temperatures at depth generally vary between 4-8ºC (Ljøen and Svansson, 1972). Cold and dense water forming over the central North Sea during particularly cold winters reaches the Skagerrak within a few months and consequently cascades down into the basin, where it replaces less dense water (Ljøen and Svansson, 1972). This new water thereafter slowly warms up with the upper layer generally over a few years. Another renewal occurs when a cold winter is strong enough to generate colder and denser water than the deep water. Recent studies aim to reconstruct past winter climate based on Skagerrak deep-water renewal (Brückner and Mackensen, 2006; Butruille et al., in press). Indeed, since the general circulation pattern in the Skagerrak was established around 8500 years ago (Gyllencreutz, 2005), it may be assumed that the deep-water renewal process was also established at that time and have monitored winter temperature variability since then.

Past temperatures reconstructions based on foraminifera shells at different depth from the Skagerrak carry different seasonal signals (Butruille et al., in press). Indeed, in the deep basin, the foraminifera grow their shells in a water that retains a winter signal all year around, and therefore paleotemperature reconstructions from the deep basin represent winter variability. In contrast, the water temperature at intermediate depth reflects seasonal variability. Foraminifera generally grow their shells following a planktonic bloom, mostly occurring in the Skagerrak between spring to autumn (Joint and Pomroy, 1993; Blanz et al, 2005). Therefore, at intermediate depth, the water temperature will reflect spring to autumn temperatures when the foraminifera grow their shells, and consequently paleotemperature reconstructions from foraminifera at intermediate depth represent the warm season variability.

6.4. Approach and Methods

High resolution times series of winter and the warm season temperatures were established in the Skagerrak from the mid- to the late Holocene (Butruille et al., in press), allowing us to explore millennial to multidecadal variability. Winter temperature reconstructions are based on benthic foraminifera Mg/Ca and $\delta^{18}O$ records from gravity-core IOW225514 (57"50.279'N, 842.226'E; 420m water depth). Warm season temperature reconstructions are based on benthic foraminifera Mg/Ca records from gravity-core IOW225517 (57"40.002'N, 7'05.465'E; 293m water depth). These records are presented and discussed in Butruille et al. (in press). The age models are based on seven and twelve dates for core IOW225514 and IOW225517, respectively.

6.4.1. The time series and their resolution

Time series analyses are performed on different records of the Skagerrak in order to explore the variability for different seasons. For warm season variability, we used the intermediate-water temperature record between 6900 and 4800 cal. yrs BP (Butruille et al., in press; Figure 6.1), where the record has a high-resolution. For the cold season, the high-resolution temperature (DWT) and $\delta^{18}O$ records of Skagerrak deep water, between 6800 and 750 cal. yrs BP, both expected to reflect winter thermal variability (Butruille et al., in press; Figure 6.1).

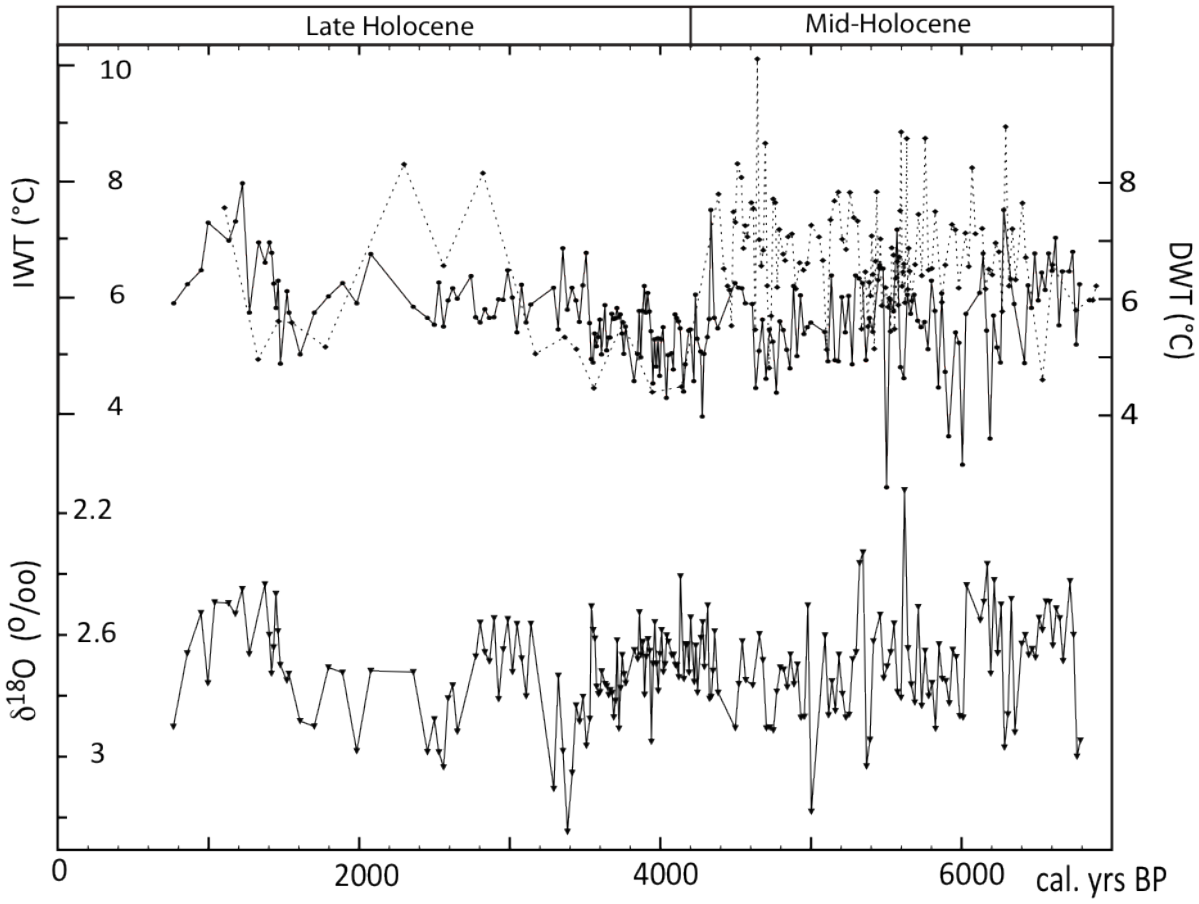

Figure 6.1: Top: Skagerrak deep and intermediate-water temperatures based on *Melonis barleeanus* Mg/Ca-thermometry of core IOW225514 and IOW225517, respectively. Bottom: Oxygen isotopes of *M.barleeanus* from the core IOW225514.

Table 6.1 present the resolution in different sections of the cores. The resolution of sampling varies around 10 to 30 years between 2500 and 6800 cal years BP for the deep-water Mg/Ca and $\delta^{18}O$ records from core IOW225514. Prior to 2500 cal. years BP, the resolution varies around 50 to 100 years mostly (Table 6.1). For the intermediate-water Mg/Ca record from core IOW225517, the resolution during the period of interest (6900-4400 cal years BP) varies between 5 to 25 years. There are however a few gaps with missing material in both records. The intervals of different average time between the data in the table is due to a linear interpolation between the radiocarbon dates, assuming linear accumulation between the level dated.

Table 6.1: Average time between the data in cores IOW225514 and IOW225517. The different intervals are the result of linear interpolation between the radiocarbon dates, assuming linear accumulation between the level dated.

Deep-water records (DWT and $\delta^{18}O$) IOW225514		**Intermediate-water temperatures (IWT) IOW225517**	
Cal. yr BP	**Average time (yrs)**	**Cal. yr BP**	**Average time (yrs)**
6800-4500	20	6900-5660	20
4500-3500	10	5660-5560	5
3500-2500	30	5560-5370	10
2500-1500	50-100	5370-4800	25
1500-1400	15	4800-4400	15
1400-770	50-100		

6.4.2. Time series analyses

Spectral analyses

In order to identify persistent cycles in the time series and to compare the variability pattern of different variables, spectral analyses were performed using the REDFIT software (Schulz and Mudelsee, 2002). This method reduces the background noise (or "white noise") by dividing the time series into overlapping segments while calculating the average spectra. Spectra of paleoclimatic time series frequently show a continuous decrease of spectral amplitude with increasing frequency (the so-called "red-noise"), which can sufficiently be explained with a first-order autoregressive (AR1) process (Hasselmann, 1976). For evenly sampled time series, the process is almost straightforward but needs an interpolation, thus reddening the signal. REDFIT allows to estimate the AR1 parameter, directly from unevenly spaced time series, then tests the hypothesis that the time series originated from an AR1 process by comparing the spectrum of the time series with the one from the AR1 model (Schulz and Mudelsee, 2002), thus avoiding the reddening of the signal due to the bias of the Fourier transform. A critical false-alarm level of (1-1/n)*100% was calculated, following Thomson (1990).

Wavelet transforms

We also applied wavelet transforms to the time series of winter temperatures (core IOW225514), in order to identify and investigate potential changes in periodicity across the last 6800 years, since spectral analysis can be ineffective at detecting non-stationary periodicities, or at giving information about how they vary in strength or frequency over time. With wavelet analysis, a time series can be studied at multiple scales (i.e. at low and high frequencies) simultaneously, and non-stationary periodicities can be detected (Lau and Weng, 1995; Torrence and Compo, 1998). The software PAST (Hammer et al., 2001) is used to perform the wavelet transforms on time series. A significance level of p=0.005 was chosen for the analyses.

6.5. RESULTS

Time series analyses of Skagerrak deep and intermediate records display several distinct peaks in the frequency domain corresponding to significant periodicities (Figure 6.2). The periodicities reported are maxima and may not represent narrow, well-defined periodicities but rather broader bands of quasi-periodic variability. Peaks that reach the critical false-alarm level (here generally around 99%) are considered relevant and will be discussed. Peaks exceeding the 95% false-alarm are only discussed if they are found in the different spectra.

A significant peak is visible around 1100 years in the $\delta^{18}O$ record of the deep water (Figure 6.2). It is matched in the DWT spectrum by a peak around 1000 years. The latter does not reach the critical false-alarm for its spectrum, but since it is above the 95% false-alarm level, and matches the peak in the $\delta^{18}O$ record, it is considered significant. The IWT record analyzed only spans around 3000 years, therefore there is no information about millennial-scale periodicity from this record.

High resolution, enough to trace multidecadal to centennial variability, is found between 6800 and 3500 in the DWT and deep $\delta^{18}O$ records and between 4400 and 7000 in the IWT record. The DWT and $\delta^{18}O$ records (Figure 6.2) present high frequency variability, with cycles centered around 70, 80-90, 100 and 110 years. Only the 100 year peaks reach the critical false-alarm of 99% in both records, but since peaks around 70, 80-90 and 110 years exceed the 95% false-alarm and are found in both records, they are considered relevant. Cycles

around 50 years and possibly 160 and 580 years are found in the intermediate-water record, yet only the 50 years peak appeared to exceed the critical false-alarm and is similar to periodicities in the other records (Figure 6.2), and is therefore discussed.

According to the wavelet transform, millennial variability is evident along the entire record of DWT (Figure 6.3). High-resolution between 6800 and 3500 cal. years BP allows the investigation of multidecadal to centennial variability on this section of the deep-water record. According to the wavelet analyses, multidecadal to centennial variability is mostly pronounced between 7000 and 5000 cal. years BP. It is also evidenced between 4200 and 3500 cal. years BP, although with less significance.

6.6. Discussion

A near millennial cyclicity is apparent in both DWT and $\delta^{18}O$ records, monitoring Skagerrak deep-water renewal and, as such, winter conditions. In addition, the wavelet transform on the DWT shows a persistence of the millennial variability over the entire record (Figure 6.3).

During the Holocene, millennial cyclicity in climate is generally associated with the Bond events (Bond et al., 1997; Bond et al., 2001). Bond events are reported to have a near 1500-year periodicity (Bond et al., 1997; Bond et al., 2001). They are expected to be mainly driven by a weakening of the Atlantic Meridional Overturning Circulation (AMOC) and by sun activity which have an internal variability around 1500-2000 and 1000 years, respectively (Bond et al., 1997, 2001; Bianchi and McCave, 1999; Debret et al., 2007; Thornalley et al., 2009). However, a review of several cold relapses based on timeseries of temperature, humidity/precipitation and reconstructions of glacier advances show that the events are not strictly regular or cyclic (Wanner et al., 2011).

Nevertheless, rapid episodes of strong deep-water renewal in the Skagerrak roughly coincide with Bond events at least between 6800 and 770 cal. years BP (Butruille et al., in press). Therefore, we expect climate variability associated with Bond events from the North Atlantic to have a strong impact on winter conditions over the North Sea region. That is to say, reduced AMOC and strong iceberg discharge into the North Atlantic in the mid-Holocene are associated with periods of particularly cold winters in Northern Europe. A reduced AMOC would lead to a decreased transport of warmth from the tropics towards the poles, most

likely inducing an increased extension of sea ice during boreal winter over the Nordic seas thus amplifying the cooling over Northern Europe (Wanner and Bütikofer, 2008).

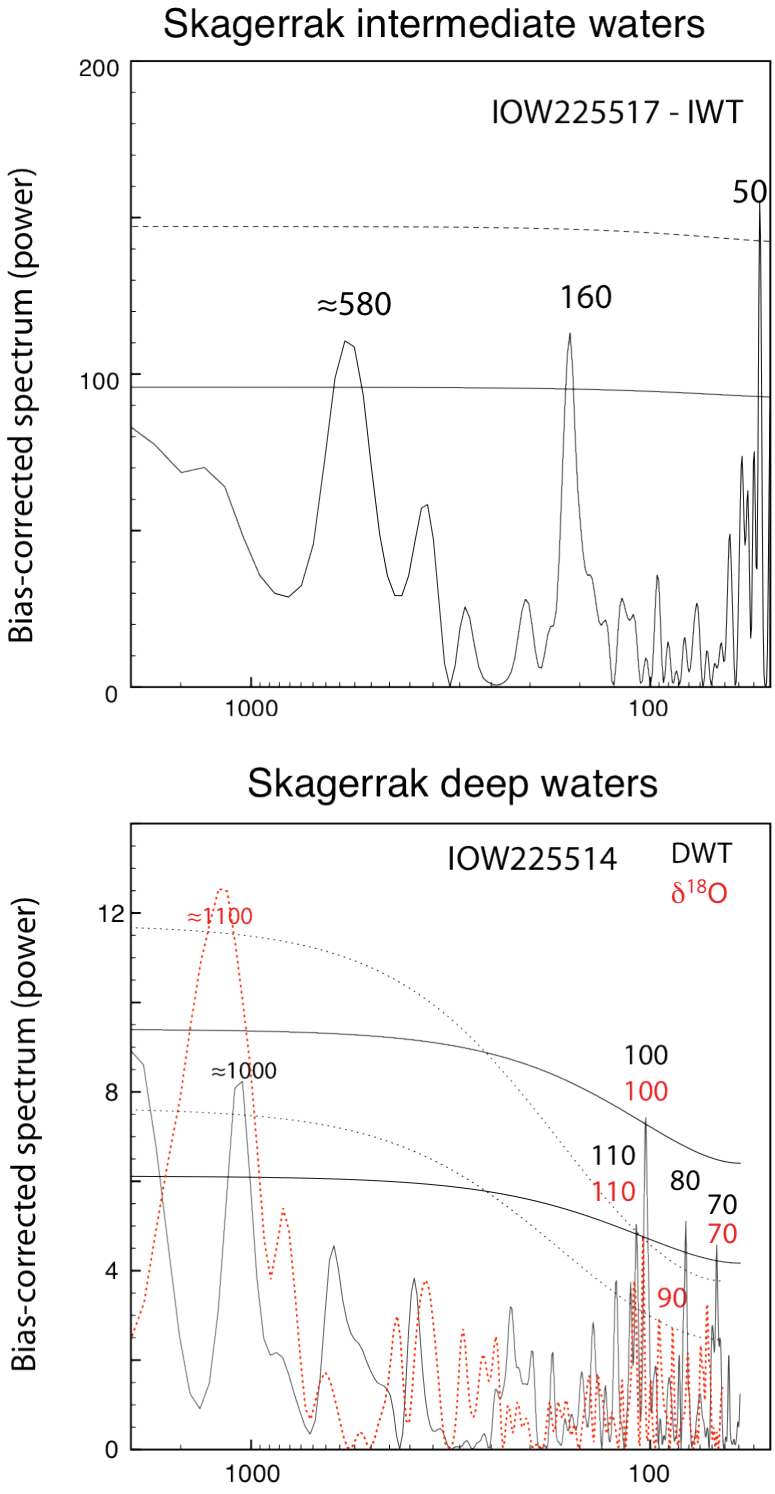

Figure 6.2: Spectral analysis on sea surface, intermediate and deep records from the western Skagerrak. The top figure shows analysis on IWT from core IOW225517, and the bottom figure, analysis on deep-water temperatures (DWT) and $d^{18}O$ from core IOW225514. In all representations, the top line represents the critical false-alarm for the designated spectrum (generally around 99%) and the bottom line the 95% false-alarm curve. Peaks exceeding the 95% curve are highlighted and will be discuss in the text.

Significant multidecadal variability in the 70 to 110 year band is evidenced in Skagerrak deep-water records, while cycles around 50 years are found in the intermediate temperature record. This high frequency variability is most likely linked to internal variability of the ocean/atmosphere system. Indeed, similar multidecadal variability between ≈30-130 years has been identified in a variety of proxies, instrumental records and modeling studies, and is considered an intrinsic dynamics of the thermohaline circulation in the North Atlantic with its principal expression in the SST fields (Atlantic Multidecadal Oscillation - AMO) (Schlesinger and Ramankutty, 1994; Delworth and Mann, 2000; Gray, 2004; Knight et al., 2005; Hubeny et al., 2006; Sicre et al., 2008; Knudsen et al., 2011; Wyatt et al., 2012; Ólafsdóttir et al., 2013). Since the instrumental Atlantic SST records only span about 150 years, it is difficult to discern whether the AMO is persistent during the Holocene as a periodic driver in the climate system or if it is only an impermanent feature. However, an increasing number of data-based studies, also supported by simulations, show that multidecadal variability similar to the AMO occurred over the Holocene and appears similarly intrinsic to the ocean-atmosphere variability (see Knudsen et al., 2011 and references therein; Wei and Lohmann, 2012). In addition, observations and modeling studies suggest that the NAO/AO variability is partially driven by North Atlantic SSTs (Sutton and Hodson, 2003). There are evidence of a non-stationary correlation between AMO and NAO (Walter and Graf, 2002; Wyatt et al., 2012), and frequency of 60-80 years has also been attributed to the NAO (Rossi et al., 2011). Interestingly, Skagerrak deep-water renewal is known to reflect the variability of the NAO during part of the 20th century (Tunberg and Nelson, 1998; Hagberg and Tunberg, 2000, Brückner and Mackensen, 2006) and possibly over the last millennium (Brückner and Mackensen, 2006). The multidecadal variability found in Skagerrak winter records therefore suggests a close association with the North Atlantic (NAO, AMO and atmosphere-ocean couplings). Our results therefore support the hypothesis that multidecadal to centennial climate variability, most likely related to a North-Atlantic/atmospheric modulation, the AMOC, the AMO and potentially the NAO, was prominent at least between 3500 and 6800 cal. years BP. This is supported for the last millennium by time series analysis on shells of long-lived bivalve mollusks from the North Sea representing annually-resolved climatic conditions (Holland et al., 2014).

Additionally, according to Skagerrak climate records, Bond events 3 and 4 seem to be associated with instability in the climate system (Figure 6.3). Stronger multidecadal and centennial variability in winter conditions, most likely related to the North Atlantic, is increased during and just after those particular cold events. Bond event 4 seems to have been associated with centennial variability and the subsequent period with multidecadal variability, at least during winter. This is however only based on one record and further high resolution investigations on winter climate variability during the Bond events are needed.

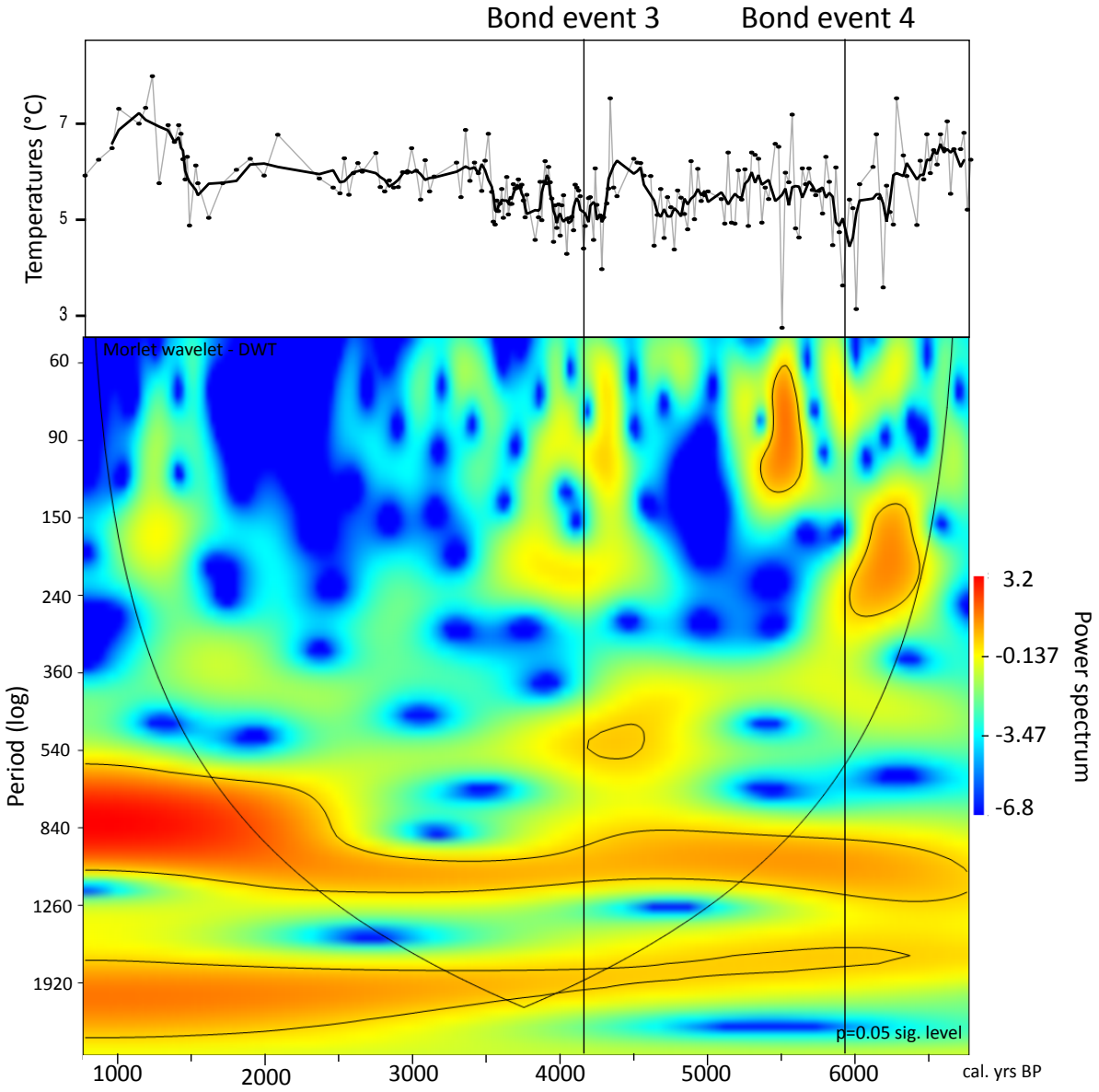

Figure 6.3: Morlet wavelet transform on the deep-water temperatures (core IOW225514). The contoured area represent the significance level (p>0.005). Area below the black line is the cone of influence (COI), representing the region of the wavelet spectrum in which edge effects become important.

6.7. CONCLUSION

We analyzed time series of winter temperature reconstructions based on deep-water records from the Skagerrak for the last 6800 years, and of summer temperature reconstructions based on intermediate-water records from the Skagerrak for the period between 6900 and 4800 cal. yrs BP, using spectrum analyses and wavelet transforms. The analyses revealed significant cycles of 60 to 110 years as well as 1000-1100 years cycles in the deep-water records, and significant cycles of 50 years in the intermediate record. The millennial variability in the winter thermal reconstructions deduced from Skagerrak deep-water records can be attributed to ice-drifted events evidenced from the North Atlantic (Bond events). The multidecadal to centennial variability is most likely the result of an influence of the AMO/AMOC and possibly the NAO on winter conditions in Northern Europe during the last 6800 years. Increased instability in winter conditions seem to be associated with the cold Bond events. Strong centennial variability in winter temperatures is evidenced during Bond event 4, followed by strong multidecadal variability in the next ca. 500 years.

Acknowledgements: We thank Carsten Lemmen for his introduction to the REDFIT software and for his assistance thereafter. The work has been founded by the DFG SPP 1400 project "Early Monumentality and Social Differentiation".

7. DISCUSSION ON THE POTENTIAL INFLUENCE OF CLIMATE ON THE DEVELOPMENT OF NEOLITHIC SOCIETIES IN NORTHERN GERMANY AND SOUTHERN SCANDINAVIA

This chapter is divided in 3 subchapters that will lead to potential manuscripts to be submitted. A manuscript on: “Decrease in summer temperatures during the Neolithic preceding a change in cultivars” is planned with Wiebke Kirleis; A manuscript on: “Shifts in the economy of Denmark late Neolithic and early Bronze Age communities at time of abrupt climate changes” is planned with Johannes Müller.

The discussion is the work of Camille Butruille, with the contributions of Johannes Müller, Wiebke Kirleis, Martin Hinz, Veronica R. Krossa, and thanks to the many discussions raised at the different conferences Camille Butruille participated in.

7.1. INTRODUCTION

While the Holocene is generally considered a period of fairly stable climate conditions compared to the last glacial and deglacial period, several abrupt cold spells are documented over its course. It is largely acknowledged that those changes are one of the drivers of social development during the Holocene (e.g. Gibbons, 1993; DeMenocal et al., 2000; Staubwasser et al., 2003; Burroughs, 2005; Dixit et al., 2014; Gronenborn et al., 2014). In northern Germany and southern Scandinavia, the first occurrence of agricultural practices are documented around 6000 cal. yrs BP (Sørensen and Karg, 2014), with a fully developed agrarian society around 5500 cal. yr BP (Müller, 2011; Dörfler et al., 2012; Feeser et al., 2012; Kirleis et al., 2012; Sørensen and Karg, 2014). Interestingly, farmer communities were already established for more than a millennia in central Germany (Guilaine, 2000), and there is evidence of contact and trade between the hunter-gatherer-fishers to the North and those Neolithic farmer groups to the South (Hartz et al., 2007). There is an ongoing debate about whether the sudden adoption of agricultural techniques by the Mesolithic groups of northern Germany and southern Scandinavia could have been influenced by climate change (Bonsall et al., 2002; Shennan et al., 2013; Sørensen and Karg, 2014). It is argued that Mesolithic groups in the region, well adapted to their environment, were most likely vulnerable to climate change and resulting environment changes.

Shennan and coauthors (2013) consider that there is no relation between climate and the onset of a population boost at the transition from the Mesolithic to the Neolithic in the region. However, their study is based on the comparison of archaeological evidence with climate reconstructions from remote archives in the high-latitudes North Atlantic. Pollen-based temperature reconstruction from Europe reveal large gradients between temperature evolution in northwestern and northeastern Europe (Davis et al., 2003). This suggest the need of climate reconstructions based on archives close to the archaeological sites to deduce the regional signal and to be able to assess the role of climate on the local communities. Moreover, the pollen reconstructions also show differential evolution of winter and summer temperatures over the Holocene, with a general cooling of the summer temperatures while the winter temperatures increased, following the respective insolation evolution. The mid-Holocene is therefore expected to have more pronounced seasonality.

Additionally, abrupt changes sometimes are only documented in either one of the two seasons (Davis et al., 2003). Therefore, it is necessary to reconstruct climate variability of both seasons in order to answer the question of climate change and its influence on past societies.

Here we use new winter and the warm season thermal reconstructions from the Skagerrak (Butruille et al., in press) in order to determine the potential impact of climate on the evolution of regional past communities. The focus is made on the transition from the Mesolithic to the Neolithic in Northern Germany and Southern Scandinavia, with the introduction of farming, but the discussion will also extend to the intervals of the evolution of farming practices during the Neolithic and the beginning of the Bronze Age in the region.

7.2. Working Area

7.2.1. Regional climate

The present day climate in northwest Europe and southern Scandinavia is strongly governed by large-scale atmospheric pressure systems that govern the storm tracks over the North Atlantic and the continent (e.g., Hurrell, 1995; Hurrell et al., 2003). Fluctuations in the strength of these features lead to a predominance of continental or maritime conditions in the region. Continental conditions are characterized by Westerlies shifted towards southern Europe and the dominance of dry air masses from Siberia. Conditions during summers are dry and warm, while winters are cold and dry. In contrast, maritime climate are characterized by strong Westerlies shifted North, bringing warm and moist air masses towards northern Europe and an increase in the frequency of storms (e.g., Hurrell, 1995; Hurrell et al., 2003).

7.2.2. Different seasons recorded in the Skagerrak

The Skagerrak is the deepest part of the otherwise shallow North Sea, with its maximum water depths of more than 700 m (Rodhe, 1987). In the present day, the surface layer is permanently stratified mainly due to the outflow of fresh Baltic Sea water, in addition to a

thermal stratification component during summer (Otto et al., 1990). The main circulation occurs around 200m water depth and variations in the temperatures at this depth represent the interannual atmospheric variations (Ljøen and Svansson, 1972). However, there is a significant contrast in the long-term variations of temperatures between waters above and below the sill depth at about 300m (Ljøen and Svansson, 1972). Below the sill, variations in temperatures are governed by the renewal of the deep water, when cold and dense water from the central North Sea cascades down into the deepest parts of the basin after a cold winter. The new established water mass slowly warms up over a year or two until a new renewal is triggered. The deep-water temperatures are therefore expected to monitor atmospheric winter temperatures (Ljøen and Svansson, 1972).

Using paleothermometry based on benthic foraminifera, it is possible to reconstruct past variations in Skagerrak temperatures at different water depth, representative of different seasons. Accordingly, reconstructions at intermediate depth would most likely represent warm season temperature variations, as we expect foraminifera to grow their shells after a planktonic bloom occurring in spring to autumn in the region. In contrast reconstructions from foraminifera at high depth though mainly growing in the warm season here report winter temperature variability as the deep water keeps a winter signal all year around (Butruille et al., in press).

7.3. DISCUSSION

7.3.1. Abrupt winter cooling prior to the adoption of agriculture in northern Germany and southern Scandinavia

The late Mesolithic in the region, represented by the Ertebølle culture, consisted of communities of hunter-gatherer-fishers established in southern Scandinavia and northern Germany between 7400 and 6100 cal. yrs BP (see Hartz et al. 2007 and references therein). The transition from the Mesolithic to the Neolithic is generally defined by the development from hunter-gatherer-fisher groups to the beginning of agriculture and animal husbandry. The first evidence of cereal cultivation trace back to 6100 - 6000 cal. yrs BP, although still associated to a hunter-gatherer-fisher subsistence. Around 5700-5500 cal. yrs BP, farming

strategies were fully adopted by the Funnel Beaker Culture (or Trichterrandbecherkultur, TRB) (Müller, 2011; Dörfler et al., 2012; Feeser et al., 2012; Kirleis et al., 2012; Sørensen and Karg, 2014). The TRB groups covered a large part of northern Europe, from the Netherlands in the West to Poland in the East, and from northern Germany to southern Sweden. Around 3100 cal. years BP, their communities declined and forests recovered, until the late Neolithic around 4900 cal. yrs BP and the Single Grave Culture (Müller, 2011; Feeser et al., 2012; Hinz et al., 2012).

The adoption of agriculture by the Mesolithic groups is thought to be partly driven by climate change and associated environmental changes, although this is still under debate (Bonsall et al., 2002; Shennan et al., 2013; Sørensen and Karg, 2014). A study on population change (Shennan et al., 2013) found no connection between climate change and the onset of agriculture in the region. However, the climate archives used by these authors are from locations most likely too remote to represent the regional climate of northern Germany and southern Scandinavia.

New temperatures reconstructions from the central Skagerrak (cores IOW225514 and IOW225517) based on benthic foraminifera paleothermometry show that while the warm season seemed to stay in prolonged warm conditions, winter temperatures also abruptly decreased in the central Skagerrak between 6200 and 5900 cal. yrs BP (Butruille et al., in press; chapter 5; Figure 7.1). Furthermore, time series analyses on winter temperature reconstructions from Skagerrak show that this cold relapse was associated with strong instability in the winter climate (chapter 5). Increased occurrence of severe winters over Northern Germany is also evidenced from lacustrine records based on micropaleonthological and microgeochemical analyses on varves (Zahrer, 2012). Additionally, alkenone-based SST reconstructions from eastern Skagerrak also show an abrupt cooling at 6200 cal. yrs BP (Krossa, personal communication, 2015) right before a demographic boom in the region (Hinz et al., 2012). Yet, SST records from central Skagerrak (cores IOW225514 and IOW225517) do not show such an abrupt cooling at 6200 cal. yrs BP, but stayed relatively warm until c. 5000 cal. yrs BP (Krossa, personal communication, 2015). This could be explain by the fact that a change from a maritime regime towards a continental regime was recorded in the eastern Skagerrak core due to proximity to the continent but not in the western Skagerrak, where the conditions stayed under the influence of the open Atlantic (Krossa, personal communication, 2015).

In the view of these results, the major climatic factor that could have influenced the onset of agriculture in northern Germany and southern Scandinavia appears inherent to winter variability. In present day, continental-dominated conditions over northern Europe, associated with dry and cold winters, generally result in late onset of spring and late frosts events, both resulting in a shortening of the vegetation growing season, as well as an increased Baltic sea-ice extent (see D'odorico et al., 2002 and references therein). Most likely, the cold relapse around 6200 cal. yrs BP provoked similar changes in the climate and environment conditions of Mesolithic groups.

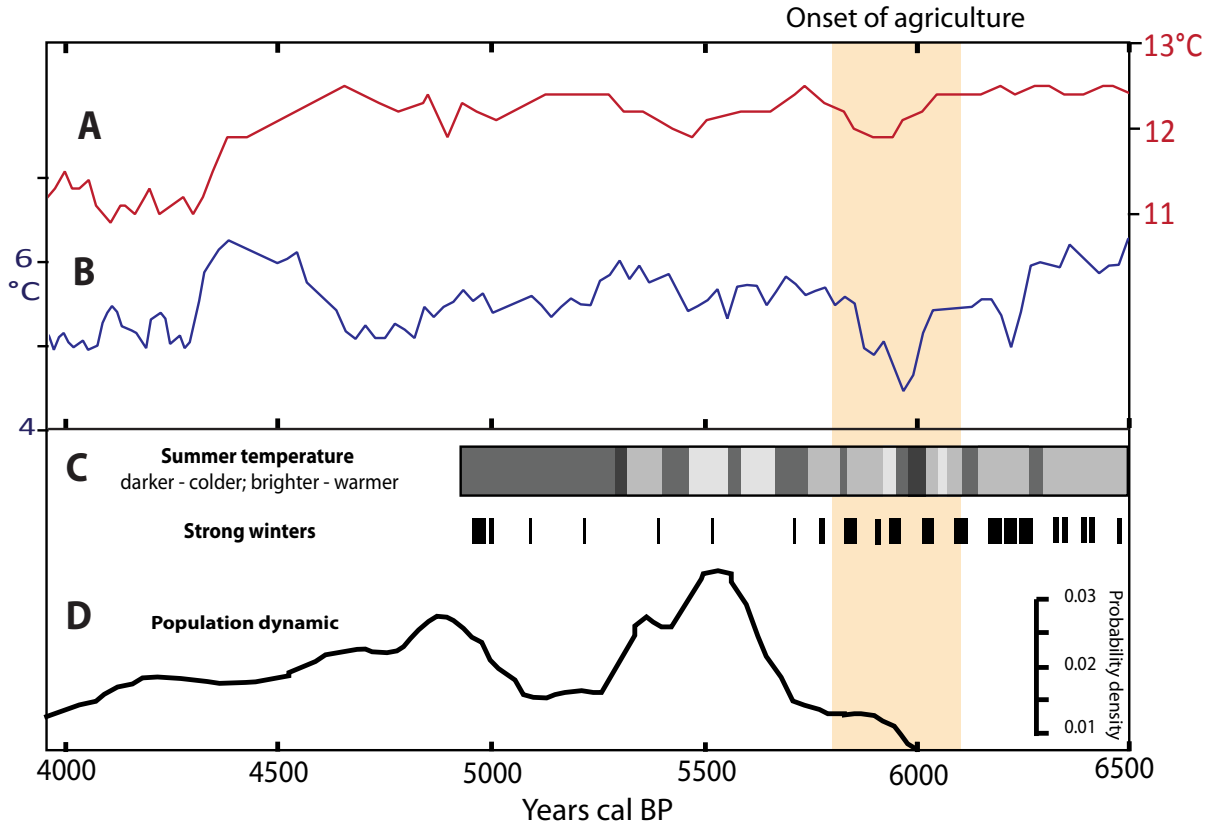

Figure 7.1: Comparison of regional climate records (Butruille et al., in press; Zahrer, 2012) and changes in population density (Hinz et al., 2012). A-B; 5-points running mean of intermediate-water temperatures (A) and deep-water temperatures (B) reconstructions, representing the regional warm season and winter conditions, respectively (Butruille et al., in press); C: Winter and summer conditions based on micropaleonthological and geochemical analyses from lake Belau in northern Germany (Zahrer, 2012); D: Sum-calibrated probabilities from northern Germany and southern Scandinavia, representing the population density of the region (Hinz et al., 2012). The highlighted area represents the onset of agriculture.

Changes in the marine environment, a delayed onset of spring and a shortening of the vegetation growing season must have affected the economy of hunter-gatherer-fisher communities and potentially encouraged the adoption of different subsistence strategies. As

cereal cultivation and animal husbandry were already known from communities in the South (Hartz et al., 2007), hunter-gatherer-fishers of northern Germany and southern Scandinavia might have progressively adopted these techniques, until they became the main way of subsistence in the region. The change in subsistence was not only progressive but it was also not simultaneous to the change in winter conditions. Indeed, first evidence for cereal cultivation are documented around a century after the beginning of the abrupt cooling.

Finally, our results underline the necessity to develop proxies to reconstruct regional winter temperatures, together with other temperature reconstructions. Most temperature reconstruction underestimate the range of climate deterioration since they only document the warm season variability. However, as we just demonstrated for the Skagerrak during the Neolithic, some abrupt climate change can be mainly inherent to winter variability.

7.3.2. Decrease in summer temperatures during the Neolithic preceding a change in cultivars

At the onset of agriculture around 6100-6200 cal. yrs BP, the first crops cultivated are mainly an assemblage of emmer, barley and free threshing wheat coming from a southeastern and a southwestern influence (Kirleis and Fischer, 2014). Around 5700 cal. yrs BP, a significant change in the crop assemblage occurs, before a fully agrarian system is developed in the region (Kirleis et al., 2014). Indeed, free threshing wheat is abandoned and emmer and barley become the main cultivars (Kirleis and Fischer, 2014). The change is mainly attributed to soil depletion and probably to cultural choice, whereas no evidence of a climate influence is found. The authors compare the cultivar assemblages to climate reconstructions based on lake micropaleonthological and geochemical analyses in northern Germany (Zahrer, 2012). These climate records indicate a diminution of the seasonality between 5810 and 5441 cal. yrs BP, with a stronger decrease in seasonality centered around 5710 cal. yrs BP. However, Kirleis and Fischer attributed the decrease in seasonality to milder winter conditions that would still be suitable for free threshing wheat. Interestingly, there is also a change in our Skagerrak temperature reconstructions around 5700 cal. yrs BP. Yet, it is not entirely attributed to an increase in winter temperatures after c. 5900 cal. yrs BP, as reflected in the deep-water temperatures (DWT), but also to a subsequent decrease in summer

temperatures at 5700 cal. yrs BP, culminating around 5500 cal. yrs BP, as reflected in the intermediate-water temperatures (IWT) (Butruille et al., in press; Figure 7.2).

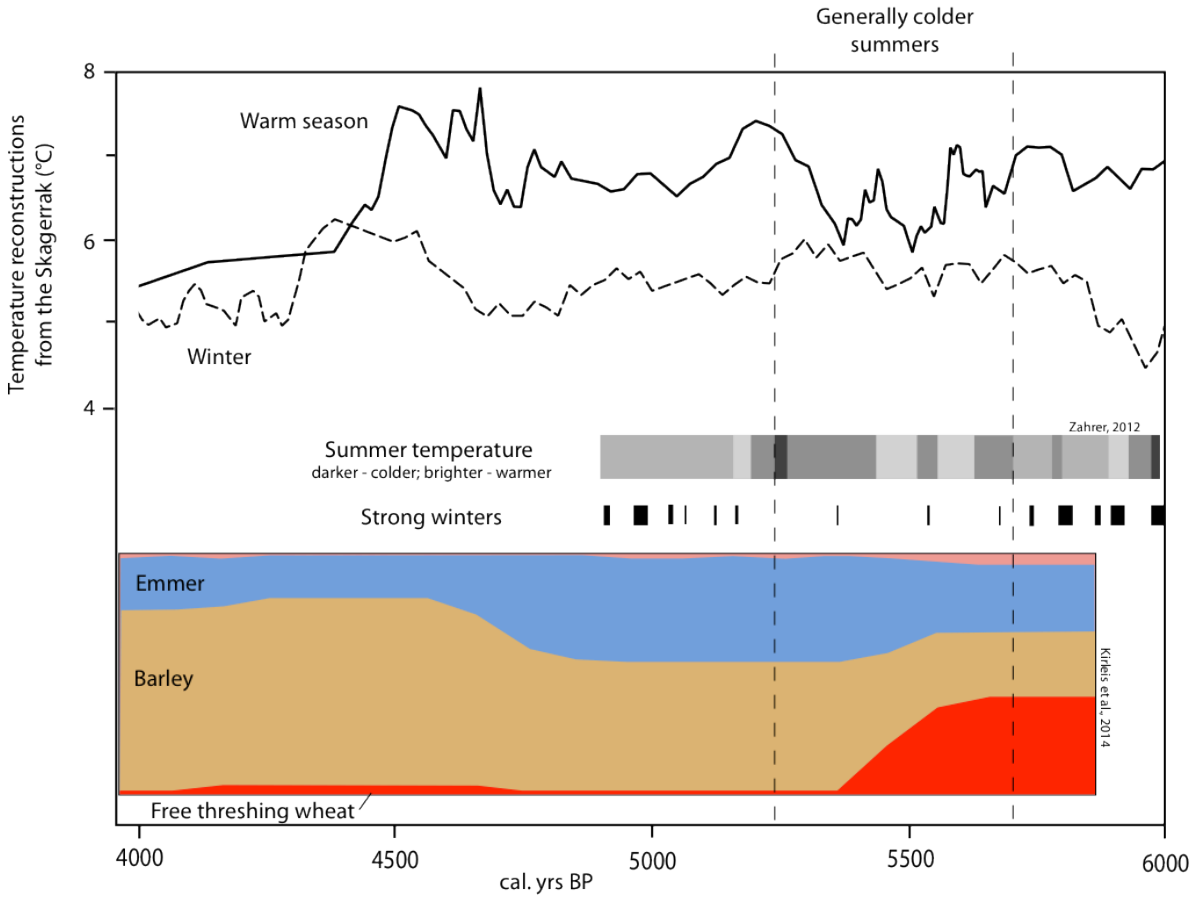

Figure 7.2: Warm season and winter temperature estimates based on intermediate and deep-water temperature reconstructions (5-points running mean) from the Skagerrak (Butruille et al., in press) and from lake Belau in northern Germany (Zahrer, 2012), and the evolution of the main crops used by agrarian communities in northern Germany (Kirleis and Fischer, 2014).

This suggests that the decrease in the overall seasonal gradient was two-timed, with first an increase in winter conditions around 5900 cal. yrs BP, that would still be suitable for free threshing wheat, but followed by a decrease in summer temperatures at 5700 cal. yrs BP, also reflected in the results by Zahrer (2012), that could have influenced the change in the crop assemblages, as *Triticum durum* (tetraploid free threshing wheat) needs relatively warm summers. Additionally, sea surface temperature (SST) reconstructions from eastern Skagerrak (Krossa, personal communication, 2015) show a slight decrease synchronous to the IWT, supporting the idea of cooler summer temperatures. Furthermore, strong decadal instability is recorded in the winter thermal condition centered around 5700 cal. yrs BP

(chapter 6). Even though climate change may not be the main reason for the shift in the cereal cultivation, changes in climate conditions preceded this shift by less than a century. Since *Triticum durum* (tetraploid free threshing wheat) needs relatively warm summers while *Triticum aestivum* (hexaploid free threshing wheat) has a high demands on soil quality (see Kirleis and Fischer, 2014), a decrease in summer temperatures together with a decrease in soil quality might have therefore influence the change in crop cultivation around the 5700 cal. yrs BP "event".

7.3.3. Shifts in the economy of Denmark late Neolithic and early Bronze Age communities at time of abrupt climate changes

A recent study about continuation or discontinuation of social practices, reflected in the material culture from archaeological sites dated between around 4450 to 3450 BP in Denmark, northern Germany and central Germany aim to compare the different regions regarding internal developments and the integration of innovations, and to understand why, how and when they were made (Müller, in Meller (in print)). In Denmark, three phases are identified in the economy, based on the increase in metal objects and the decrease in flint dagger production rates, together with the differences in house development. A first period of economic boom is identified prior to c. 4100 cal. yrs BP, followed by a period of crisis between c. 4100 and 3700 cal. yrs BP. Finally, another period boom in the economy is documented after c. 3700 cal. yrs BP. One of the hypothesis for the sudden crisis between c. 4100 and 3700 cal. yrs BP is that strong winter cooling at 4300 cal. yrs BP evidenced from Skagerrak climate reconstructions (Butruille et al., in press; chapter 5), could have lead to worse conditions for agriculture, as the growing season for vegetation must have shorten. Moreover, an increase in winter precipitations after 4000 cal. yrs BP is suggested by glaciers advance in Norway (Nesje et al., 2001), while winters were still cold according to Skagerrak reconstructions. Wet and cold winters most likely led to pervasive frost during spring and worsen conditions for agriculture.

Acknowledgements: We thank Johannes Müller, Wiebke Kirleis, Martin Hinz and Veronica R. Krossa for the discussion on the different subjects. The work has been founded by the DFG SPP 1400 project "Early Monumentality and Social Differentiation".

8. CONCLUSIONS

This PhD-thesis aims to evaluate the potential impact of climate change during the mid-Holocene on past societies in northern Germany and southern Scandinavia. Benthic foraminifera Mg/Ca and stable isotopes were used to reconstruct regional atmospheric paleotemperature. They were performed on two marine core sites in the Skagerrak covering the mid- and late Holocene (core IOW225514 in the deep basin and core IOW225517 at intermediate depth). The Skagerrak is the depocentre of the North Sea and as such provides high-resolution cores, allowing us to explore multidecadal to centennial variability of Holocene climates. The temperature variations at intermediate depth reflects seasonal changes in atmospheric temperatures over the region, while they reflect the renewal of the deep waters linked to winter temperatures over the region in the deep basin. We therefore consider that since benthic foraminifera grow their shells between spring and autumn, following planktonic blooms (Joint and Pomroy, 1993; Blanz et al, 2005 and references therein), the temperature signal of the ambient water incorporated in the shells at that time reflects spring to autumn (the "warm season") temperatures at intermediate depth, and winter temperatures in the deep basin. Therefore, temperature reconstructions based on benthic foraminifera paleothermometry from the intermediate and deep Skagerrak provides a new insight into the warm season and winter atmospheric temperatures over northern Germany and southern Scandinavia during the Holocene.

The cores cover the last ca. 7000 years. Their chronologies have been completed with two and five radiocarbon dates to enable the exploration of millennial to multidecadal climate variability in the region. The chronologies were also improved by establishing robust chronostratigraphies of the marine core, using remarkable events found in both marine and terrestrial archives. Tephra chronology in Skagerrak sediments turned out only little successful, probably hampered by (post)depositional processes, at least for the mid-Holocene, as the tephra particles reaching the region are apparently too light to settle in one specific layer after the eruptions. However, pollen analyses from the Skagerrak reflect on-land environmental changes during the mid-Holocene, when using the radiocarbon age model with a reservoir age of 400 years, which is therefore adopted in this study. Time series

analyses were additionally performed in order to identify potential cyclicity intrinsic to the ocean-atmosphere variability, as well as periods of climate instability. The results were then confronted to archaeological reports of societal changes.

Reconstructions of the warm season temperatures over the Skagerrak region, based on Skagerrak intermediate-water temperatures (IWT), show the expected insolation-induced cooling from the mid- to the late Holocene. The Holocene thermal optimum (HTO) in our records abruptly ends around 4400-4300 cal. yrs BP, roughly supporting an end of the mid-Holocene at 4200 cal. yrs BP as recently proposed by Walker et al. (2012). In contrast, regional winter temperature reconstructions, based on Skagerrak deep-water temperatures (DWT), indicate a warming from the mid- to the late Holocene, following the increase in winter insolation, as previously evidenced on a supra-regional scale (Davis et al., 2003). The mid-Holocene in the Skagerrak region is characterized by a winter thermal minimum ending with a prolonged cold period between 4300 and 3500 cal. yrs BP. The late Holocene corresponds to a prolonged period of generally mild winters starting abruptly at 3500 cal. yrs BP and culminating during the Medieval Warm Period between ca. 1400 to 900 cal. yrs BP. The mid-Holocene in the region is therefore characterized by strong seasonality, which decreases during the late Holocene. This supports the general pattern observed in many paleoclimate reconstructions from the region and the North Atlantic, showing a continental-dominated mid-Holocene period followed by a maritime-dominated late Holocene interval starting around 4200-3500 cal. yrs BP (e.g. Snowball et al., 1999; Nesje et al., 2001; Risebrobakken et al., 2003; Moros et al., 2004; Bjune et al., 2005; Bakke et al., 2008; Krossa et al., 2015).

The warm season temperatures in the Skagerrak region do not show repeated cooling periods associated with the North Atlantic Bond events, similarly to many high-resolution paleotemperature reconstructions tracing mean annual or summer temperatures from northern Europe (e.g. Seppä and Birks, 2001; Seppä et al., 2009; Erbs-Hansen et al., 2011a). The end of the HTO in the warm season record is marked by a strong cooling (-2°C for the IWT), that marks the beginning of a prolonged phase of milder summers that prevailed over the late Holocene. The onset of a mild summer phase do roughly correspond to Bond event 3, though. Winter temperature reconstructions based on Skagerrak DWT indicate repetitive episodes of strong winter cooling roughly corresponding to the Bond events. They are also associated with periods of low winter precipitation as evidenced in glacier fluctuations from

western Norway (Nesje et al., 2001). The coldest period correlates with Bond event 4 during the mid-Holocene, and is only evidenced during winter in our records. This suggests that changes in the North Atlantic circulation associated with Bond events had a stronger influence on winter atmospheric variability during the mid-Holocene than they did on the warm season variability. We propose that the weakening of the Atlantic Meridional Overturning Circulation (AMOC) and extension of Arctic Sea ice, associated with the Bond events (Denton et al., 2005; Wanner and Bütikofer, 2008; Wanner et al., 2014, and references therein), under relatively low winter insolation, intensified the cooling during winter time as already suggested for the last deglaciation and the early Holocene (Denton et al., 2005). The following Bond events are also marked in the winter thermal reconstructions, although to weaker extends. The period of transition between the mid- and the late Holocene in the winter thermal reconstructions, between 4300 and 3500 cal. yrs BP, also starts abruptly simultaneous to Bond event 3, as for the warm summer thermal reconstructions.

Additionally, spectral analyses based on the DWT and IWT records reveal strong periodicities of 60 to 120 years and of 50 years in the winter and warm season temperatures, respectively. These cyclicities are most likely linked to internal variability of the ocean/atmosphere system. Similar multidecadal variability between ≈30-130 years has been identified in numerous studies as an intrinsic dynamic of the thermohaline circulation in the North Atlantic and the Atlantic Multidecadal Oscillation (AMO) (Schlesinger and Ramankutty, 1994; Delworth and Mann, 2000; Gray, 2004; Knight et al., 2005; Hubeny et al., 2006; Sicre et al., 2008; Knudsen et al., 2011; Wyatt et al., 2012; Ólafsdóttir et al., 2013). Additionally, frequency of 60-80 years has also been attributed to the NAO (Rossi et al., 2011). The multidecadal variability found in Skagerrak winter records therefore suggests a close association with the North Atlantic (NAO, AMO and atmosphere-ocean coupling) for the last 6800 years. Moreover, wavelet transforms applied on the DWT record show that Bond events 3 and 4 are associated with instability in winter. Increased centennial winter variability related to the North Atlantic, seems to prevail during those cold events, while multidecadal variability seems more pronounced subsequent to Bond event 4.

Finally, we compared the winter and warm season temperature reconstructions to the social evolution of northern Germany and southern Scandinavia during the mid-Holocene. The transition from the Mesolithic to the Neolithic, characterized by the introduction of

agricultural practices in the region between 6100-6000 cal. yrs BP, appears to follow a rapid cooling event affecting winter variability which onset occurs 100 to 150 years earlier. This cooling is associated with Bond event 4 in the North Atlantic and most likely lead to important environmental changes such as a change in the vegetation growing season, as well as an increased Baltic sea-ice extent that could have in turn lead an impoverishment of the marine ecosystems (see D'odorico et al., 2002 and references therein). Such impacts on the environment of the Mesolithic hunter-gather-fisher groups could have influenced them to adopt cereal cultivation and animal domestication as new way of subsistence. Another change in the regional thermal conditions could have potentially impacted the Neolithic economy. Indeed, after the first introduction of agrarian techniques, a shift in the main cultivars is reported around 5700 cal. yrs BP (Wiebke and Fischer, 2014). Simultaneously, a period of mild summers is reported in our IWT, that could have been unfavourable to the cultivation of free threshing wheat. At last, the early Bronze Age in the region is characterized by a period of crisis between 4100 and 3700 in between two periods of economical boom evidenced in the material culture (Müller et al, in print). The beginning of the crisis period follows by about 200 years the onset of a prolonged period of colder winter and milder summers in the Skagerrak region. This could have lead to worse conditions for agriculture, as the growing season for vegetation must have shorten.

In the end, this study showed the strong potential of Skagerrak as a regional archive for paleoclimate reconstruction. The particularity of Skagerrak deep-water renewal also gives the exceptional opportunity to explore winter thermal variability and study for instance the seasonal variability of Bond events in the region. Our reconstructions trace back to the mid-Holocene, around 6800 years BP. Further investigations, using deep-water cores covering the whole Holocene would bring additional knowledge on Holocene winter thermal conditions at a high resolution and allow us to explore earlier Bond events for instance. Our work also shows that, without falling into a deterministic concept of climate control, a multi-disciplinary approach can lead to better understanding of the potential influence of climate on past societies. Moreover, it gives the paleoclimalogists the opportunity to directly compare their results to societal-related issues. We therefore believe that encouraging the cooperation between paleoclimatologists and archaeologists would benefit to both sides.

REFERENCES

Alley R.B., Mayewski P.A., Sowers T., Stuiver M., Taylor K.C. and Clark P.U. (1997) Holocene climatic instability: A prominent, widespread event 8200 yr ago. *Geology* 25(6): 483–486.

Andersen C., Koç N. and Moros M. (2004) A highly unstable Holocene climate in the subpolar North Atlantic: evidence from diatoms. *Quaternary Science Reviews* 23(20-22): 2155–2166.

Austin W.E.N., Cage a. G. and Scourse J.D. (2006) Mid-latitude shelf seas: a NW European perspective on the seasonal dynamics of temperature, salinity and oxygen isotopes. *The Holocene* 16(7): 937–947.

Bakke J., Lie Ø., Dahl S., Nesje A. and Bjune A. (2008) Strength and spatial patterns of the Holocene wintertime westerlies in the NE Atlantic region. *Global and Planetary Change* 60(1-2): 28–41.

Bianchi G.G. and McCave I.N. (1999) Holocene periodicity in the North Atlantic climate and deep-ocean ow south of Iceland. *Nature* 397(6719): 515–517.

Björck S., Koç N. and Skog G. (2003) Consistently large marine reservoir ages in the Norwegian Sea during the Last Deglaciation. *Quaternary Science Reviews* 22: 429–435.

Bjune A.E., Bakke J., Nesje A. and Birks H.J.B. (2005) Holocene mean July temperature and winter precipitation in western Norway inferred from palynological and glaciological lake-sediment proxies. *The Holocene* 15(2): 177–189.

Blanz T., Emeis K.-C. and Siegel H. (2005) Controls on alkenone unsaturation ratios along the salinity gradient between the open ocean and the Baltic Sea. *Geochimica et Cosmochimica Acta* 69(14): 3589–3600.

Bond G., Kromer B., Beer J., Muscheler R., Evans M.N., Showers W., et al. (2001) Persistent solar influence on North Atlantic climate during the Holocene. *Science (New York, N.Y.)* 294(5549): 2130–2136.

Bond G., Showers W., Chesseby M., Lotti R., Almasi P., DeMenocal P., et al. (1997) A Pervasive Millennial-Scale Cycle in North Atlantic Holocene and Glacial Climates. *Science* 278(5341): 1257–1266.

Bonsall C., Macklin M.G., Anderson D.E. and Payton R.W. (2002) Climate change and the adoption of agriculture in north-west Europe. *European Journal of Archaeology* 5(1): 9–23.

Brückner S. (2008) Climatic and hydrographic variability in the late Holocene Skagerrak as deducted from benthic foraminiferal proxies. Ph. D. Thesis - Alfred Wegener Institut für Polar- und Meeresforschung, Bremerhaven, 139.

Brückner S. and Mackensen A. (2006) Deep-water renewal in the Skagerrak during the last 1200 years triggered by the North Atlantic Oscillation : evidence from benthic foraminiferal d18O. *The Holocene* 16(3): 331– 340.

Brückner S. and Mackensen A. (2008) Organic matter rain rates, oxygen availability, and vital effects from benthic foraminiferal δ 13 C in the historic Skagerrak, North Sea. *Marine Micropaleontology* 66(3-4): 192–207.

Burroughs W. (2005) *Climate change in prehistory: The end of the reign of chaos*. Cambridge University Press, 372.

Butruille C., Krossa V.R., Schwab C. and Weinelt M. ((n.d.)) Reconstruction of mid- to late Holocene winter temperatures in the Skagerrak region using benthic foraminifera Mg/Ca and δ18O. *The Holocene*.

Cappers R.T.J. and Raemaekers D.C.M. (2008) Cereal Cultivation at Swifterbant? Neolithic Wetland Farming on the North European Plain. *Current Anthropology* 49(3): 385–402.

D'odorico P., Yoo J. and Jaeger S. (2002) Changing Seasons : An Effect of the North Atlantic Oscillation ? *Journal of Climate* 15(4): 435–445.

Davis B., Brewer S., Stevenson A.C. and Guiot J. (2003) The temperature of Europe during the Holocene reconstructed from pollen data. *Quaternary Science Reviews* 22: 1701–1716.

Debret M., Bout-Roumazeilles V., Grousset F., Desmet M., Mcmanus J.F., Massei N., et al. (2007) The origin of the 1500-year climate cycles in Holocene North-Atlantic records. *Climate Of The Past* 3(4): 569–575.

Delworth T.L. and Greatbatch R.J. (2000) Multidecadal Thermohaline Circulation Variability Driven by Atmospheric Surface Flux Forcing. *Journal of Climate* 13(9): 1481–1495.

Delworth T.L. and Mann M.E. (2000) Observed and simulated multidecadal variability in the Northern Hemisphere. *Climate Dynamics* 16(9): 661–676.

DeMenocal P., Ortiz J., Guilderson T., Adkins J., Sarnthein M., Baker L., et al. (2000) Abrupt onset and termination of the African Humid Period rapid climate responses to gradual insolation forcing.pdf. Quaternary Science.

Denton G., Alley R., Comer G. and Broecker W. (2005) The role of seasonality in abrupt climate change. *Quaternary Science Reviews* 24(10-11): 1159–1182.

Dixit Y., Hodell D. and Petrie C. (2014) Abrupt weakening of the summer monsoon in northwest India~ 4100 yr ago. *Geology*.

Dörfler W., Feeser I., van den Bogaard C., Dreibrodt S., Erlenkeuser H., Kleinmann A., et al. (2012) A high-quality annually laminated sequence from Lake Belau, Northern Germany: Revised chronology and its implications for palynological and tephrochronological studies. *The Holocene* 22(12): 1413–1426.

Dugmore A.J., Cook G.T., Shore J.S. and Newton A.J. (1995) Radiocarbon dating tephra layers in britain and iceland. *Radiocarbon* 37(2): 379–388.

Elderfield H., Yu J., Anand P., Kiefer T. and Nyland B. (2006) Calibrations for benthic foraminiferal Mg/Ca paleothermometry and the carbonate ion hypothesis. *Earth and Planetary Science Letters* 250(3-4): 633–649.

Emeis K.-C., Struck U., Blanz T., Kohly A. and Voß M. (2003) Salinity changes in the central Baltic Sea (NW Europe) over the last 10 000 years. *The Holocene* 13(3): 411–421.

Erbs-Hansen D.R., Knudsen K.L., Gary a. C., Gyllencreutz R. and Jansen E. (2011a) Holocene climatic development in Skagerrak, eastern North Atlantic: Foraminiferal and stable isotopic evidence. *The Holocene* 22(3): 301–312.

Erbs-Hansen D.R., Knudsen K.L., Gary A.C., Jansen E., Gyllencreutz R., Scao V., et al. (2011b) Late Younger Dryas and early Holocene palaeoenvironments in the Skagerrak, eastern North Atlantic: a multiproxy study. *Boreas* 40(4): 660–680.

Erlenkeuser H. (1985) Distribution of 210Pb with depth in core GIK 15530-4 from the Skagerrak. *Norsk geologisk tidsskrift* 65: 27–34.

Erlenkeuser H. and Pederstad K. (1984) Recent sediment accumulation in Skagerrak as depicted by 210Pb-dating. *Norsk geologisk tidsskrift* 64(2): 135–152.

Fairbanks R. (1989) A 17, 000-year glacio-eustatic sea level record: influence of glacial melting rates on the Younger Dryas event and deep-ocean circulation. *Nature* 342: 637–642.

Feeser I., Dörfler W., Averdieck F.-R. and Wiethold J. (2012) New insight into regional and local land-use and vegetation patterns in eastern Schleswig- Holstein during the Neolithic. *M. Hinz/ J. Müller (Hrsg.), Siedlung , Grabenwerk, Großsteingrab. Studien zu Gesellschaft, Wirtschaft und Umwelt der Trichterbechergruppen im nördlichen Mitteleuropa. Frühe Monumentalität und soziale Differenzierung 2*, 159 – 190.

Gibbons A. (1993) How the akkadian empire was hung out to dry. *Science* 261(5124): 985.

Gooday A.J. (2003) Benthic foraminifera (protista) as tools in deep-water palaeoceanography: Environmental influences on faunal characteristics. *Advances in Marine Biology* 46: 1–90.

Gouveia C., Trigo R., DaCamara C., Libonati R. and Pereira J. (2008) The North Atlantic Oscillation and European vegetation dynamics. *International Journal of Climatology* 28: 1835 – 1847.

Gray S.T. (2004) A tree-ring based reconstruction of the Atlantic Multidecadal Oscillation since 1567 A.D. *Geophysical Research Letters* 31(12): L12205.

Greaves M., Caillon N., Rebaubier H., Bartoli G., Bohaty S., Cacho I., et al. (2008) Interlaboratory comparison study of calibration standards for foraminiferal Mg/Ca thermometry. *Geochemistry, Geophysics, Geosystems* 9: Q0810.

Gronenborn D., Strien H., Dietrich S. and Sirocko F. (2014) “Adaptive cycles” and climate fluctuations: a case study from Linear Pottery Culture in western Central Europe. *Journal of Archaeological Science* 51: 73–83.

Guilaine J. (2000) La diffusion de l'agriculture en Europe: une hypothèse arythmique. *Zephyrus: Revista de prehistoria y arqueología* 53/54.

Gyllencreutz R., Backman J., Jakobsson M., Kissel C. and Arnold E. (2006) Postglacial palaeoceanography in the Skagerrak. *The Holocene* 16(7): 975–985.

Gyllencreutz R., Jakobsson M. and Backman J. (2005) Holocene sedimentation in the Skagerrak interpreted from chirp sonar and core data. *Journal of Quaternary Science* 20(1): 21–32.

Hagberg J. and Tunberg B.G. (2000) Studies on the Covariation between Physical Factors and the Long-Term Variation of the Marine Soft Bottom Macrofauna in Western Sweden. *Estuarine, Coastal and Shelf Science* 50: 373–385.

Hall V.A. and Pilcher J.R. (2002) Late-Quaternary Icelandic tephras in Ireland and Great Britain: detection, characterization and usefulness. *The Holocene* 12(2): 223–230.

Hammer O., Harper D. and Ryan P. (2001) PAST: paleontological statistics software package for education and data analysis. *Palaeontologia Electronica* 4(1): 4–9.

Hartz S., Lübke H. and Terberger T. (2007) From fish and seal to sheep and cattle : new research into the process of neolithisation in northern Germany. (Lüning 2002): 567–594.

Harwood A.J.P., Dennis P.F., Marca A.D., Pilling G.M. and Millner R.S. (2008) The oxygen isotope composition of water masses within the North Sea. *Estuarine, Coastal and Shelf Science* 78(2): 353–359.

Hass H.C. (1996) Northern Europe climate variations during late Holocene: evidence from marine Skagerrak. *Palaeogeography, Palaeoclimatology, Palaeoecology* 123(1-4): 121–145.

Hasselmann K. (1976) Stochastic climate models Part I. Theory. *Tellus* 28(6): 473–485.

Hebbeln D., Knudsen K.-L., Gyllencreutz R., Kristensen P., Klitgaard-Kristensen D., Backman J., et al. (2006) Late Holocene coastal hydrographic and climate changes in the eastern North Sea. *The Holocene* 16(7): 987–1001.

Heier-Nielsen S., Heinemeier J., Nielsen H. and Rud N. (1995) Recent reservoir ages for Danish fjords and marine waters. *Radiocarbon* 37(3): 875–882.

Hinz M., Feeser I., Sjögren K.-G. and Müller J. (2012) Demography and the intensity of cultural activities: an evaluation of Funnel Beaker Societies (4200–2800 cal BC). *Journal of Archaeological Science* 39: 3331–3340.

Holland H., Schöne B., Lipowsky C. and Esper J. (2014) Decadal climate variability of the North Sea during the last millennium reconstructed from bivalve shells (Arctica islandica). *The Holocene* 24(7): 771–786.

Hubeny J., King J. and Santos A. (2006) Subdecadal to multidecadal cycles of Late Holocene North Atlantic climate variability preserved by estuarine fossil pigments. *Geology* 34(7): 569–572.

Hurrell J.W. (1995) Decadal trends in North Atlantic Oscillation: Regional Temperatures and Precipitation. *Science* 269(5224): 676–679.

Hurrell J.W., Kushnir Y., Ottersen G. and Visbeck M. (2003) An overview of the North Atlantic Oscillation. *The North Atlantic Oscillation: climatic significance and environmental impact*, 1–35.

Jevrejeva S., Moore J. and Grinsted A. (2003) Influence of the Arctic Oscillation and El Niño‐Southern Oscillation (ENSO) on ice conditions in the Baltic Sea: The wavelet approach. *Journal of Geophysical Research* 108: 10–11.

Joint I. and Pomroy A. (1993) *Phytoplankton biomass and production in the southern North Sea*. , 16.

Jones P., Harpham C. and BM V. (2014) Winter responding proxy temperature reconstructions and the North Atlantic Oscillation. *Journal of Geophysical Research: Atmospheres* 119(11): 6497–6505.

Kirleis W. and Fischer E. (2014) Neolithic cultivation of tetraploid free threshing wheat in Denmark and Northern Germany: implications for crop diversity and societal dynamics of the Funnel Beaker Culture. *Vegetation History and Archaeobotany* 23(S1): 81–96.

Kirleis W., Klooß S., Kroll H. and Müller J. (2011) Crop growing and gathering in the northern German Neolithic: a review supplemented by new results. *Vegetation History and Archaeobotany* 21(3): 221–242.

Kirleis W., Klooß S., Kroll H. and Müller J. (2012) Crop growing and gathering in the northern German Neolithic: a review supplemented by new results. *Vegetation History and Archaeobotany* 221–242.

Knight J., Allan R., Folland C., Vellinga M. and Mann M. (2005) A signature of persistent natural thermohaline circulation cycles in observed climate. *Geophysical research letters* 32(20).

Knudsen M., Seidenkrantz M.-S., Jacobsen B. and Kuijpers A. (2011) Tracking the Atlantic Multidecadal Oscillation through the last 8,000 years. *Nature communication* 2: 178.

Koslowski G. and Loewe P. (1994) The western Baltic sea ice season in terms of a mass‐related severity index: 1879–1992. *Tellus A* 46: 66–74.

Kristjánsdóttir G.B. (2005) Holocene climatic and environmental changes on the Iceland shelf: d18O, Mg/Ca, and tephrochronology of core MD99-2269. Ph. D. Thesis - University of Colorado, Boulder, Colo.

Kristjánsdóttir G.B., Lea D.W., Jennings a. E., Pak D.K. and Belanger C. (2007) New spatial Mg/Ca-temperature calibrations for three Arctic, benthic foraminifera and reconstruction of north Iceland shelf temperature for the past 4000 years. *Geochemistry Geophysics Geosystems* 8(3): 1–27.

Krossa V.R., Moros M., Blanz T., Jansen E. and Schneider R. (2015) Late Holocene Baltic Sea outflow changes reconstructed using C37: 4 content from marine cores. *Boreas* 44(1): 81–93.

Kuehn S.C., Froese D.G. and Shane P. a. R. (2011) The INTAV intercomparison of electron-beam microanalysis of glass by tephrochronology laboratories: Results and recommendations. *Quaternary International* 246(1-2): 19–47.

Laskar J., Robutel P., Joutel F., Gastineau M., Correia A.C.M. and Levrard B. (2004) A long-term numerical solution for the insolation quantities of the Earth. *Astronomy and Astrophysics* 428: 261–285.

Lau K.-M. and Weng H. (1995) Climate signal detection using wavelet transform: how to make a time series sing. *Bulletin of the American Meteorological Society* 76: 2391–2402.

Lea D., Mashiotta T. and Spero H. (1999) Controls on magnesium and strontium uptake in planktonic foraminifera determined by live culturing. *Geochimica et Cosmochimica Acta* 63(16): 2369–2379.

Leduc G., Schneider R., Kim J. and Lohmann G. (2010) Holocene and Eemian sea surface temperature trends as revealed by alkenone and Mg/Ca paleothermometry. *Quaternary science reviews* 29: 989–1004.

Liu Z., Zhu J., Rosenthal Y., Zhang X., Otto-Bliesner B.L., Timmermann A., et al. (2014) The Holocene temperature conundrum. *Proceedings of the National Academy of Sciences* 111(34): E3501–E3505.

Ljøen R. and Svansson A. (1972) Long-term variations of subsurface temperatures in the Skagerrak. *Deep Sea Research* 19: 277–288.

Locarnini R.A., Mishonov A.V., Antonov J.I., Boyer T.P., Garcia H.E., Baranova O.K., et al. (2010) *World Ocean Atlas 2009, vol. 1: temperature*. , 184.

Mangini a., Spötl C. and Verdes P. (2005) Reconstruction of temperature in the Central Alps during the past 2000 yr from a δ18O stalagmite record. *Earth and Planetary Science Letters* 235(3-4): 741–751.

Mangini a., Verdes P., Spötl C., Scholz D., Vollweiler N. and Kromer B. (2007) Persistent influence of the North Atlantic hydrography on central European winter temperature during the last 9000 years. *Geophysical Research Letters* 34(2): L02704.

Martin P. and Lea D. (2002) A simple evaluation of cleaning procedures on fossil benthic foraminiferal Mg/Ca. *Geochemistry, Geophysics, Geosystems* 3(10): 8401.

Mayewski P., Rohling E., Curtstager J., Karlen W., Maasch K., Davidmeeker L., et al. (2004) Holocene climate variability. *Quaternary Research* 62(3): 243–255.

Mikalsen G. and Sejrup H.P. (2000) Oxygen Isotope Composition of Fjord and River Water in the Sognefjorden Drainage Area, Western Norway. Implications for Paleoclimate Studies. *Estuarine, Coastal and Shelf Science* 50(4): 441–448.

Moore P., Webb J. and Collison M. (1991) *Pollen analysis. London, etc.: Hodder & Stoughton*. Blackwell Science, 216.

Moreno A., Pérez A., Frigola J., Nieto-Moreno V., Rodrigo-Gámiz M., Martrat B., et al. (2012) The Medieval Climate Anomaly in the Iberian Peninsula reconstructed from marine and lake records. *Quaternary Science Reviews* 43: 16–32.

Moros M., Emeis K., Risebrobakken B., Kuijpers A., Snowball I., Mcmanus J., et al. (2004) Sea surface temperatures and ice rafting in the Holocene North Atlantic: climate influences on northern Europe and Greenland. *Quaternary Science Reviews* 23(20-22): 2113–2126.

Müller J. (2011) *Megaliths and Funnel Beakers: Societies in Change 4100-2700 BC*. Amsterdam: Drieendertigste Kroon-Voordracht.

Müller J. ((n.d.)) Crisis – what crisis? Innovation: different approaches to climatic change around 2200 BC. In: Meller H (ed) *4200 BP event*. Halle: Landesmuseum Halle.

Nesje A., Matthews J. a., Dahl O., Berrisford M.S. and Andersson C. (2001) Holocene glacier fluctuations of Flatebreen and winter-precipitation changes in the Jostedalsbreen region, western Norway, based on glaciolacustrine sediment records. *The Holocene* 11(3): 267–280.

Nürnberg D., Bijma J. and Hemleben C. (1996) Assessing the reliability of magnesium in foraminiferal calcite as a proxy for water mass temperatures. *Geochimica et Cosmochimica Acta* 60(5): 803–814.

O'Brien S.R., Mayewski P.A., Meeker L.D., Meese D.A., Twickler M.S. and Whitlow S. (1995) Reconstructed from a Greenland Ice Core. *Science* 270: 1962–1964.

Ólafsdóttir K.B., Geirsdóttir Á., Miller G.H. and Larsen D.J. (2013) Evolution of NAO and AMO strength and cyclicity derived from a 3-ka varve-thickness record from Iceland. *Quaternary Science Reviews*. Elsevier Ltd 69: 142–154.

Olsen J., Anderson N.J. and Knudsen M.F. (2012) Variability of the North Atlantic Oscillation over the past 5,200 years. *Nature Geoscience*. Nature Publishing Group 5(11): 808–812.

Omstedt A. and Chen D. (2001) Influence of atmospheric circulation on the maximum ice extent in the Baltic Sea. *Journal of Geophysical Research: Oceans* 106: 4493–4500.

Oppo D.W., McManus J.F. and L C.J. (2003) Deepwater variability in the Holocene Epoch. *Nature communications* 422: 277–278.

Otto L., Zimmerman T., Furnes G., Mork M., Saetre R. and Becker G. (1990) Review of the physical oceanography of the North Sea. *Netherlands Journal of Sea Research* 26(2-4): 161–238.

Parker A.G., Goudie A.S., Anderson D.E., Robinson M.A. and Bonsall C. (2002) A review of the mid-Holocene elm decline in the British Isles. *Progress in Physical Geography* 26(1): 1–45.

Pilcher J.R. and Hall V.A. (1996) Tephrochronological studies in northern England. *The Holocene* 6(1): 100–105.

Raitzsch M., Kuhnert H., Groeneveld J. and Bickert T. (2008) Benthic foraminifer Mg/Ca anomalies in South Atlantic core top sediments and their implications for paleothermometry. *Geochemistry Geophysics Geosystems* 9(Q05010).

Reimer P.J., Bard E., Bayliss A., Beck J.W., Blackwell P.G., Bronk Ramsey C., et al. (2013) IntCal13 and Marine13 radiocarbon age calibration curves 0-50,000 years cal BP. *Radiocarbon* 55(4): 1869–1887.

Risebrobakken B., Jansen E., Andersson C., Mjelde E. and Hevrøy K. (2003) A high-resolution study of Holocene paleoclimatic and paleoceanographic changes in the Nordic Seas. *Palaeoceanography* 18(1).

Robson J., Sutton R. and Smith D. (2012) Initialized decadal predictions of the rapid warming of the North Atlantic Ocean in the mid 1990s. *Geophysical Research Letters* 39: L19713.

Rodhe J. (1987) The large-scale circulation in the Skagerrak ; interpretation of some observations. *Tellus A* 39(1-3): 245–253.

Rodhe J. and Holt N. (1996) Observations of the transport of suspended matter into the Skagerrak along the western and northern coast of Jutland. *Journal of Sea Research* 35(1-3): 91–98.

Rossi A., Massei N. and Laignel B. (2011) A synthesis of the time-scale variability of commonly used climate indices using continuous wavelet transform. *Global and Planetary Change*. Elsevier B.V. 78: 1–13.

Schlesinger M.E. and Ramankutty N. (1994) An oscillation in the global climate system of period 65-70 years. *Nature* 367: 723–726.

Schmidt M., Spero H. and Lea D. (2004) Links between salinity variation in the Caribbean and North Atlantic thermohaline circulation. *Nature* 428: 160–163.

Schulz M. and Mudelsee M. (2002) REDFIT: estimating red-noise spectra directly from unevenly spaced paleoclimatic time series. *Computers & Geosciences* 28(3): 421–426.

Seppä H., Birks H., Giesecke T., Hammarlund D., Alenius T., Antonsson K., et al. (2007) Spatial structure of the 8200 cal yr BP event in northern Europe. *Climate of the Past* 3: 225–236.

Seppä H. and Birks H.J.B. (2001) July mean temperature and annual precipitation trends during the Holocene in the Fennoscandian tree-line area: pollen-based climate reconstructions. *The Holocene* 11(5): 527–539.

Seppä H., Bjune A., Telford R., Birks H. and Veski S. (2009) Last nine-thousand years of temperature variability in Northern Europe. *Climate Of The Past* 5: 523–535.

Shackleton N. (1974) Attainment of isotopic equilibrium between ocean water and the benthonic foraminifera genus Uvigerina: Isotopic changes in the ocean during the last glacial. *Colloques Internationaux du C.N.R.S.* 219: 203–209.

Shennan S., Downey S., Timpson A., Edinborough K., Colledge S., Kerig T., et al. (2013) Regional population collapse followed initial agriculture booms in mid-Holocene Europe. *Nature communications* 4.

Sicre M.-A., Yiou P., Eiríksson J., Ezat U., Guimbaut E., Dahhaoui I., et al. (2008) A 4500-year reconstruction of sea surface temperature variability at decadal time-scales off North Iceland. *Quaternary Science Reviews* 27(21-22): 2041–2047.

Snowball I., Sandgren P. and Petterson G. (1999) The mineral magnetic properties of an annually laminated Holocene lake-sediment sequence in northern Sweden. *The Holocene* 9(3): 353–362.

Sørensen L. and Karg S. (2014) The expansion of agrarian societies towards the north – new evidence for agriculture during the Mesolithic/Neolithic transition in Southern Scandinavia. *Journal of Archaeological Science*. Elsevier Ltd 51: 98–114.

Spangehl T., Cubasch U., Raible C.C., Schimanke S., Körper J. and Hofer D. (2010) Transient climate simulations from the Maunder Minimum to present day: Role of the stratosphere. *Journal of Geophysical Research* 115.

Staubwasser M., Sirocko F., Grootes P. and Segl M. (2003) Climate change at the 4.2 ka BP termination of the Indus valley civilization and Holocene south Asian monsoon variability. *Geophysical Research Letters* 30(8): 1425.

Stockmarr J. (1971) Tablets with spores used in absolute pollen analysis. *Pollen et Spores* 13: 615–621.

Sutton R.T. and Hodson D.L.R. (2003) Influence of the Ocean on North Atlantic Climate Variability 1871 – 1999. *Journal of Climate* 16: 3296–3313.

Svansson A. (1975) *Physical and chemical oceanography of the Skagerrak and the Kattegat. I. Open Sea Conditions. Report of Fishery Board of Sweden Institute of Marine Research No. 1.*, 88.

Thomson D. (1990) Time series analysis of Holocene climate data. *Philosophical Transactions of the Royal Society of London. Series A, Mathematical and Physical Sciences* 330(1615): 601–616.

Thornalley D.J.R., Elderfield H. and McCave I.N. (2009) Holocene oscillations in temperature and salinity of the surface subpolar North Atlantic. *Nature* 457(7230): 711–714.

Tinz B. (1996) On the relation between annual maximum extent of ice cover in the Baltic Sea and sea level pressure as well as air temperature field. *Geophysica* 32: 319–341.

Torrence C. and Compo G.P. (1998) A Practical Guide to Wavelet Analysis. *Bulletin of the American Meteorological Society*. American Meteorological Society 79: 61–78.

Trouet V., Esper J., Graham N.E., Baker A., Scourse J.D. and Frank D.C. (2009) Persistent positive North Atlantic oscillation mode dominated the Medieval Climate Anomaly. *Science* 324(5923): 78–80.

Trouet V., Scourse J.D. and Raible C.C. (2012) North Atlantic storminess and Atlantic Meridional Overturning Circulation during the last Millennium: Reconciling contradictory proxy records of NAO variability. *Global and Planetary Change*. Elsevier B.V. 84-85: 48–55.

Tunberg B. and Nelson W. (1998) Do climatic oscillations influence cyclical patterns of soft bottom macrobenthic communities on the Swedish west coast? *Marine Ecology Progress Series* 170: 85–94.

Van den Bogaard C., Dörfler W., Glos R., Nadeau M.-J., Grootes P.M. and Erlenkeuser H. (2002) Two tephra layers bracketing late Holocene paleoecological changes in northern Germany. *Quaternary Research* 57: 314–324.

Van den Bogaard C. and Schmincke H.-U. (2002) Linking the North Atlantic to central Europe: a high-resolution Holocene tephrochronological record from northern Germany. *Journal of Quaternary Science* 17(1): 3–20.

Villiers S. de, Greaves M. and Elderfield H. (2002) An intensity ratio calibration method for the accurate determination of Mg/Ca and Sr/Ca of marine carbonates by ICP‐AES. *Geochemistry, Geophysics, Geosystems* 3(1): 1001.

Vorren K.-D., Blaauw M., Wastegård S., Van Der Plicht J. and Jensen C. (2007) High-resolution stratigraphy of the northernmost concentric raised bog in Europe: Sellevollmyra, Andøya, northern Norway. *Boreas* 36(3): 253–277.

Walker M., Berkelhammer M., Björck S., Cwynar L.C., Fisher D.A., Long A.J., et al. (2012) Formal subdivision of the Holocene Series/Epoch: a Discussion Paper by a Working Group of INTIMATE (Integration of ice‐core, marine and terrestrial records) and. *Journal of Quaternary Science* 27(7): 649–659.

Walker M., Johnsen S., Rasmussen S., Popp T., Steffensen J.P., Gibbard P., et al. (2009) Formal definition and dating of the GSSP (Global Stratotype Section and Point) for the base of the Holocene using the Greenland NGRIP ice core, and selected auxiliary records. *Journal of Quaternary Science* 24(1): 3–17.

Walter K. and Graf H. (2002) On the changing nature of the regional connection between the North Atlantic Oscillation and sea surface temperature. *Journal of geophysical research* 107(D17): 4338.

Wanner H., Beer J., Bütikofer J., Crowley T.J., Cubasch U., Flückiger J., et al. (2008) Mid- to Late holocene climate change : an overview. *Quaternary Science Reviews* 27: 1791–1828.

Wanner H. and Bütikofer J. (2008) Holocene Bond Cycles: real or imaginary. *Geografie* 4(113): 338–349.

Wanner H., Mercolli L., Grosjean M. and Ritz S.P. (2014) Holocene climate variability and change; a data-based review. *Journal of the Geological Society* 172(2): 254–263.

Wanner H., Solomina O., Grosjean M., Ritz S.P. and Jetel M. (2011) Structure and origin of Holocene cold events. *Quaternary Science Reviews*. Elsevier Ltd 30(21-22): 3109–3123.

Wastegård S. (2005) Late Quaternary tephrochronology of Sweden: a review. *Quaternary International* 130(1): 49–62.

Wei W. and Lohmann G. (2012) Simulated atlantic multidecadal oscillation during the holocene. *Journal of Climate* 25: 6989–7002.

Weltje G.J. and Tjallingii R. (2008) Calibration of XRF core scanners for quantitative geochemical logging of sediment cores: Theory and application. *Earth and Planetary Science Letters* 274: 423–438.

Wyatt M.G., Kravtsov S. and Tsonis A. a (2012) Atlantic Multidecadal Oscillation and Northern Hemisphere's climate variability. *Climate Dynamics* 38(5-6): 929–949.

Xoplaki E., Luterbacher J., Paeth H., Dietrich D., Steiner N., Grosjean M., et al. (2005) European spring and autumn temperature variability and change of extremes over the last half millennium. *Geophysical Research Letters* 32(15): L15713.

Zahrer J. (2012) *Hochauflösende Rekonstruktion der kontinentalen Klima-und Umweltentwicklung während der Trichterbecherzeit in Seeeinzugsgebieten*. Dissertation an der Christian-Albrechts-Universität zu Kiel: Shaker-Verlag Aachen.

Zillén L., Wastegård S. and Snowball I. (2002) Calendar year ages of three mid-Holocene tephra layers identified in varved lake sediments in west central Sweden. *Quaternary Science Reviews* 21: 1583–1591.

LIST OF FIGURES

Figure 5.2: Evolution of instrumental temperatures at different depths in the Skagerrak basin, depicting the difference between the intermediate and the deep-waters annual variability between 1947 and 1969 CE (from Ljøen and Svansson, 1972). The cores used in this study are represented at their respective depth on a profile of the Skagerrak basin.

Figure 5.3: Winter air temperatures from central England (mean of December, January and February, from the HadCET dataset) and Skagerrak deep-water temperatures (bottle data from the Ocean Data View, measurements below 400m) between 1950 and 1960 CE. The thicker lines represent a five years average.

Figure 5.4: Top: Age-depth relation of radiocarbon calibrated age model for core IOW225514 and IOW225517. Bottom: Ca/K ratio from XRF measurements for core IOW225514 and IOW225517. XRF measurements were performed on XRF Avaatech core scanner from Kiel University, with the following settings: 15 seconds measurement time in a 1.2x1 cm rectangle, operated at 10kV and 30kV.

Figure 5.5: *M. barleeanus* Mg/Ca on intermediate (IOW225517) and deep (IOW225514) cores and *M. barleeanus* $\delta^{18}O$ of the deep core, and derived temperature reconstructions. The error bar indicates analytical error for Mg/Ca reconstructions. The stable isotope record is corrected for vital effect and ice volume (see references in the methods).

Figure 5.6: A) Winter and summer insolations at 58°N (Laskar et al., 2004), B) Skagerrak sea surface temperatures, core IOW225514 (Krossa, personal communication, 2015), C) intermediate and deep-water temperatures, D) deep-water salinity (represented by δw), E) winter precipitations documented from Norway (Nesje et al., 2001). Note that the solid lines in B, C, and D represent a 5 points running mean. Periods of relatively cold and less saline deep waters are highlighted by grey areas.

Figure 6.1: Top: Skagerrak deep and intermediate-water temperatures based on *M.barleeanus* Mg/Ca-thermometry of core IOW225514 and IOW225517, respectively. Bottom: Oxygen isotopes of *M.barleeanus* from the core IOW225514.

Figure 6.2: Spectral analysis on sea surface, intermediate and deep records from the western Skagerrak. The top figure shows analysis on IWT from core IOW225517, and the bottom figure, analysis on deep-water temperatures (DWT) and $d^{18}O$ from core IOW225514. In all representations, the top line represents the critical false-alarm for the designated spectrum (generally around 99%) and the bottom line the 95% false-alarm curve. Peaks exceeding the 95% curve are highlighted and will be discuss in the text.

Figure 6.3: Morlet wavelet transform on the deep-water temperatures (core IOW225514). The contoured area represent the significance level ($p>0.005$). Area below the black line is the cone of influence (COI), representing the region of the wavelet spectrum in which edge effects become important.

Figure 7.1: Comparison of regional climate records (Butruille et al., in press; Zahrer, 2012) and changes in population density (Hinz et al., 2012). A-B; 5-points running mean of intermediate-water temperatures (A) and deep-water temperatures (B) reconstructions, representing the regional warm season and winter conditions, respectively (Butruille et al., in press); C: Winter and summer conditions based on micropaleonthological and geochemical analyses from lake Belau in northern Germany (Zahrer, 2012); D: Sum-calibrated probabilities from northern Germany and southern Scandinavia, representing the population density of the region (Hinz et al., 2012). The highlighted area represents the onset of agriculture.

Figure 7.2: Warm season and winter temperature estimates based on intermediate and deep-water temperature reconstructions (5-points running mean) from the Skagerrak (Butruille et al., in press) and from lake Belau in northern Germany (Zahrer, 2012), and the evolution of the main crops used by agrarian communities in northern Germany (Kirleis and Fischer, 2014).

LIST OF TABLES

ACKNOWLEDGMENTS

First and foremost, I want to thank my supervisors Mara Weinelt and Ralph Schneider, for giving me the opportunity to work on this subject. I was really blessed to be able to work on paleoclimatology with an archaeological perspective, as it has always been a subject of interest for me. I am thankful to them both for their guidance and their advices through my PhD years. In particular, I am grateful to my main supervisor, Mara Weinelt, for being available as often as possible for discussion. Mara is also really enthusiastic about the collaboration with archaeologists and has encouraged me to participate in various meetings, workshops or conferences with them.

The present project is part of the Priority Program 1140 “Early Monumentality and Social Differentiation, On the origin and development of Neolithic large-scale buildings and the emergence of early complex societies in Northern Central Europe”, and is founded by the DFG (Deutsche Forschungsgemeinschaft ; German Research Foundation). Additionally, it is part of the Graduate School “Human Development in Landscapes”, which founded my scholarship. Although I was not directly affiliated to the Institute of Geosciences in Kiel, I have benefited from the knowledge of my colleagues there and I am thankful for the many meetings and discussion about each other subjects.

I would like to thank Dieter Garbe-Schönberg for his help on both XRF and Mg/Ca procedures and to Ann Holbourn, Markus Regenberg and Tim Bolliet for their help on the different foraminifera preparations. Many thanks to Marie-José Nadeau and Nils Andersen for the quick handling of my samples on radiocarbon and stable isotopes, and for answering my questions on the subjects. Many thanks also to Carsten Lemmen who helped me with the time series analyses and introduced me to REDFIT. I am very grateful to the colleagues who also helped me with the redaction and the review of my work. In particular to Guillaume Leduc, Janne Repschläger, Christian Schwab and Veronica R. Krossa. Thank you also Veronica and Guillaume for all the nice discussions work-related or not, when we shared an office. Thank you Veronica also for your support and advices, I am glad we could help and rely on each other for our common subject.

Many thanks also to all my colleagues in archaeology, directly connected to my own subject or not. First of all, I am grateful to Johannes Müller, director of the pre- and proto-history institute (UFG) in Kiel, for his enthusiasm and his interest in my work, and for the numerous exchanges. I am also thankful to Walter Dörfler and Christel van den Bogaard for helping me with tephra and pollen analyses, and for the many discussions on the subject. Many thanks also to the technicians of the pollen laboratory of the UFG for their help, and the Hiwis that helped me with the many cleaning procedures. Thank you to Martin Hinz, Wiebke Kirleis and again Johannes Müller for their help with the different aspects of archaeology I could integrate into my work. I would like to thank all my colleagues from the UFG, for the fascinating talks and anecdotes about their own work and for their kindness. Thanks to Jutta Kneisel, Doris and Carsten Mischka, Christoph Rinne, Christian Horn, Ines Reese and many others. I also want to thank all my colleagues from the Graduate School "Human development in Landscape" (GSHDL). Many of them are or were PhD students with me and it was like a big family. From the Graduate School, I want to thank Rhina Colunge Peters in particular, for her help and patience with all the administrative aspects of the graduate school at the beginning of my work in the GSHDL.

I would like to thank my friends for all the support they gave me through those years. I am very glad to have met some very important friends in Kiel, and without you I would never have managed those difficult years. Thank you Fabi, Martin, Marta, Vincent, Daniel, Miriam, Thies, Steffi, David, Florian, Nicole, and Marion. You are all very dear to me. Many thank also in particular to Florian, Miriam, Thies, Jutta and Fabi for helping me with my health or with the complexity of the German administration. A special thanks to Vanessa, my long-lasting friend from France, you are always there to share some fun time when I am back in France and I am looking forward to welcoming you in Kiel anytime.

Pour finir, je voudrais remercier toute ma famille. Un énorme merci à mes parents pour leur soutien inconditionnel et leur aide que ce soit au niveau moral, intellectuel, financier, organisationnel ou gastronomique (petits plats et restaurants). Merci aussi à mes frères, Julien et Florent, qui malgré la distance ont toujours été prêts à m'aider pour mon travail ou pour me changer les idées. C'est aussi ça l'esprit COGIP. Merci à mes oncles, tantes, cousins et cousines (et petite cousine) pour leur soutien. Et enfin merci à mes grand-parents, Clara, Marcel et Martha, qui nous auront quitté trop tôt, et Elise et Daniel qui j'espère seront encore avec nous longtemps… Je vous aime.

ANNEXES

Geochemical analyses on tephra particles

	SiO2	TiO2	Al2O3	FeO	MnO	MgO	CaO	Na2O	K2O	P2O5	F	SO3	Cl	Σ(total analyses)
IOW225514														
180cm	71,83	0,21	14,25	3,71	0,1	0	2,28	4,84	2,48	0	0,2	0,02	0,08	98,42
	75,42	0,15	13,33	1,9	0,05	0	1,43	4,64	2,89	0,01	0,08	0	0,09	95,35
	75,51	0,15	13,1	2,02	0,07	0	1,43	4,61	2,95	0	0,07	0	0,09	97,35
	75,8	0,09	13,33	1,82	0,09	0,01	1,25	4,4	3,06	0	0,06	0	0,09	95,5
	72,76	0,19	14,24	2,89	0,11	0,15	2,01	4,96	2,45	0,06	0,04	0,03	0,1	97,53
	67,77	0,38	14,42	6,25	0,17	0,14	3,38	5	2,13	0,08	0,14	0	0,15	93,67
	75,5	0,08	13,19	1,98	0,06	0,03	1,43	4,63	2,85	0	0,14	0,02	0,09	95,02
	75,43	0,11	13,47	2,01	0,01	0,02	1,37	4,5	2,87	0,02	0,09	0,01	0,09	95,08
	71,73	0,3	13,5	3,82	0,1	0,2	1,33	5,03	3,59	0,06	0,14	0,02	0,18	96,32
	71,66	0,3	13,58	3,86	0,17	0,21	1,34	5,05	3,54	0,02	0,09	0,02	0,17	98,93
	71,61	0,29	13,69	3,63	0,12	0,21	1,39	5,16	3,51	0,02	0,17	0,01	0,19	98,32
	75,08	0,14	13,47	1,95	0,11	0	1,3	4,85	2,87	0	0,17	0	0,08	98,44
	75,63	0,11	13,3	1,65	0,06	0	1,17	5,02	2,87	0	0,13	0	0,06	97,53
	75,84	0,08	13,3	1,65	0,04	0,01	1,18	4,78	2,95	0,02	0,06	0,01	0,1	96,73
	75,21	0,12	13,29	2,03	0,04	0,02	1,36	4,74	2,95	0	0,12	0,01	0,09	97,69
	75,25	0,1	13,26	2	0,1	0,02	1,44	4,74	2,94	0,02	0,04	0	0,09	97,13
	75,7	0,1	13,23	1,69	0,09	0,02	1,37	4,65	2,98	0,01	0,08	0	0,09	96,76
	75,16	0,09	13,52	1,86	0,04	0,03	1,44	4,72	2,89	0,01	0,13	0,01	0,09	95,78
IOW225517														
97 cm	75,22	0,1	13,07	2,12	0,06	0,02	1,32	4,87	2,84	0,04	0,17	0	0,19	93,97
	67,1	0,42	15,09	5,28	0,2	0,52	3,3	5,64	2,09	0,09	0,01	0,01	0,23	93,88
	75,1	0,14	13,2	1,82	0,09	0,01	1,37	5,18	2,86	0,01	0,08	0	0,13	94,01
	73,1	0,17	13,88	2,9	0,1	0,16	1,98	5,04	2,53	0	0,06	0,02	0,07	97,06
	75,43	0,1	13,14	2,02	0,06	0,04	1,38	4,71	2,9	0	0,09	0,01	0,13	93,6
	76,24	0,09	12,96	1,56	0,02	0,01	1,27	4,72	2,9	0	0,11	0	0,11	94,99
155 cm	67,26	0,41	14,79	6,5	0,21	0,21	3,55	4,91	1,99	0,03	0,05	0	0,1	97,37

Pollen counts

CORE IOW225517

	Depth	213	224	232	241	249	257	266	272	280	290	295	300
	Yrs BP	5382	5474	5537	5594	5644	5798	5998	6132	6310	6533	6644	6755
Pollen type													
Acer (MAPLE)		+	0	0	0	0	0	0	0	0	0	0	0
Alnus (ALDER)		7	8	12	13	20	7	8	18	13	2	6	5
Anthemis-type		0	0	0	0	0	0	0	0	1	0	0	0
Artemisia (MUGWORT)		4	5	8	5	4	1	0	2	2	0	0	0
Betula (BIRCH)		14	9	9	9	9	7	5	12	8	6	8	12
Bidens-type		+	0	+	0	0	1	0	0	0	0	0	1
Calluna (LING)		0	0	0	0	2	0	3	+	0	+	0	0
Carpinus		0	0	1	0	1	0	0	0	+	0	0	0
Caryophyllaceae p,p,		0	0	0	0	0	0	0	0	0	0	1	0
Cereal-type		0	0	+	2	0	0	1	1	+	0	0	0
Chenopodiaceae		4	2	2	0	+	0	1	2	+	1	0	3
Corylus (HAZEL)		9	4	3	5	10	8	3	8	5	6	9	8
Brassicaceae		2	0	0	0	1	0	1	2	0	0	0	0
Cyperaceae p,p,		1	0	0	1	0	0	0	0	0	0	0	0
Empetrum		0	1	1	0	0	0	0	0	0	0	0	0
Fagus (BEECH)		0	0	1	1	2	1	0	2	2	1	0	+
Filipendula		0	0	1	0	0	0	0	0	0	0	0	0
Frangula alnus		0	0	0	0	0	0	0	0	+	0	0	0
Fraxinus (ASH)		1	1	1	0	2	1	0	1	+	0	0	0
Gentiana pneumonanthe-type		0	0	0	0	0	0	0	0	0	0	1	0
Poaceae		4	2	3	2	2	3	6	0	3	+	0	1
Hystrichaceae		562	384	447	484	347	459	445	242	362	450	611	825
Corroded grains		1	2	1	1	1	1	2	0	1	0	1	0
Liguliflorae		0	0	0	0	0	0	0	0	0	0	0	1
Lycopodium clavatum		0	0	0	1	1	0	1	1	+	1	+	3
Myriophyllum alternifl,		0	0	+	0	0	0	0	0	0	0	0	0
Pediastrum		2	2	2	1	1	1	0	1	0	0	1	2
Picea (SPRUCE)		1,5	1	2,5	0	1,5	2	1	+	++	1	0	2,5
Pinus (PINE)		121	110	117,5	101,5	99,5	140	120	110	142	163,5	154	151,5
Plantago lanceolata		0	0	1	+	0	1	0	0	0	0	0	0
Polygonum aviculare		0	0	0	0	0	0	0	0	+	0	0	0
Monolete fern spore (-perine)		25	16	12	10	9	27	12	17	14	21	27	19
Polypodium vulgare		4	2	0	1	1	0	1	1	1	1	2	0
Pteridium (BRACKEN)		+	1	4	0	2	3	2	4	+	3	4	2
Quercus (OAK)		33	26	26	25	20	8	14	11	11	8	14	9
Rumex acetosa-type		0	0	0	0	0	0	0	0	1	1	0	0
Secale-type (RYE)		1	1	1	0	+	0	0	0	0	0	0	0
Silene dioica		0	0	0	0	0	+	0	0	0	0	0	0
Sorbus		0	0	0	0	0	+	0	0	0	0	0	0
Sparganium-type (Beug)		0	0	0	0	0	0	0	0	0	+	0	+
Sphagnum		8	5	4	6	8	4	4	5	4	3	7	2
Tilia cordata-type		1	+	0	3	1	1	1	1	0	+	2	1
Ulmus (ELM)		3	1	0	0	2	0	2	0	2	0	3	2
Apiaceae p,p,		1	0	0	0	0	0	0	0	0	0	0	0
unbekannte Spore		1	1	0	0	0	0	1	0	0	0	0	0
Vaccinium-type		0	0	0	0	0	0	0	0	0	0	1	0
Valerianella		0	0	1	0	0	0	0	0	0	0	0	0
Vitis		0	0	0	0	0	1	0	0	0	0	0	0

***Melonis barleeanus* Mg/Ca analyses**

CORE IOW225514

Depth	cal BP	Mg/Ca	t°C
45	769	1,48	5,92
55	861	1,55	6,25
65	952	1,60	6,49
70	998	1,79	7,31
85	1135	1,72	7,00
90	1180	1,80	7,33
95	1226	1,97	7,99
100	1272	1,45	5,76
107	1333	1,71	6,97
113	1376	1,63	6,62
117	1405	1,71	6,97
119	1420	1,67	6,79
121	1434	1,55	6,26
123	1449	1,47	5,84
125	1463	1,56	6,31
127	1478	1,28	4,88
133	1521	1,52	6,13
135	1535	1,45	5,76
137	1609	1,31	5,04
139	1703	1,45	5,76
141	1797	1,51	6,04
143	1891	1,55	6,27
145	1985	1,48	5,92
147	2078	1,66	6,77
153	2360	1,47	5,86
155	2454	1,43	5,67
157	2500	1,41	5,55
159	2530	1,56	6,28
161	2561	1,40	5,52
163	2591	1,49	5,97
165	2622	1,54	6,18
167	2652	1,50	6,00
173	2744	1,58	6,39
175	2774	1,43	5,68
177	2804	1,41	5,59
179	2835	1,46	5,82
181	2865	1,43	5,67
183	2896	1,43	5,68
185	2926	1,49	5,99
187	2957	1,49	5,98
189	2987	1,60	6,49
191	3018	1,50	6,02
193	3048	1,38	5,42
195	3079	1,55	6,24
197	3109	1,42	5,59
199	3140	1,48	5,90
209	3292	1,54	6,19
211	3322	1,39	5,47
213	3353	1,69	6,87
215	3383	1,46	5,81
217	3414	1,54	6,19
219	3440	1,49	5,97
221	3463	1,42	5,60
223	3486	1,55	6,23
225	3508	1,67	6,79
227	3531	1,41	5,58
228	3542	1,30	4,96

Depth	cal BP	Mg/Ca	t°C
229	3554	1,29	4,90
230	3565	1,38	5,40
231	3576	1,34	5,18
232	3588	1,37	5,34
233	3599	1,43	5,64
234	3610	1,31	5,04
236	3633	1,47	5,89
237	3644	1,32	5,11
238	3656	1,37	5,33
239	3667	1,37	5,33
240	3678	1,45	5,74
241	3690	1,43	5,65
242	3701	1,43	5,66
243	3712	1,46	5,84
244	3724	1,43	5,68
245	3735	1,44	5,73
246	3746	1,38	5,40
247	3758	1,32	5,05
248	3769	1,40	5,52
253	3826	1,23	4,58
255	3849	1,32	5,05
256	3860	1,45	5,79
257	3871	1,30	4,99
258	3883	1,46	5,79
259	3894	1,54	6,22
260	3905	1,45	5,76
261	3917	1,52	6,10
262	3928	1,45	5,78
263	3939	1,39	5,44
264	3951	1,23	4,54
265	3962	1,36	5,30
266	3973	1,27	4,83
267	3985	1,36	5,32
268	3996	1,25	4,67
269	4007	1,36	5,30
270	4019	1,40	5,51
272	4041	1,18	4,29
273	4053	1,31	5,03
275	4075	1,32	5,06
276	4087	1,27	4,78
277	4098	1,44	5,73
278	4109	1,43	5,67
279	4121	1,42	5,61
280	4132	1,40	5,49
282	4155	1,20	4,40
283	4166	1,28	4,87
285	4189	1,39	5,45
286	4200	1,39	5,47
288	4223	1,23	4,58
289	4234	1,51	6,07
290	4245	1,36	5,31
292	4268	1,32	5,09
293	4279	1,13	3,97
294	4291	1,31	5,05
296	4313	1,37	5,34
297	4325	1,43	5,65
298	4336	1,85	7,53

Depth	cal BP	Mg/Ca	t°C
300	4359	1,43	5,67
301	4382	1,40	5,49
306	4496	1,55	6,27
307	4519	1,54	6,19
308	4542	1,53	6,18
309	4565	1,48	5,92
311	4611	1,48	5,91
312	4634	1,21	4,46
313	4656	1,32	5,10
314	4679	1,42	5,64
315	4702	1,24	4,62
316	4725	1,39	5,47
317	4748	1,35	5,26
318	4771	1,20	4,38
319	4794	1,42	5,61
320	4817	1,39	5,46
321	4840	1,33	5,12
322	4862	1,27	4,80
323	4885	1,54	6,22
324	4908	1,31	5,01
325	4931	1,51	6,06
326	4954	1,38	5,39
327	4977	1,40	5,51
328	5000	1,42	5,59
332	5091	1,39	5,43
333	5114	1,29	4,92
334	5137	1,58	6,40
335	5160	1,29	4,94
336	5183	1,29	4,92
337	5206	1,50	6,03
338	5229	1,38	5,42
339	5251	1,51	6,05
340	5274	1,28	4,87
341	5297	1,58	6,40
342	5320	1,57	6,35
343	5343	1,55	6,27
344	5366	1,29	4,94
345	5389	1,43	5,67
346	5412	1,38	5,43
348	5457	1,62	6,58
349	5480	1,61	6,52
350	5503	0,96	2,75
351	5526	1,49	5,98
352	5549	1,45	5,78
353	5572	1,76	7,19
354	5595	1,27	4,82
355	5618	1,24	4,63
356	5641	1,51	6,07
357	5663	1,44	5,74
358	5686	1,51	6,07
359	5709	1,42	5,62
360	5732	1,40	5,51
361	5755	1,42	5,60
362	5778	1,33	5,13
363	5801	1,56	6,31
364	5824	1,45	5,79
365	5847	1,21	4,47

Depth	cal BP	Mg/Ca	t°C
366	5869	1,52	6,09
367	5892	1,26	4,74
368	5915	1,08	3,63
370	5961	1,38	5,42
371	5984	1,35	5,24
372	6007	1,01	3,14
373	6030	1,44	5,74
377	6121	1,52	6,10
378	6144	1,67	6,78
379	6167	1,39	5,45
380	6190	1,08	3,59
381	6213	1,44	5,71
382	6236	1,33	5,16
383	6259	1,29	4,90
384	6281	1,85	7,53
386	6327	1,57	6,34
387	6350	1,48	5,91
390	6419	1,29	4,89
391	6442	1,54	6,23
392	6465	1,46	5,84
393	6487	1,67	6,78
394	6510	1,49	5,97
395	6533	1,59	6,45
396	6556	1,53	6,15
397	6579	1,67	6,78
398	6602	1,60	6,48
399	6625	1,73	7,05
400	6648	1,41	5,54
401	6670	1,60	6,47
403	6716	1,60	6,47
404	6739	1,67	6,81
405	6762	1,34	5,21
406	6785	1,55	6,25

***Melonis barleeanus* Mg/Ca analyses**

CORE IOW225517

depth	cal BP	Mg/Ca	t°C
10	1101	1,85	7,53
20	1324	1,29	4,91
26	1458	1,41	5,57
30	1547	1,41	5,54
40	1771	1,33	5,12
60	2293	2,05	8,29
70	2555	1,61	6,53
80	2817	2,01	8,14
100	3165	1,31	5,00
110	3359	1,36	5,29
114	3437	1,32	5,08
120	3553	1,20	4,41
130	3747	1,41	5,55
140	3941	1,19	4,34
150	4135	1,21	4,43
159	4381	1,91	7,77
160	4416	1,60	6,48
161	4441	1,53	6,18
162	4454	1,52	6,11
163	4467	1,40	5,49
164	4480	1,83	7,46
165	4493	1,78	7,28
166	4507	2,05	8,30
168	4533	1,99	8,06
169	4546	1,68	6,83
170	4559	1,77	7,22
171	4573	1,72	7,03
173	4599	1,87	7,62
174	4612	1,84	7,52
175	4625	1,38	5,42
176	4639	2,63	10,12
177	4652	1,71	6,98
178	4665	1,61	6,53
179	4678	1,67	6,80
180	4691	2,15	8,65
181	4705	1,53	6,18
182	4718	1,26	4,76
183	4731	1,43	5,66
184	4744	1,89	7,69
185	4757	1,87	7,62
186	4771	1,53	6,16
187	4784	1,75	7,16
189	4810	1,65	6,73
190	4823	1,63	6,62
191	4843	1,72	7,03
192	4869	1,74	7,08
193	4894	1,52	6,13
194	4920	1,62	6,58
195	4946	1,59	6,45
196	4971	1,62	6,57
197	4997	1,77	7,23
199	5048	1,72	7,03
200	5074	1,63	6,62
201	5100	1,32	5,07
202	5125	1,79	7,33
203	5151	1,88	7,65
204	5177	1,92	7,81
205	5202	1,71	6,99
206	5228	1,67	6,81
207	5254	1,92	7,80
208	5279	1,80	7,37
209	5305	1,79	7,30
210	5331	1,39	5,43
211	5356	1,59	6,42
212	5373	1,39	5,48
213	5382	1,55	6,24
214	5390	1,50	6,01
215	5398	1,73	7,05
216	5407	1,58	6,38
217	5415	1,32	5,09
218	5423	1,63	6,61
219	5432	1,92	7,81
220	5440	1,56	6,28
221	5449	1,60	6,49
222	5457	1,72	6,99
223	5465	1,46	5,84
226	5490	1,53	6,15
228	5507	1,46	5,81
229	5515	1,49	5,97
230	5524	1,38	5,39
231	5531	1,68	6,84
233	5544	1,65	6,72
234	5550	1,39	5,43
236	5562	1,56	6,32
237	5569	1,63	6,60
238	5575	1,47	5,85
239	5581	1,64	6,68
240	5587	1,83	7,48
241	5594	2,21	8,85
242	5600	1,53	6,17
243	5606	1,59	6,42
244	5612	1,62	6,56
245	5619	1,47	5,89
247	5631	2,18	8,74
248	5637	1,52	6,12
249	5644	1,68	6,83
250	5650	1,59	6,44
251	5664	1,48	5,92
252	5686	1,61	6,55
253	5709	1,82	7,42
254	5731	1,57	6,36
255	5753	2,18	8,74
256	5776	1,59	6,46
257	5798	1,60	6,48
258	5820	1,83	7,47
260	5865	1,48	5,90
261	5887	1,61	6,54
263	5931	1,78	7,24
264	5954	1,75	7,15
265	5976	1,53	6,14
267	6020	1,74	7,10
268	6043	1,61	6,52
269	6065	2,03	8,23
270	6087	1,74	7,08
272	6132	1,76	7,17
273	6154	1,52	6,13
274	6176	1,60	6,47
275	6199	1,58	6,37
276	6221	1,70	6,92
277	6243	1,66	6,77
278	6265	1,44	5,74
279	6288	2,24	8,94
280	6310	1,53	6,18
281	6332	1,76	7,17
282	6354	1,56	6,29
284	6399	1,87	7,62
285	6421	1,64	6,67
290	6533	1,23	4,55
293	6599	1,61	6,55
300	6755	1,45	5,76
304	6844	1,48	5,94
305	6867	1,48	5,93
306	6889	1,53	6,18
307	6911	1,66	6,75
310	6978	1,38	5,39
360	8258	2,58	9,97
361	8284	1,74	7,08
362	8309	1,79	7,32
363	8347	1,76	7,19
364	8396	1,73	7,05
370	8692	1,75	7,16
400	10174	1,98	8,04
410	10667	1,74	7,12
420	11161	1,75	7,16
430	11655	1,90	7,74
440	12149	2,00	8,13
450	12642	1,81	7,40

Melonis barleeanus **$\delta^{18}O$ raw and corrected for vital effect and ice volume (ve.vi)**

CORE IOW225514

depth	age BP	$\delta^{18}O$	$\delta^{18}O$ ve.iv
45	769	2,63	2,90
55	861	2,39	2,66
65	952	2,25	2,53
70	998	2,48	2,76
75	1043	2,22	2,49
85	1135	2,22	2,50
90	1180	2,26	2,53
95	1226	2,17	2,45
100	1272	2,39	2,66
113	1376	2,16	2,43
117	1405	2,32	2,60
119	1420	2,45	2,73
121	1434	2,37	2,64
123	1449	2,19	2,47
125	1463	2,31	2,59
127	1478	2,42	2,70
133	1521	2,47	2,75
135	1535	2,45	2,73
137	1609	2,61	2,88
139	1703	2,63	2,90
141	1797	2,43	2,71
143	1891	2,45	2,72
145	1985	2,71	2,98
147	2078	2,44	2,72
153	2360	2,45	2,72
155	2454	2,71	2,99
157	2500	2,60	2,88
159	2530	2,71	2,99
161	2561	2,76	3,04
163	2591	2,53	2,81
165	2622	2,49	2,77
167	2652	2,64	2,92
175	2774	2,40	2,67
177	2804	2,28	2,56
179	2835	2,38	2,66
181	2865	2,41	2,69
183	2896	2,27	2,55
185	2926	2,54	2,81
187	2957	2,37	2,65
189	2987	2,27	2,55
191	3018	2,45	2,72
193	3048	2,29	2,56
195	3079	2,40	2,68
197	3109	2,53	2,80
199	3140	2,29	2,56
209	3292	2,83	3,11
211	3322	2,46	2,73
213	3353	2,71	2,98
215	3383	2,97	3,25
217	3414	2,78	3,05
219	3440	2,56	2,83
221	3463	2,61	2,89
223	3486	2,53	2,80
225	3508	2,69	2,96
227	3531	2,60	2,88
228	3542	2,23	2,51
229	3554	2,31	2,58
230	3565	2,34	2,61
231	3576	2,49	2,77
232	3588	2,52	2,80
233	3599	2,51	2,79
234	3610	2,44	2,72
236	3633	2,49	2,76
237	3644	2,49	2,77
238	3656	2,52	2,80
239	3667	2,51	2,78
240	3678	2,52	2,79
241	3690	2,60	2,87
242	3701	2,54	2,82
243	3712	2,34	2,62
244	3724	2,63	2,91
245	3735	2,50	2,78
246	3746	2,39	2,67
247	3758	2,45	2,73
248	3769	2,48	2,76
253	3826	2,37	2,65
255	3849	2,40	2,68
256	3860	2,25	2,53
257	3871	2,39	2,67
258	3883	2,35	2,62
259	3894	2,52	2,80
260	3905	2,40	2,67
261	3917	2,34	2,61
262	3928	2,38	2,65
263	3939	2,68	2,95
264	3951	2,42	2,70
265	3962	2,28	2,56
266	3973	2,42	2,70
267	3985	2,51	2,78
268	3996	2,39	2,66
269	4007	2,31	2,58
270	4019	2,45	2,72
271	4030	2,42	2,70
272	4041	2,33	2,60
273	4053	2,35	2,62
275	4075	2,39	2,67
276	4087	2,39	2,67
277	4098	2,42	2,70
278	4109	2,43	2,70
279	4121	2,46	2,74
280	4132	2,13	2,41
282	4155	2,47	2,75
283	4166	2,36	2,63
284	4177	2,36	2,63
285	4189	2,45	2,72
286	4200	2,27	2,54
288	4223	2,48	2,75
289	4234	2,36	2,64
290	4245	2,51	2,79
292	4268	2,33	2,61
293	4279	2,28	2,56
294	4291	2,43	2,71
296	4313	2,23	2,50
297	4325	2,53	2,81
298	4336	2,53	2,80
299	4348	2,44	2,72
300	4359	2,31	2,59
301	4382	2,51	2,79
306	4496	2,63	2,91
307	4519	2,49	2,76
308	4542	2,35	2,62
309	4565	2,47	2,75
311	4611	2,49	2,77
313	4656	2,32	2,60
314	4679	2,41	2,68
315	4702	2,63	2,91
316	4725	2,63	2,90
317	4748	2,64	2,91
318	4771	2,51	2,79
319	4794	2,43	2,71
320	4817	2,44	2,71
321	4840	2,50	2,77
322	4862	2,39	2,66
323	4885	2,49	2,76
324	4908	2,42	2,70
325	4931	2,60	2,87
326	4954	2,59	2,87
327	4977	2,23	2,50
328	5000	2,91	3,18
332	5091	2,33	2,60
333	5114	2,59	2,86
334	5137	2,48	2,75
335	5160	2,57	2,85
336	5183	2,39	2,67
337	5206	2,52	2,79
338	5229	2,60	2,87
339	5251	2,59	2,86
340	5274	2,40	2,68
341	5297	2,38	2,66
342	5320	2,09	2,36
343	5343	2,05	2,33
344	5366	2,76	3,03
345	5389	2,67	2,94
346	5412	2,35	2,62
348	5457	2,26	2,53
349	5480	2,47	2,74
350	5503	2,43	2,70
351	5526	2,38	2,66
352	5549	2,29	2,56
353	5572	2,51	2,79
354	5595	2,53	2,81
355	5618	1,85	2,12
356	5641	2,37	2,64
357	5663	2,49	2,76
358	5686	2,55	2,82
359	5709	2,23	2,51
360	5732	2,56	2,83
361	5755	2,38	2,65
362	5778	2,53	2,80
363	5801	2,48	2,76
364	5824	2,63	2,91
365	5847	2,36	2,63
366	5869	2,47	2,74
367	5892	2,48	2,75
368	5915	2,55	2,83
369	5938	2,37	2,65
370	5961	2,40	2,67
371	5984	2,59	2,87
372	6007	2,67	2,60
373	6030	2,24	2,16
377	6121	2,36	2,28
378	6144	2,30	2,22
379	6167	2,17	2,09
380	6190	2,53	2,45
381	6213	2,23	2,15
382	6236	2,47	2,39
383	6259	2,31	2,23
384	6281	2,78	2,69
385	6304	2,68	2,59
386	6327	2,30	2,21
387	6350	2,73	2,64
389	6396	2,44	2,35
390	6419	2,42	2,32
391	6442	2,49	2,39
392	6465	2,47	2,37
393	6487	2,49	2,40
394	6510	2,37	2,27
395	6533	2,41	2,31
396	6556	2,31	2,21
397	6579	2,32	2,22
398	6602	2,47	2,36
399	6625	2,35	2,24
400	6648	2,38	2,27
401	6670	2,52	2,41
403	6716	2,26	2,15
404	6739	2,43	2,32
405	6762	2,83	2,72
406	6785	2,78	2,67

Melonis barleeanus **$\delta^{18}O$ raw and corrected for vital effect and ice volume (ve.vi)**

CORE IOW225517

depth	cal BP	$\delta^{18}O$	$\delta^{18}O$ ve.iv
10	1762	2,28	2,55
20	1889	2,35	2,63
26	1968	2,47	2,74
30	2021	2,58	2,86
40	2157	2,43	2,70
60	2441	2,47	2,75
70	2589	2,52	2,79
80	2742	2,42	2,69
100	3059	2,64	2,91
110	3224	2,61	2,89
114	3292	2,45	2,72
120	3394	2,78	3,05
130	3567	2,53	2,80
140	3745	2,71	2,99
150	3927	2,56	2,84
159	4094	2,34	2,61
160	4113	2,63	2,90
161	4131	2,76	3,04
162	4150	2,40	2,67
164	4188	2,31	2,58
166	4226	2,57	2,85
167	4245	2,31	2,58
169	4284	2,63	2,90
171	4322	2,50	2,77
173	4361	2,20	2,48
174	4380	2,17	2,45
176	4419	2,36	2,64
177	4438	2,64	2,91
178	4458	2,41	2,69
179	4478	2,61	2,89
180	4497	2,44	2,72
184	4576	2,43	2,70
185	4596	2,39	2,67
187	4636	2,43	2,71
189	4676	2,45	2,72
191	4716	2,47	2,74
192	4736	2,59	2,86
194	4776	2,35	2,63
195	4797	2,44	2,72
196	4817	2,48	2,75
197	4837	2,58	2,86
199	4878	2,41	2,69
201	4919	2,41	2,68
202	4939	2,47	2,75
203	4960	2,40	2,68
204	4981	2,39	2,67
205	5001	2,38	2,66
206	5022	2,41	2,69
207	5043	2,52	2,80
208	5064	2,35	2,62
209	5084	2,59	2,87
210	5105	2,50	2,78
215	5210	2,12	2,40
218	5274	2,34	2,62
219	5295	2,36	2,63

depth	cal BP	$\delta^{18}O$	$\delta^{18}O$ ve.iv
221	5338	2,50	2,78
222	5359	2,43	2,71
226	5445	2,54	2,82
229	5510	2,55	2,83
230	5532	2,44	2,72
231	5553	2,41	2,69
233	5597	2,44	2,72
236	5663	2,45	2,72
237	5685	2,47	2,75
239	5729	2,52	2,80
241	5773	2,80	3,08
242	5795	2,47	2,74
243	5818	2,53	2,80
244	5840	2,24	2,51
245	5862	2,45	2,72
247	5907	2,56	2,84
248	5930	2,34	2,62
249	5952	2,66	2,94
250	5975	2,50	2,78
253	6043	2,15	2,42
256	6111	2,30	2,58
261	6225	2,50	2,77
263	6272	2,44	2,71
264	6295	2,39	2,67
267	6364	2,31	2,51
268	6388	2,50	2,69
269	6411	2,28	2,47
272	6481	2,54	2,74
274	6528	2,51	2,70
275	6552	2,55	2,75
276	6576	2,33	2,51
277	6599	2,48	2,66
279	6647	2,47	2,66
280	6671	2,53	2,72
281	6694	2,52	2,70
284	6766	2,45	2,64
285	6790	2,45	2,62
290	6911	2,66	2,84
293	6984	2,44	2,61
300	7155	2,60	2,76
304	7254	2,39	2,56
305	7279	2,36	2,53
306	7304	2,84	3,01
307	7329	2,58	2,74
310	7404	2,57	2,72
370	8984	2,46	2,44
400	9830	2,98	2,65
410	10121	2,31	1,94
420	10416	2,53	2,11
430	10714	2,59	2,06
440	11017	2,83	2,21
450	11325	3,17	2,44

***Melonis barleeanus* $\delta^{13}C$ raw**

CORE IOW225514

depth	cal BP	$\delta^{13}C$
45	769	-0,64
55	861	-0,76
65	952	-0,68
70	998	-0,58
75	1043	-0,58
85	1135	-0,48
90	1180	-0,45
95	1226	-0,69
100	1272	-0,76
113	1376	-0,58
117	1405	-0,77
119	1420	-0,89
121	1434	-0,91
123	1449	-1,10
125	1463	-1,23
127	1478	-0,98
133	1521	-1,15
135	1535	-1,01
137	1609	-1,18
139	1703	-1,00
141	1797	-1,07
143	1891	-1,07
145	1985	-1,04
147	2078	-1,04
153	2360	-1,04
155	2454	-1,21
157	2500	-1,34
159	2530	-1,06
161	2561	-0,89
163	2591	-0,96
165	2622	-1,10
167	2652	-0,80
175	2774	-1,20
177	2804	-0,98
179	2835	-1,27
181	2865	-1,27
183	2896	-0,98
185	2926	-1,31
187	2957	-1,10
189	2987	-1,05
191	3018	-1,04
193	3048	-1,22
195	3079	-0,85
197	3109	-1,00
199	3140	-1,03
209	3292	-1,31
211	3322	-1,12
213	3353	-1,41
215	3383	-1,02
217	3414	-1,14
219	3440	-1,11
221	3463	-1,21
223	3486	-1,07
225	3508	-1,00
227	3531	-1,06
228	3542	-1,24
229	3554	-1,07

depth	cal BP	$\delta^{13}C$
230	3565	-1,05
231	3576	-1,04
232	3588	-0,92
233	3599	-0,98
234	3610	-1,11
236	3633	-0,89
237	3644	-1,15
238	3656	-1,26
239	3667	-1,11
240	3678	-0,96
241	3690	-1,28
242	3701	-1,27
243	3712	-0,95
244	3724	-1,19
245	3735	-1,21
246	3746	-1,13
247	3758	-1,09
248	3769	-1,07
253	3826	-1,13
255	3849	-1,20
256	3860	-1,39
257	3871	-1,37
258	3883	-1,13
259	3894	-1,38
260	3905	-0,88
261	3917	-0,91
262	3928	-1,23
263	3939	-1,10
264	3951	-1,15
265	3962	-1,32
266	3973	-1,28
267	3985	-1,11
268	3996	-1,17
269	4007	-1,30
270	4019	-1,41
271	4030	-1,29
272	4041	-1,17
273	4053	-1,17
275	4075	-1,10
276	4087	-1,30
277	4098	-0,99
278	4109	-1,10
279	4121	-1,22
280	4132	-1,09
282	4155	-1,22
283	4166	-0,92
284	4177	-0,85
285	4189	-1,17
286	4200	-1,07
288	4223	-0,86
289	4234	-1,06
290	4245	-1,01
292	4268	-1,38
293	4279	-1,16
294	4291	-0,95
296	4313	-1,10
297	4325	-1,09

depth	cal BP	$\delta^{13}C$
298	4336	-0,73
299	4348	-0,96
300	4359	-1,13
301	4382	-1,32
306	4496	-1,04
307	4519	-1,25
308	4542	-1,29
309	4565	-1,28
311	4611	-1,15
313	4656	-1,58
314	4679	-1,23
315	4702	-1,18
316	4725	-1,22
317	4748	-1,00
318	4771	-1,18
319	4794	-0,85
320	4817	-1,42
321	4840	-1,40
322	4862	-1,52
323	4885	-0,97
324	4908	-1,07
325	4931	-1,34
326	4954	-1,14
327	4977	-1,30
328	5000	-0,83
332	5091	-1,07
333	5114	-1,25
334	5137	-1,32
335	5160	-1,07
336	5183	-1,12
337	5206	-1,14
338	5229	-1,14
339	5251	-1,25
340	5274	-0,92
341	5297	-1,15
342	5320	-0,76
343	5343	-1,21
344	5366	-1,18
345	5389	-1,34
346	5412	-1,34
348	5457	-1,52
349	5480	-1,26
350	5503	-1,10
351	5526	-1,14
352	5549	-1,21
353	5572	-1,30
354	5595	-1,02
355	5618	-1,44
356	5641	-0,88
357	5663	-1,15
358	5686	-1,15
359	5709	-1,19
360	5732	-1,33
361	5755	-1,30
362	5778	-1,35
363	5801	-1,24
364	5824	-1,04

depth	cal BP	$\delta^{13}C$
365	5847	-1,23
366	5869	-0,97
367	5892	-1,15
368	5915	-1,03
369	5938	-0,86
370	5961	-1,34
371	5984	-1,07
372	6007	-0,89
373	6030	-1,22
377	6121	-1,12
378	6144	-1,46
379	6167	-1,24
380	6190	-0,82
381	6213	-1,00
382	6236	-1,08
383	6259	-1,26
384	6281	-0,89
385	6304	-1,08
386	6327	-1,02
387	6350	-1,02
389	6396	-0,94
390	6419	-1,00
391	6442	-0,66
392	6465	-0,73
393	6487	-1,03
394	6510	-0,90
395	6533	-0,80
396	6556	-1,08
397	6579	-0,79
398	6602	-1,33
399	6625	-1,13
400	6648	-1,11
401	6670	-0,91
403	6716	-0,94
404	6739	-1,17
405	6762	-0,57
406	6785	-1,19

***Melonis barleeanus* $\delta^{13}C$ raw**

CORE IOW225517

depth	cal BP	$\delta^{13}C$
10	1762	-1,00
20	1889	-0,92
26	1968	-0,95
30	2021	-1,22
40	2157	-1,26
50	2297	-1,21
60	2441	-1,24
70	2589	-1,16
80	2742	-1,12
90	2898	-1,41
100	3059	-1,30
110	3224	-1,22
114	3292	-1,32
120	3394	-1,15
130	3567	-1,24
140	3745	-1,26
150	3927	-1,05
159	4094	-1,28
160	4113	-1,34
161	4131	-1,24
162	4150	-1,39
164	4188	-1,35
166	4226	-1,45
167	4245	-1,56
169	4284	-1,44
171	4322	-1,30
173	4361	-1,46
174	4380	-1,32
176	4419	-1,27
177	4438	-1,21
178	4458	-1,41
179	4478	-1,27
180	4497	-1,46
184	4576	-1,08
185	4596	-1,25
187	4636	-1,12
189	4676	-1,24
190	4696	-1,08
191	4716	-1,42
192	4736	-1,16
194	4776	-1,06
195	4797	-1,09
196	4817	-1,13
197	4837	-1,01
199	4878	-0,90
200	4898	-1,29
201	4919	-1,26
202	4939	-1,28
203	4960	-0,98
204	4981	-0,95
205	5001	-1,36
206	5022	-0,86
207	5043	-1,30
208	5064	-0,65
209	5084	-0,98
210	5105	-1,22
215	5210	-1,03
218	5274	-1,11
219	5295	-1,19
221	5338	-1,00
222	5359	-1,28
226	5445	-1,11
229	5510	-1,30
230	5532	-0,95
231	5553	-0,84
233	5597	-0,74
236	5663	-0,98
237	5685	-0,96
239	5729	-1,07
241	5773	-0,86
242	5795	-0,90
243	5818	-0,90
244	5840	-0,89
245	5862	-1,03
247	5907	-1,18
248	5930	-0,93
249	5952	-0,93
250	5975	-1,20
253	6043	-0,79
256	6111	-0,98
260	6202	-0,96
261	6225	-0,95
263	6272	-1,07
264	6295	-1,03
267	6364	-0,70
268	6388	-0,96
269	6411	-1,15
270	6434	-1,21
272	6481	-1,09
274	6528	-1,13
275	6552	-1,08
276	6576	-1,17
277	6599	-0,90
279	6647	-1,15
280	6671	-1,18
281	6694	-1,24
284	6766	-1,06
285	6790	-1,06
290	6911	-1,17
293	6984	-1,01
300	7155	-1,20
304	7254	-1,22
305	7279	-1,25
306	7304	-1,28
307	7329	-1,14
310	7404	-1,38
320	7657	-1,34
330	7914	-1,29
340	8175	-0,86
350	8441	-1,34
360	8710	-1,36
370	8984	-0,90
380	9262	-1,11
390	9544	-0,66
400	9830	-0,84
410	10121	-0,90
420	10416	-0,62
430	10714	-0,45
440	11017	-0,71
450	11325	-0,68